



Presentation Title Goes Here and Should Not Be Longer Than Two Lines

Presenter Name

Presenter Title

The Team



Prof Phil Coates
Polymer IRC



Dr Ben Whiteside
Fibre reinforcement
Micromoulding



Dr Franco Costa
Software development



Dr Russ Speight
Material characterisation



Dr Pete Hine
Fibre orientation
Micromechanics



Bushra Parveen
Short and long fibre reinforcement

Micromoulding

1. High shear rheometry

- To evaluate the validity of power law viscosity models for thin walled/micromoulded products with high shear rates

2. Flow front / shrinkage predictions

- Investigate simulation performance for micromoulded products

3. Thermal considerations

- High surface area/volume ratio for thin wall and micro scale mouldings means that boundary conditions at polymer mould interface have significant influence over product properties. Ongoing to work to investigate thermal contact resistance behaviour and validate Moldflow models

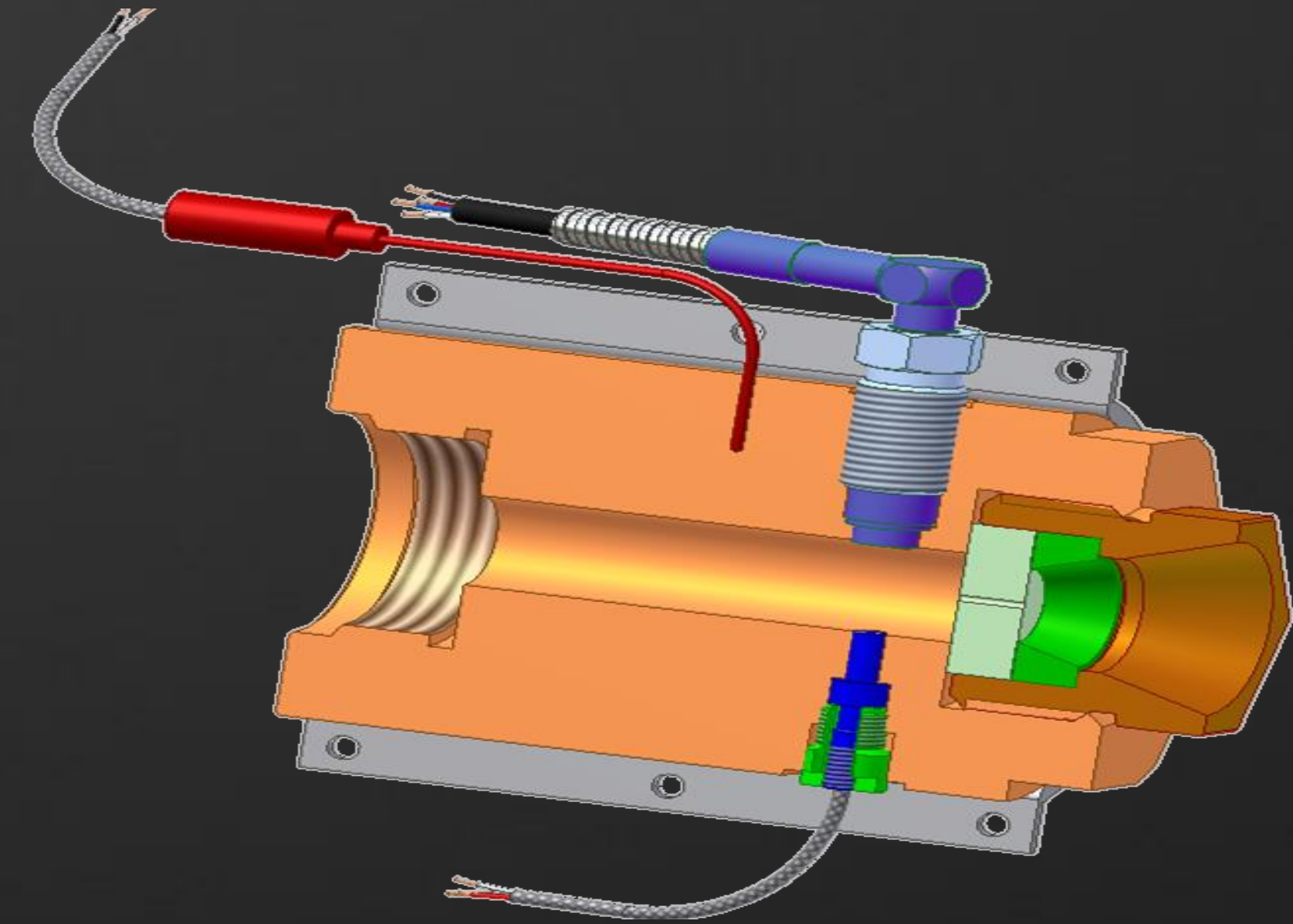
Micromoulding - Experimental details



Tests performed on Fanuc S2000i100A High Speed IMM

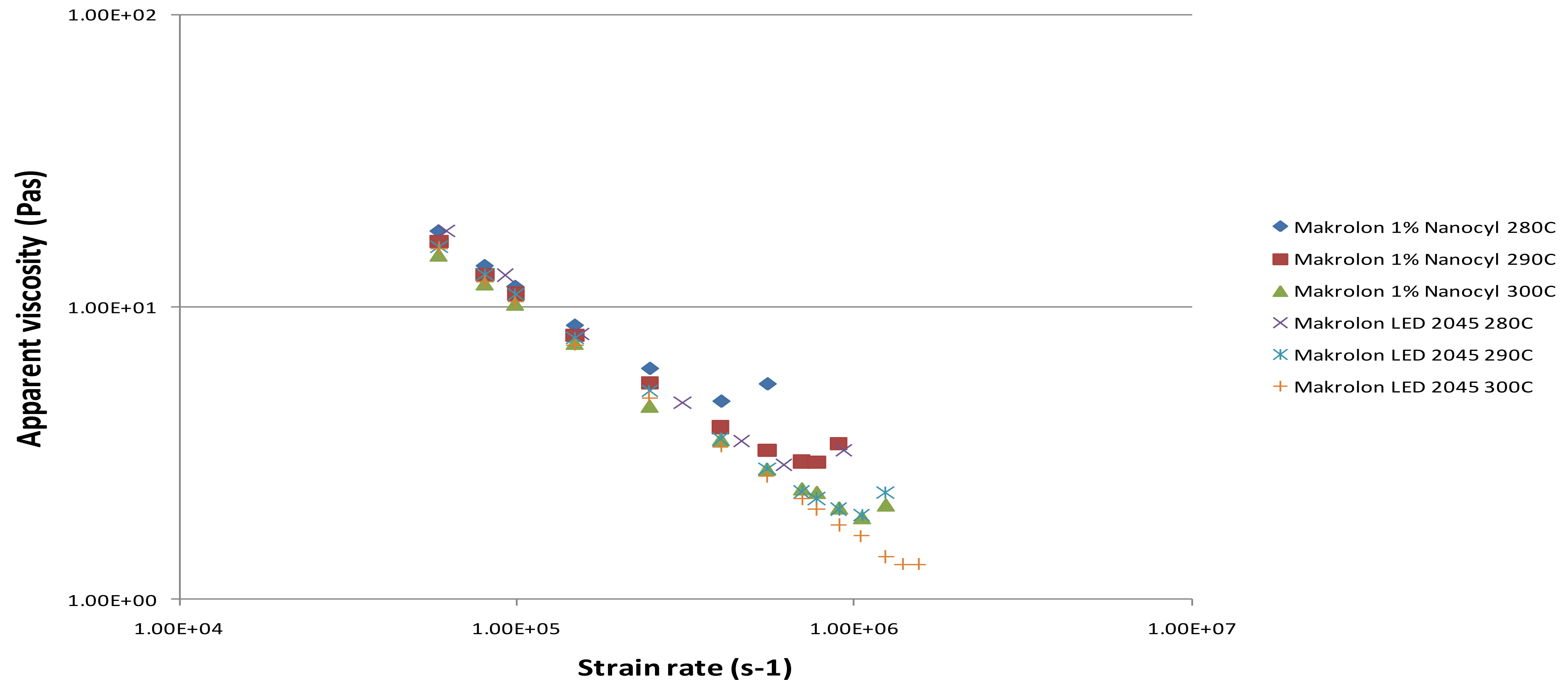
Nozzle design

- Long capillary die installed and machine allowed to soak for 30mins to ensure temperature is consistent
- Full extent of screw back (70mm) performed with no decompression
- Injection delay of 120s to allow temperature to stabilise
- 3 measurements taken at each injection velocity/shear rate
- Plateau selected by the user after each experiment
- After all velocities/shear rates are completed a zero length die is fitted and experiments repeated



- Capillary die is retained by a locking nut
- Kistler high temperature piezo-resistive nozzle sensor provides pressure and temperature information

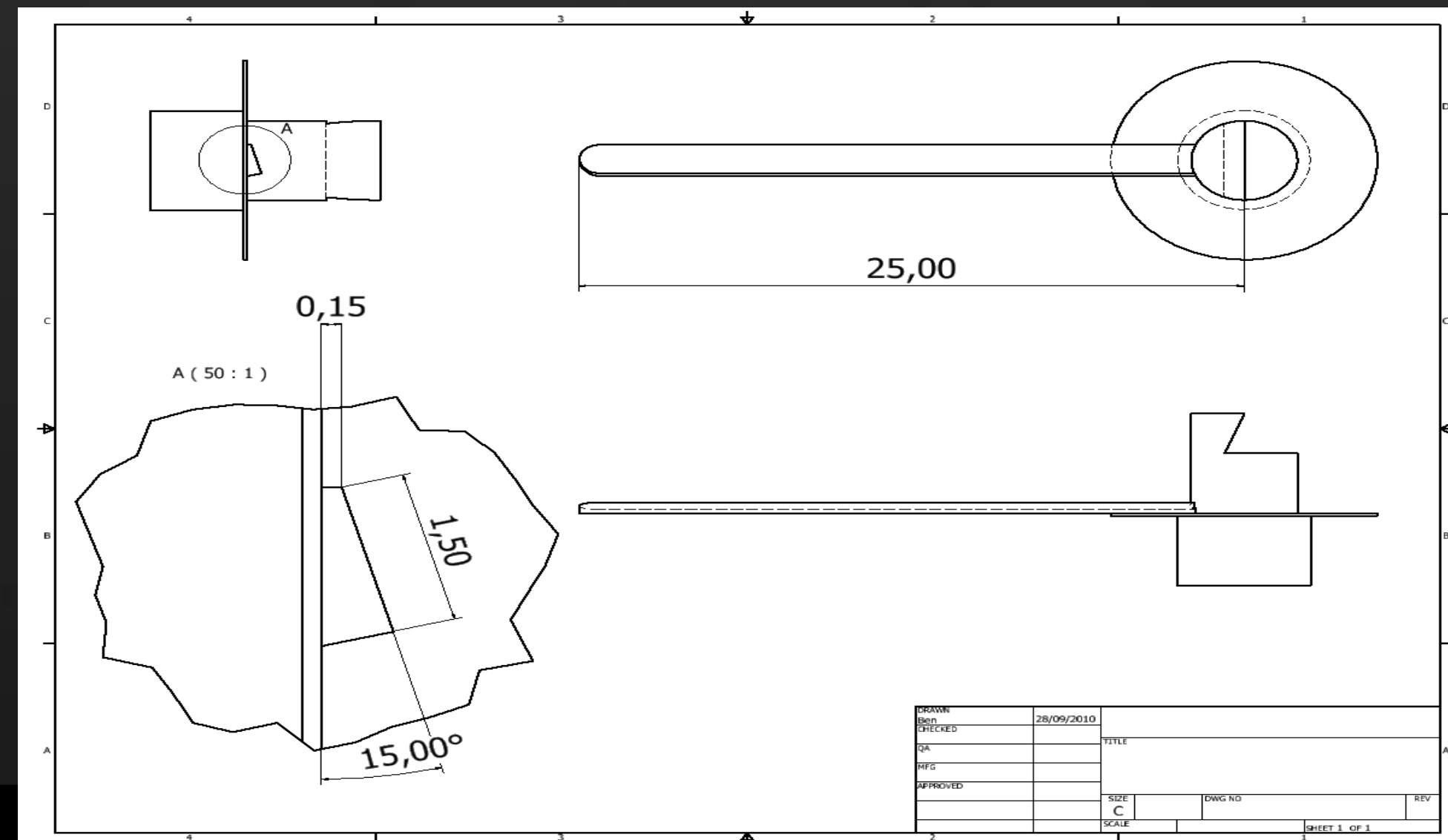
High shear rheometry data - Makrolon LED 2045/Nanocyl CNT



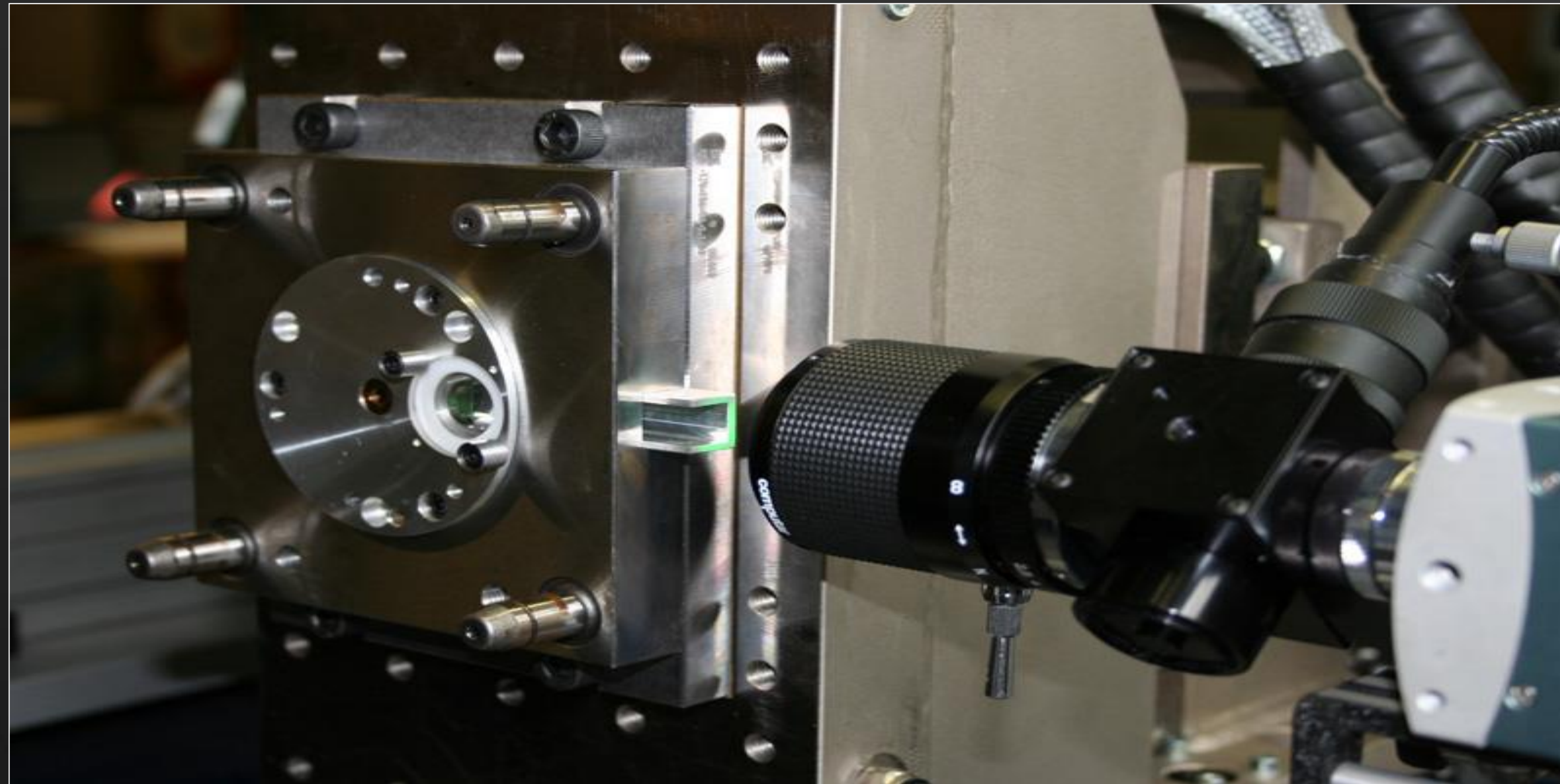
Data shows that a critical shear rate occurs, above which power law behaviour no longer exists. This critical shear rate is affected by temperature and presence of nanofillers. We must ensure that the simulation environment does not exceed this critical shear rate to ensure an accurate solution

Flow visualisation for simulation validation

- Flow visualisation a useful tool for evaluating Moldflow but it is difficult to assess differences in flow front profile as this is highly geometry dependent
- Created a new wedge shaped cavity form in order to increase sensitivity of flow front profile to process conditions

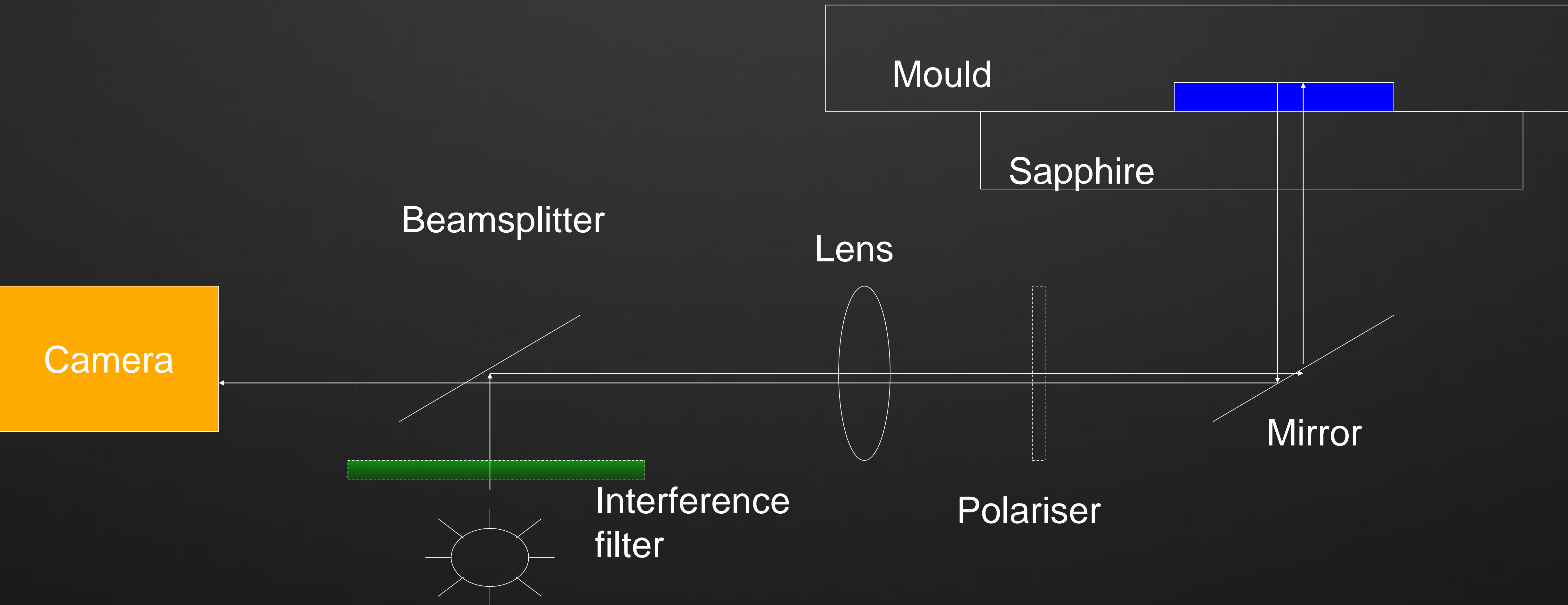


Flow visualisation



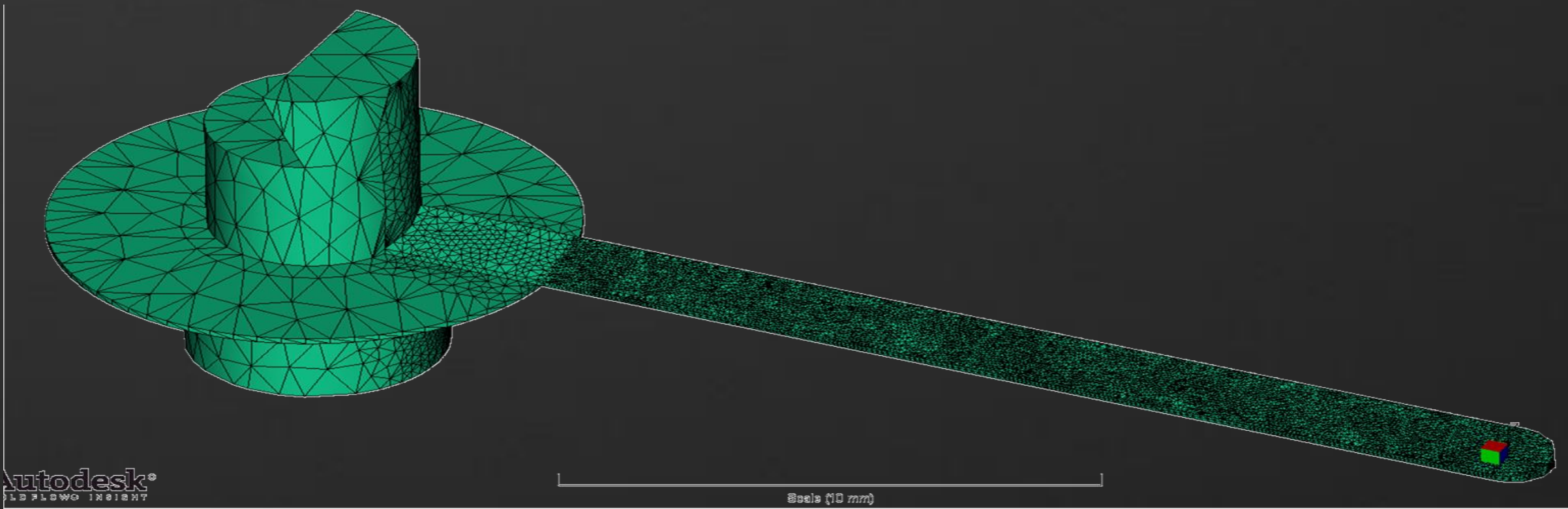
- High speed camera (>10 000 fps)
- Sapphire window in cavity
- Monochromatic lighting
- Measurement of
 - Flow front position
 - Shrinkage behaviour
 - Stress-induced birefringence

Optical Train



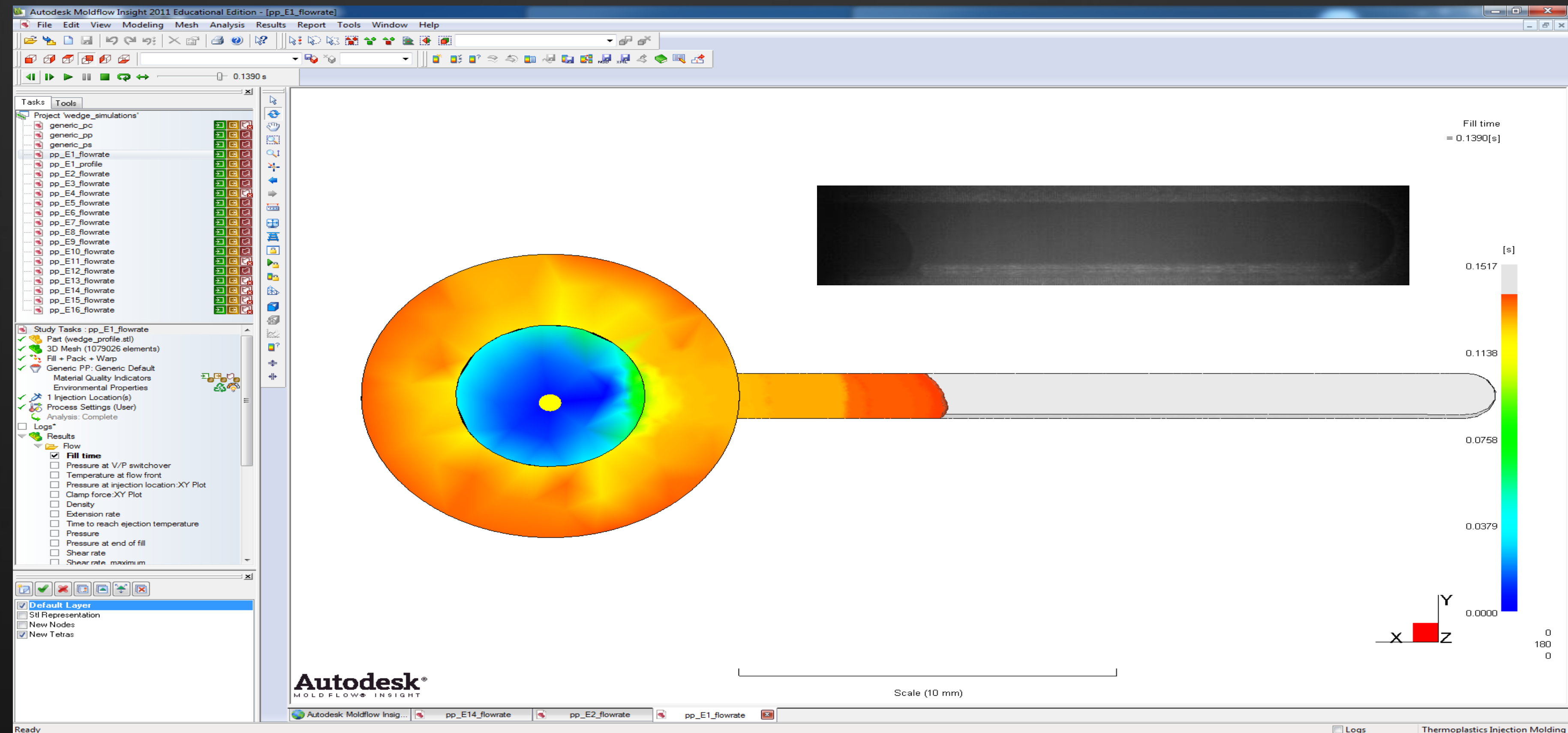
Experimental method

- DOE performed with full flow visualisation for measurements of flow front progression and shrinkage
- DOE repeated in the MF environment using flow rates calculated from injection piston area and velocity
- Work performed to optimise/refine the mesh for convergence of results with acceptable solution times

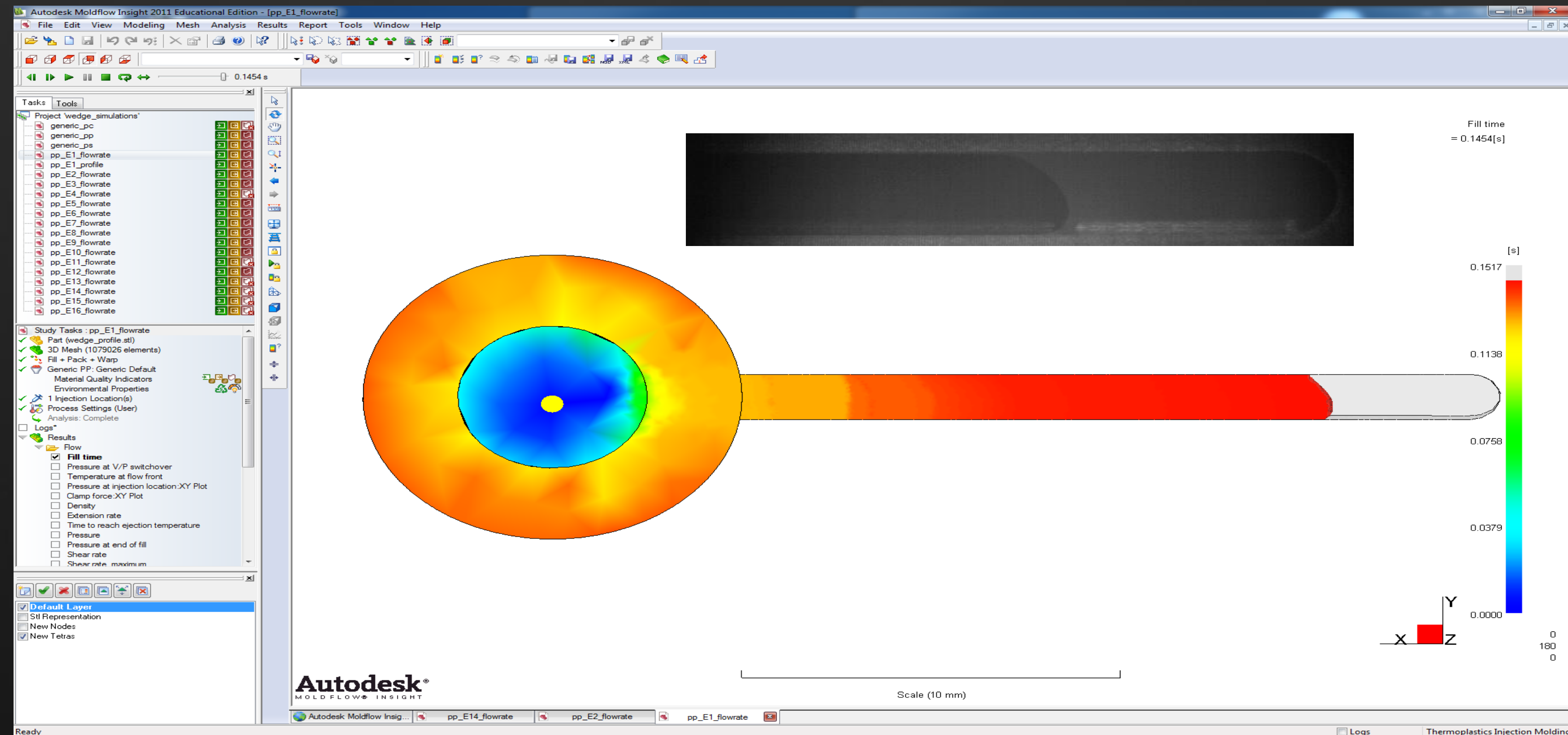


Melt T	Mould T	Injection Velocity	Hold Pressure
200	45	50	50
200	45	50	100
200	45	100	50
200	45	100	100
200	75	50	50
200	75	50	100
200	75	100	50
200	75	100	100
220	45	50	50
220	45	50	100
220	45	100	50
220	45	100	100
220	75	50	50
220	75	50	100
220	75	100	50
220	75	100	100

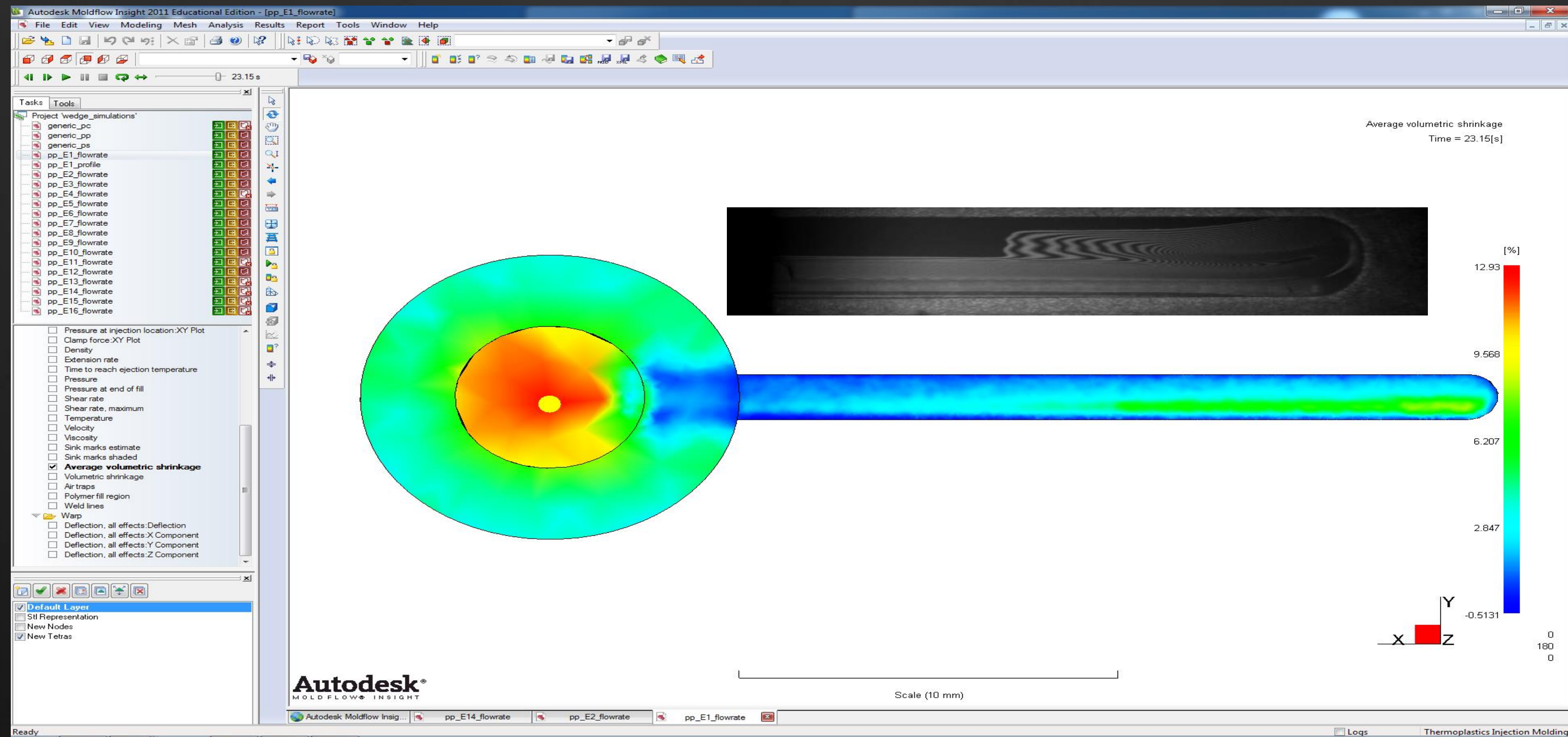
Experiment 1 – flow front



Experiment 1 – flow front



Experiment 1 – average volumetric shrinkage



Flow front profiles



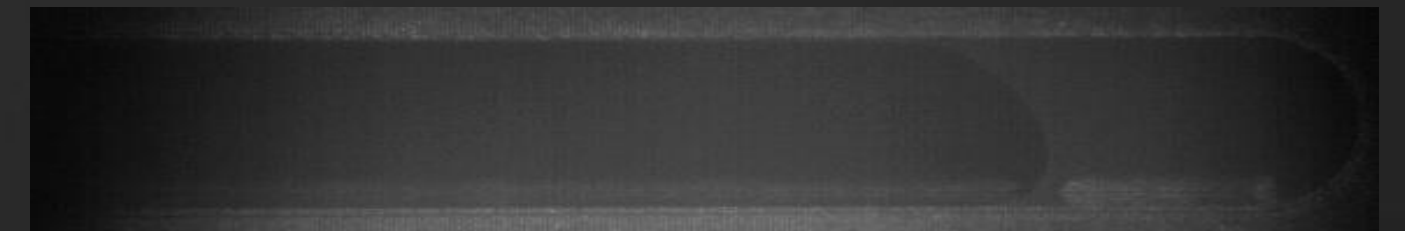
Expt 1



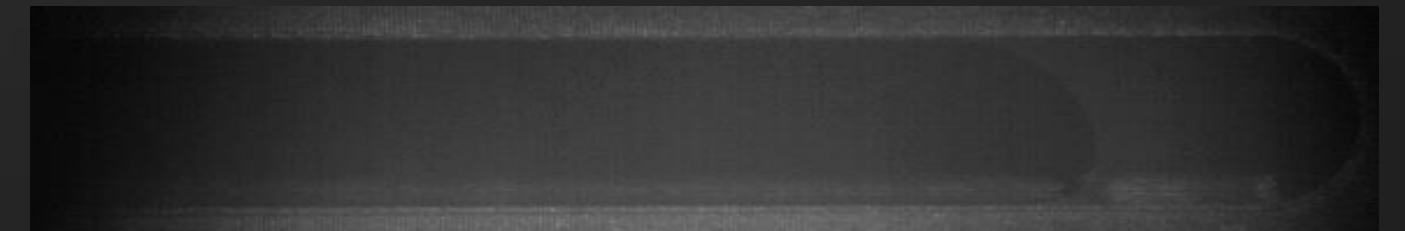
Expt 3



Expt 5



Expt 7



Expt 9



Expt 11



Expt 13

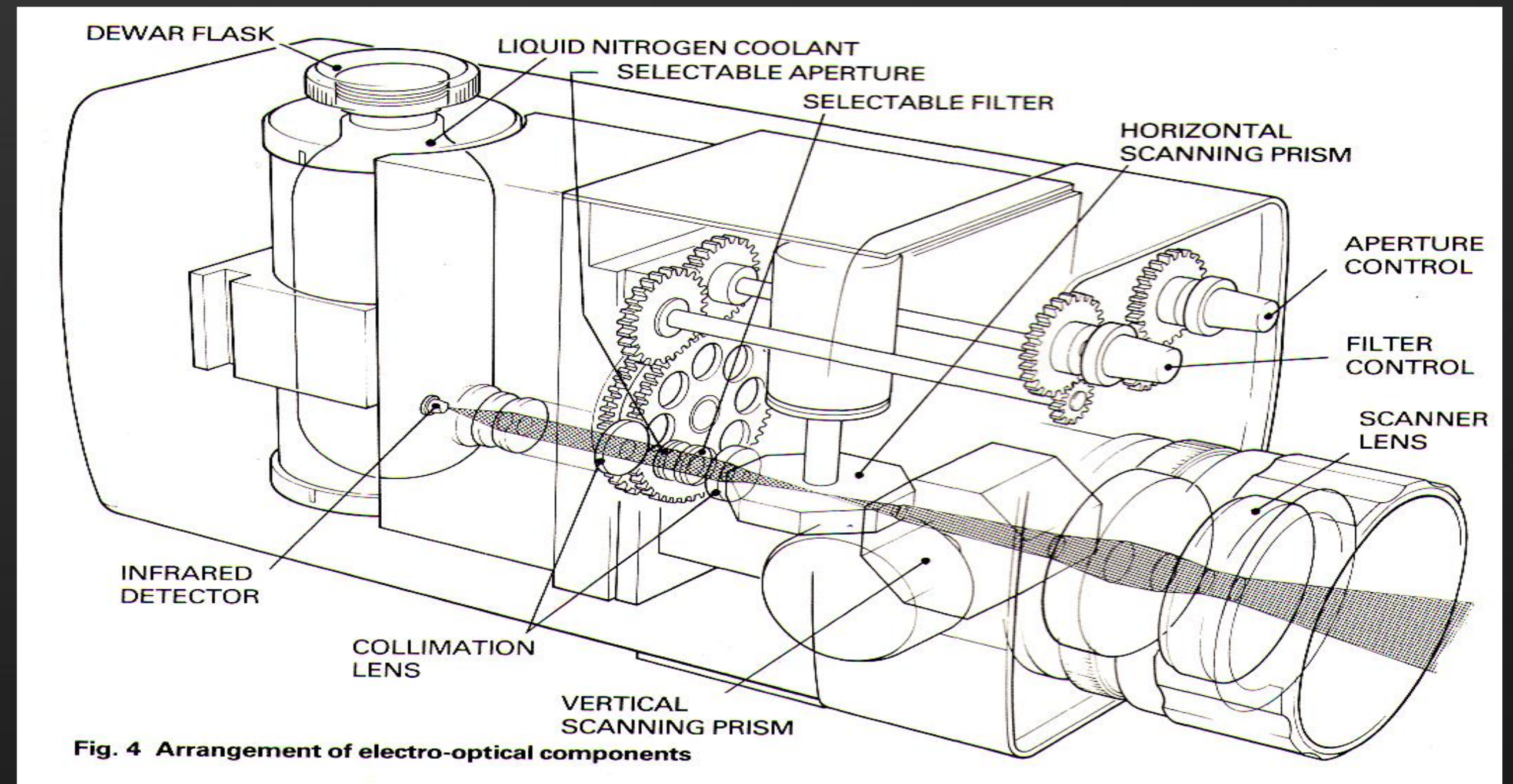


Thermal imaging system

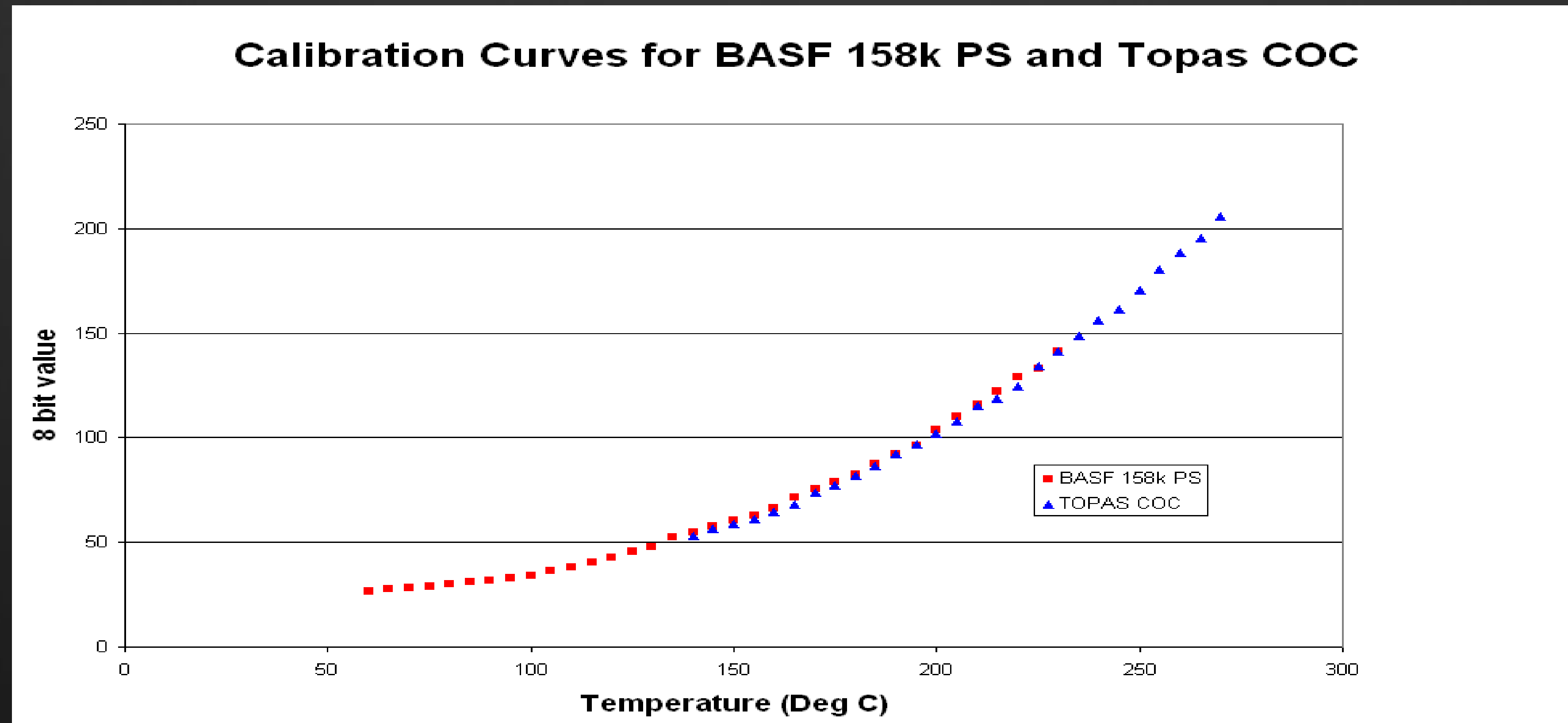
AGA thermovision system uses a single sensor and two rotating prisms to form a full field image.

By halting the vertical scanning prism, line scan images can be obtained at a rate of 2500Hz.

Analogue data output and start-of-frame signals have been intercepted and digitised to produce digital line scan thermal images.



Calibration data

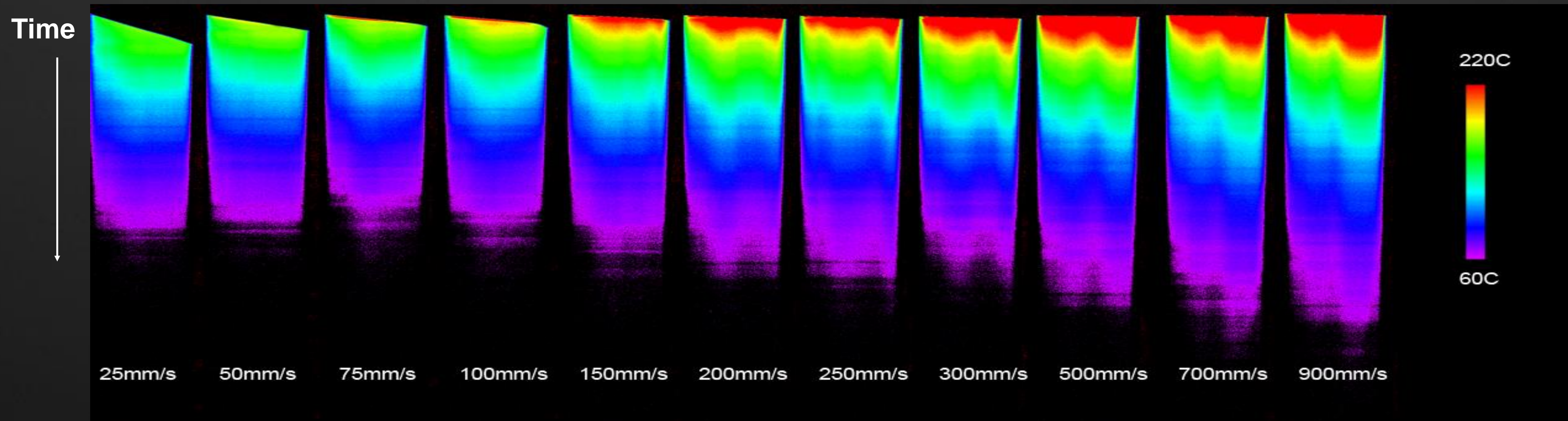


Curves for two polymers overlap – similar emissivity

No abrupt changes during phase changes

No outlying points – piecewise linear curve fit

IR Contour evolution at different injection rates – BASF 158k

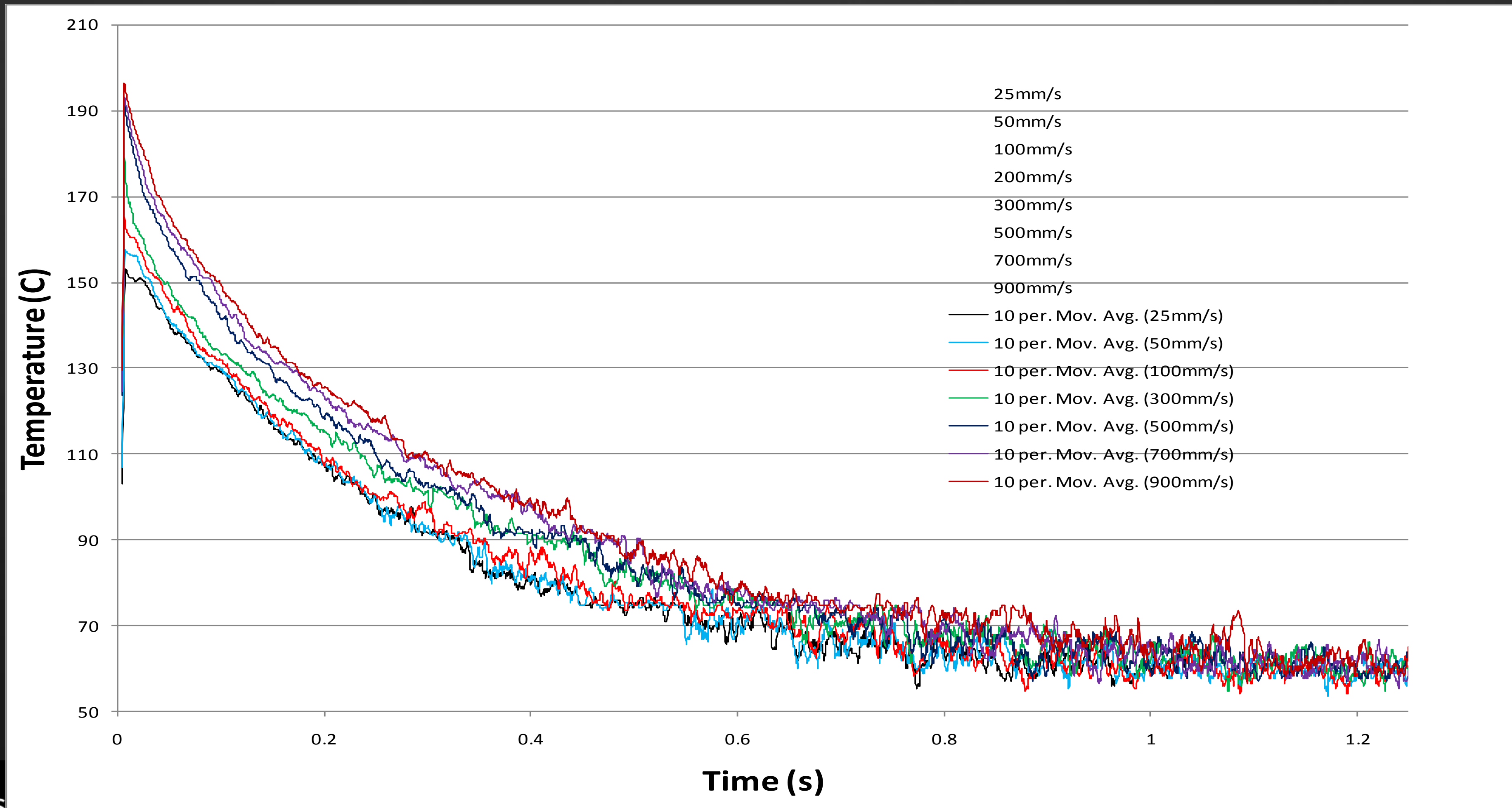


Higher velocity -> Higher measured temperatures

Increased shear heating

Decreased cooling in runner system

Cooling curves for BASF 158K PS



Part 2 – Fibre Polymer Composites

Fibre Polymer Composites

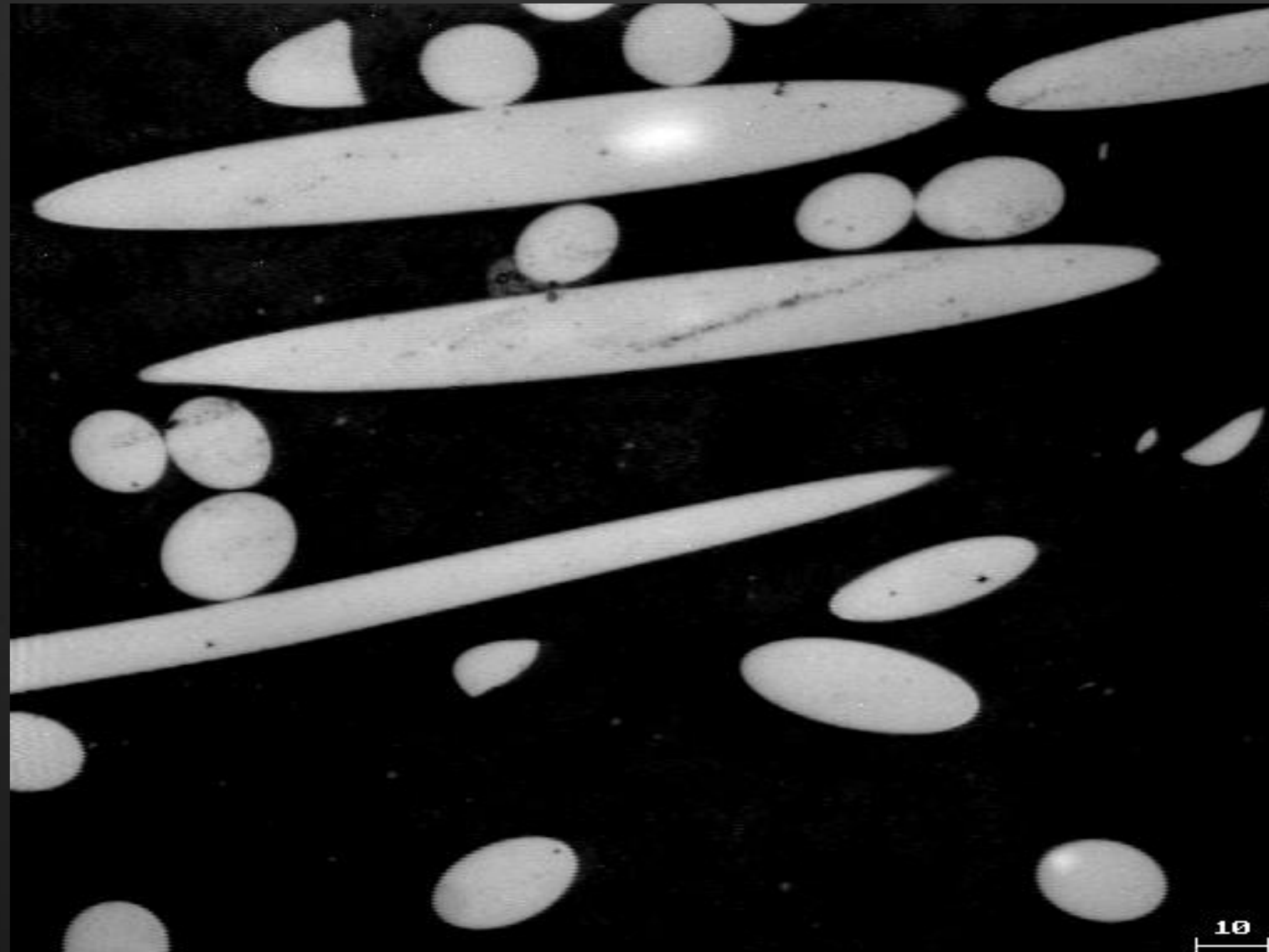
1. Experimentally determined fibre orientation
2. Fibre prediction models
3. Example geometry analysis
4. Effect on final product properties
5. Look to the future

Experimentally Determined Fibre Orientation

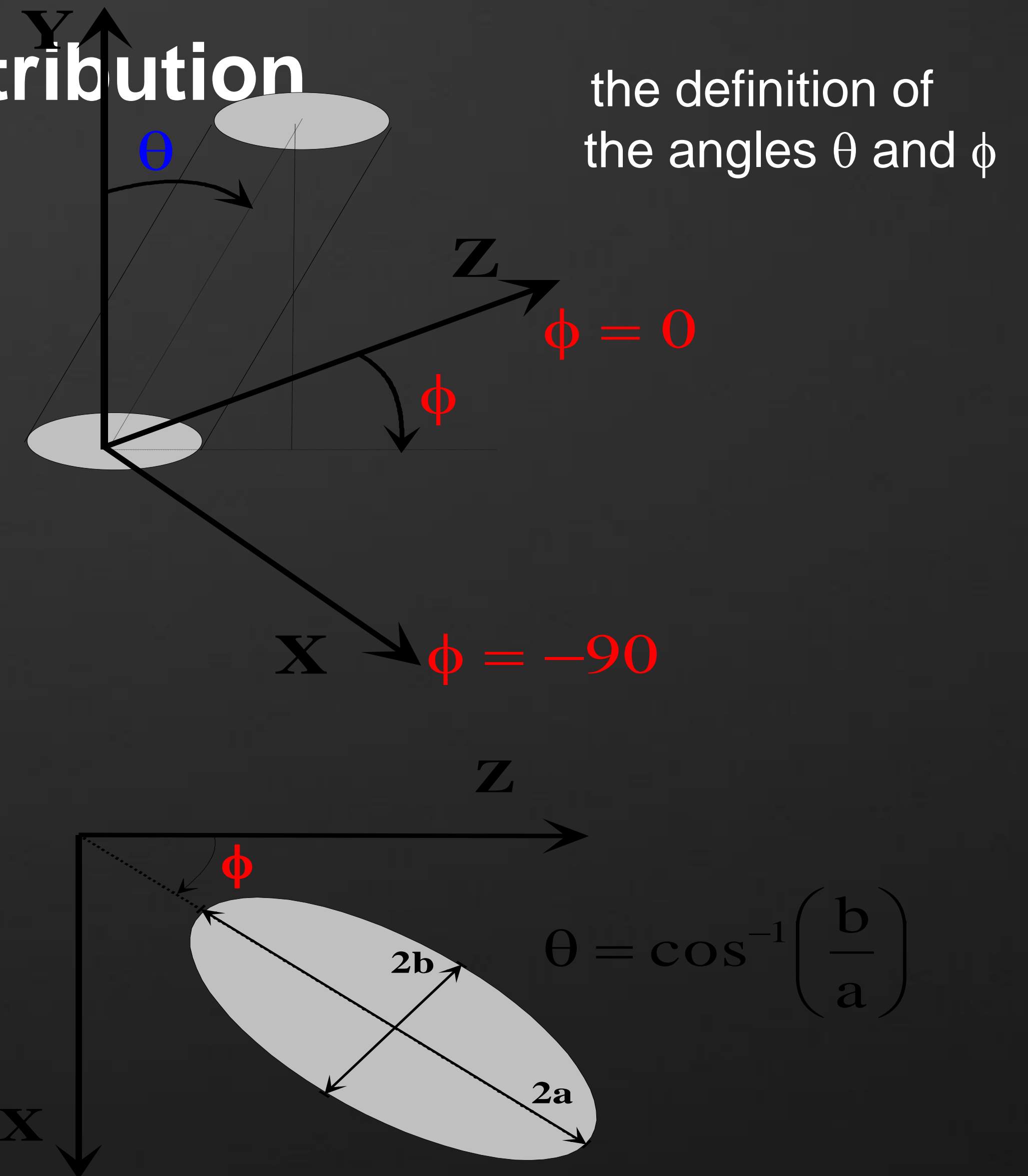
Fibre Polymer Composites

1. **Experimentally determined fibre orientation**
 - How to define fibre orientation
 - 'State of the art' fibre orientation measurement
 - Leeds based system (cutting edge technology)
 - Upgrades to exploit improved computational power
 - Example orientation distribution
 - Path through from sample preparation to final orientation plot

How to define fibre orientation distribution



a typical 2D image analysis section



the calculation of θ from the elliptical footprint

Experimentally Determined Fibre Orientation

‘State of the art’ Fibre Orientation Measurement Method

- Windows 2000 based PC (2.4 GHz P4, 2 Gb ram, 40 Gb HD)
- Microscope with computer controlled stage (movement to $1\mu\text{m}$ accuracy)
- In-house developed software

Details

- High magnification (for accurate orientation measurement)
- Large areas using frame matching (up to 25mm square)
- Large numbers of fibres to improve statistics (>1 million)
- High speed and small file sizes through on-line calculation of parameters
- Automatic scanning using auto threshold and autofocusing



Get better picture

Steps during fibre measurement

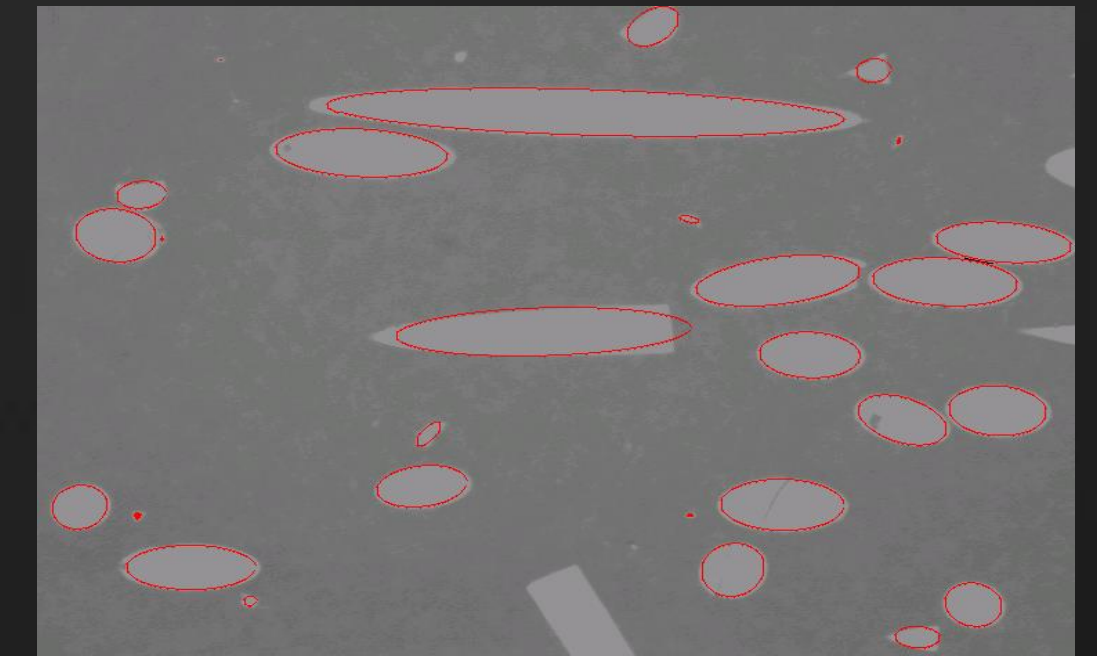
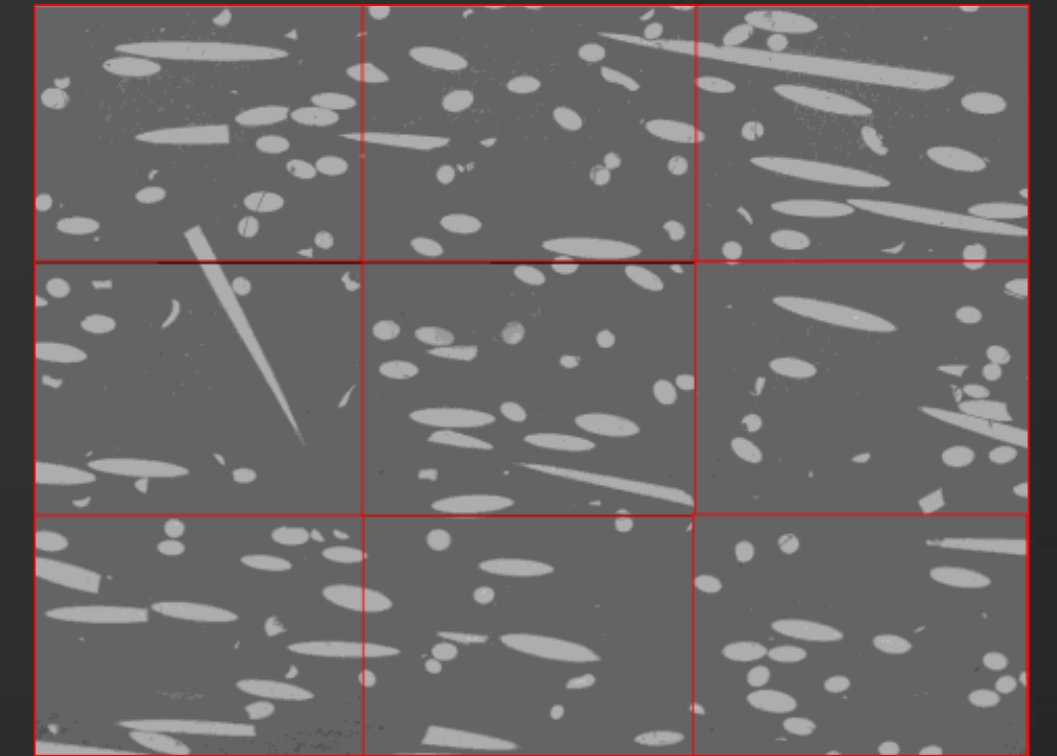
Sample Preparation

Image Capture

*Threshold
Image*

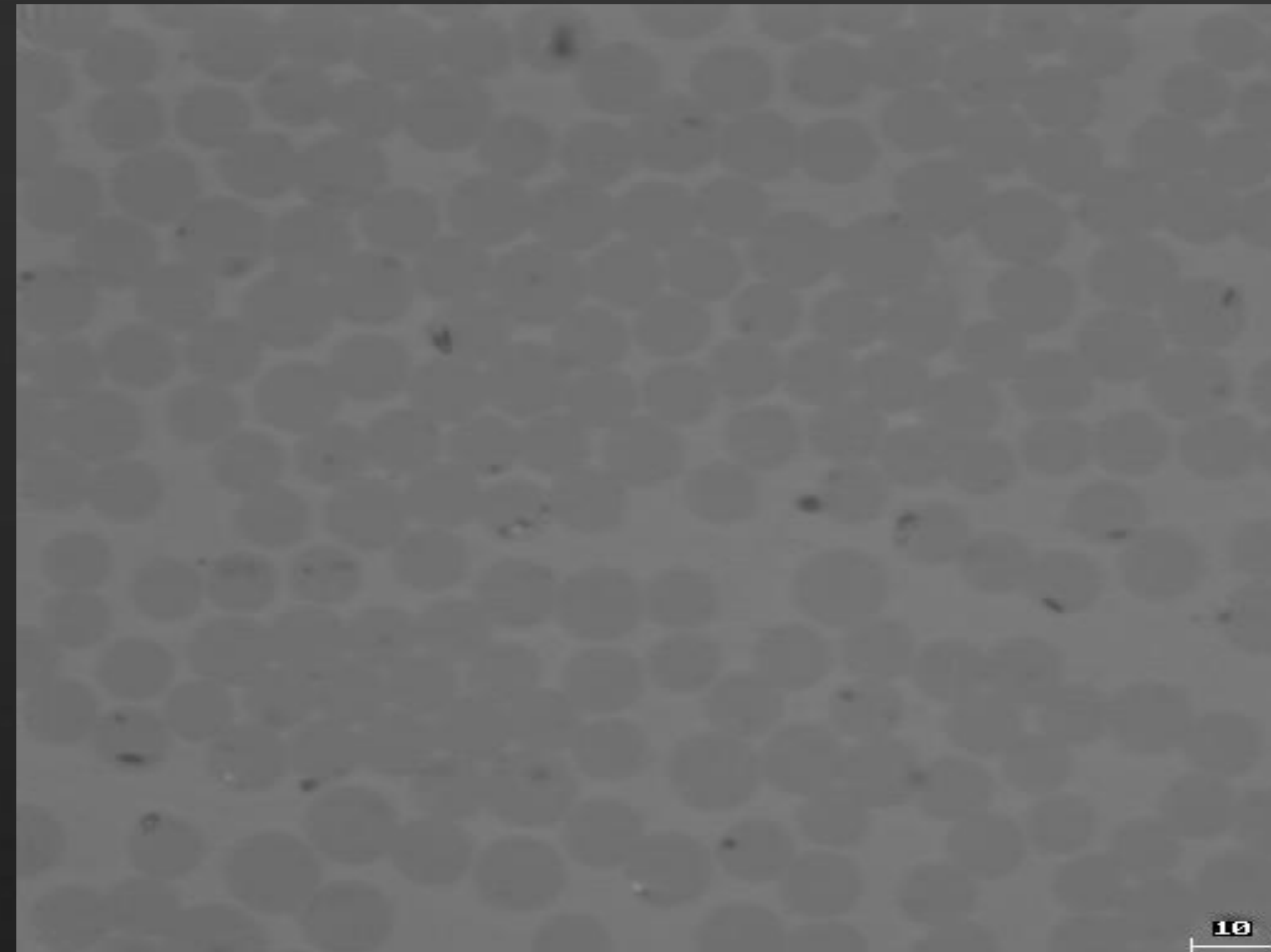
*Large Area
Reconstruction*

Ellipse Fitting

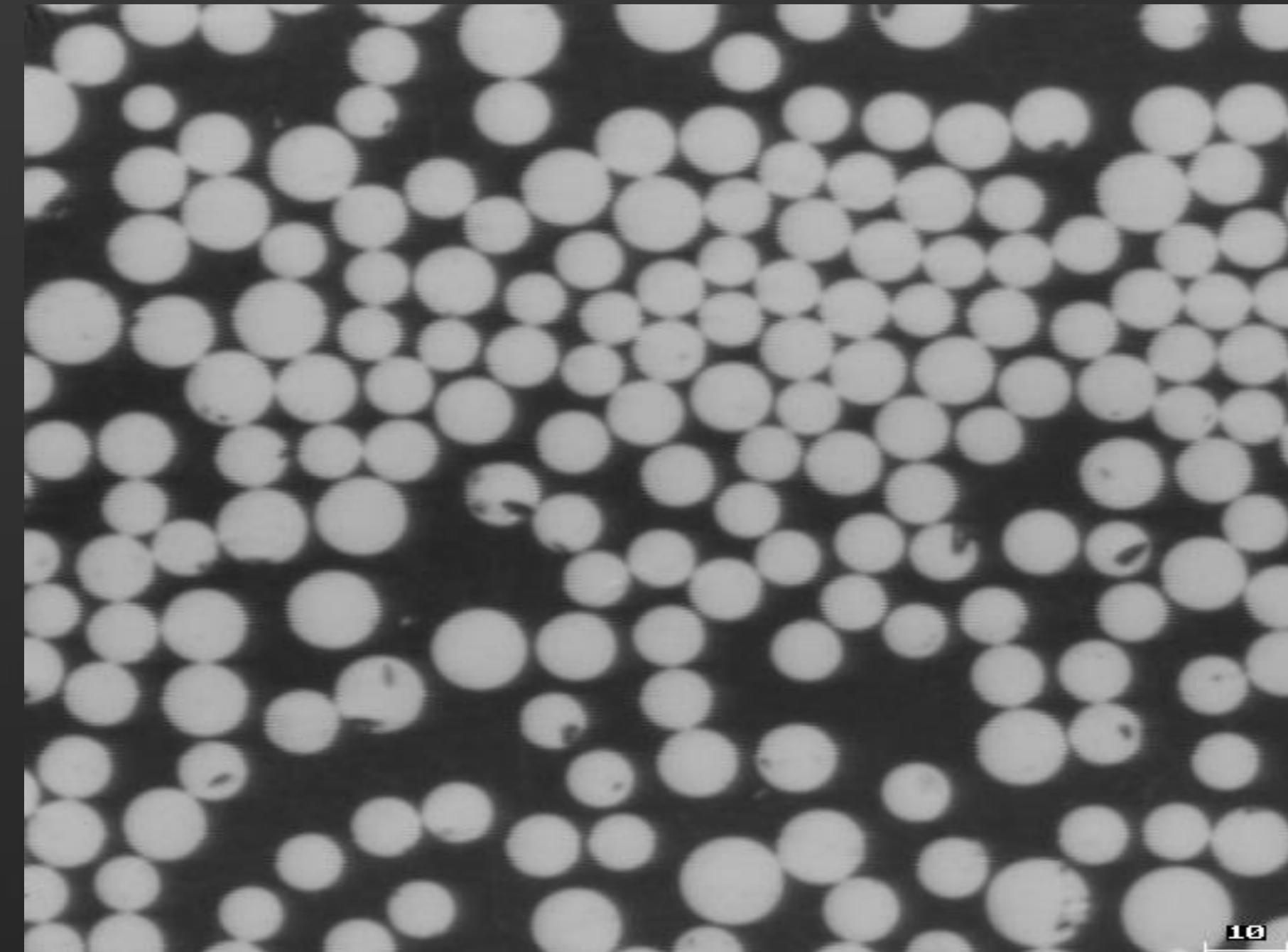


Multiple frames scanned in a raster fashion
fibres matched between frames

Elliptical parameters determined for each fiber
Single frame at high magnification
ellipse (in red)
768 x 576 pixels: 190 μ m x 150 μ m

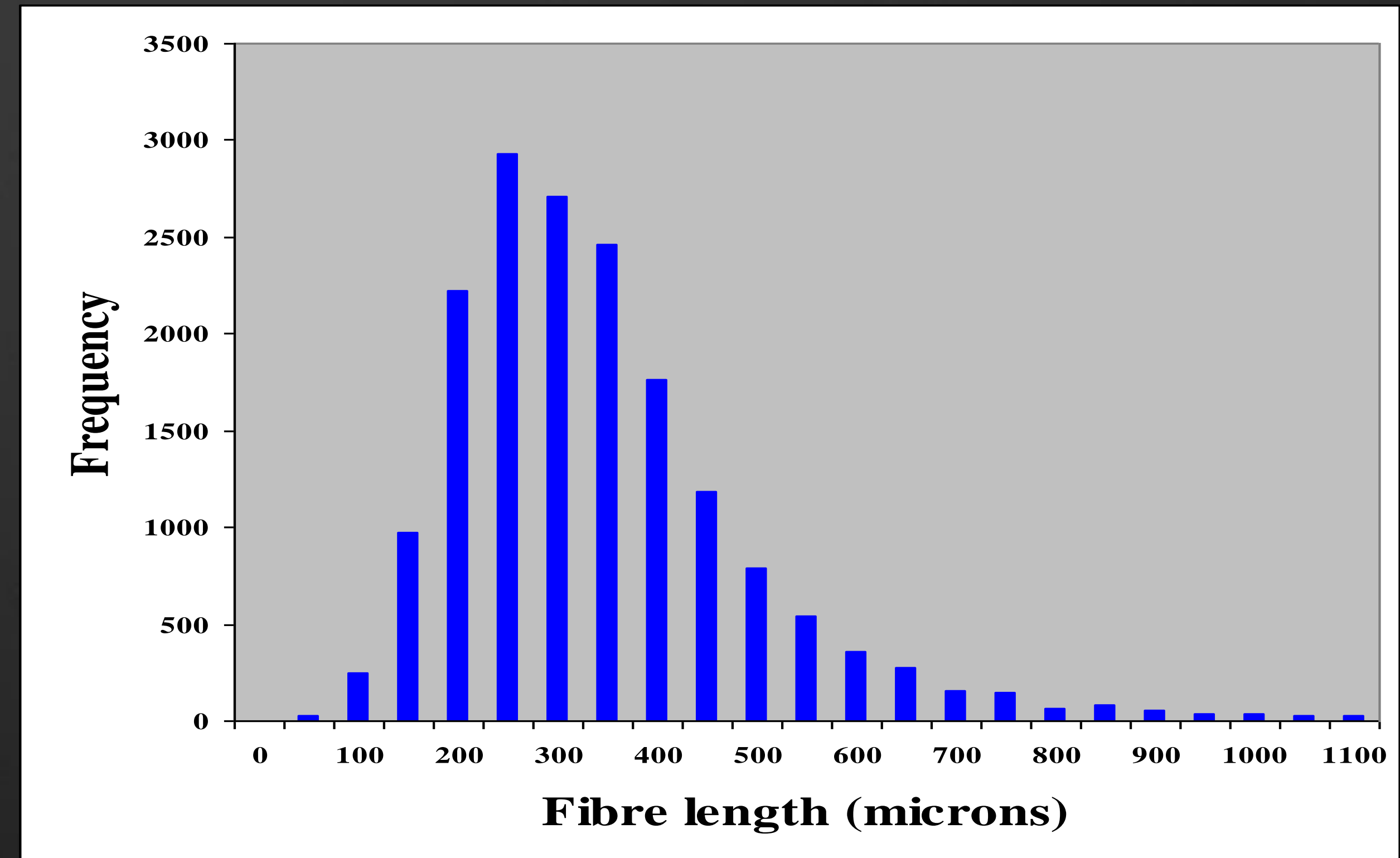
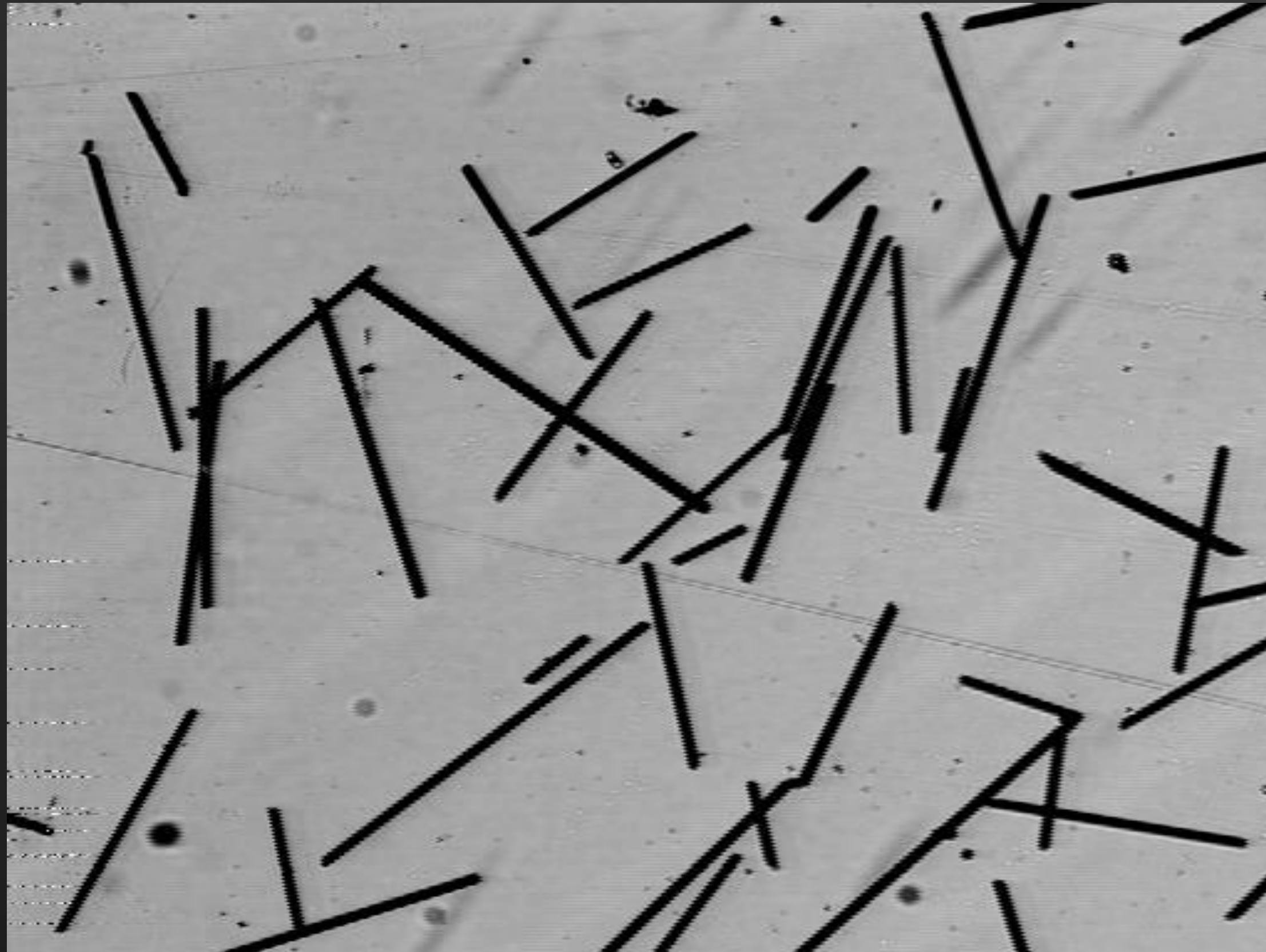


After polishing but before etching

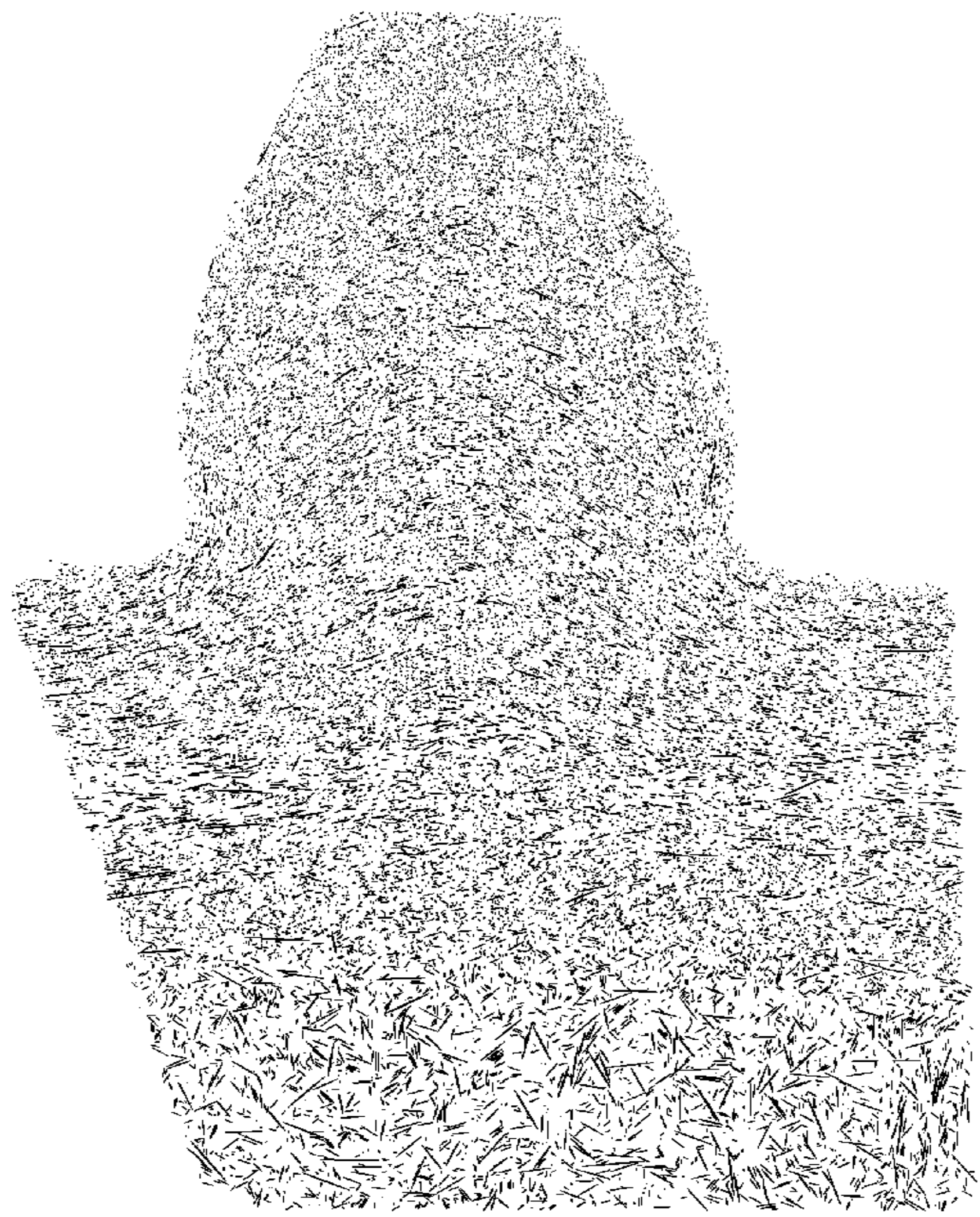


After etching using a plasma etch

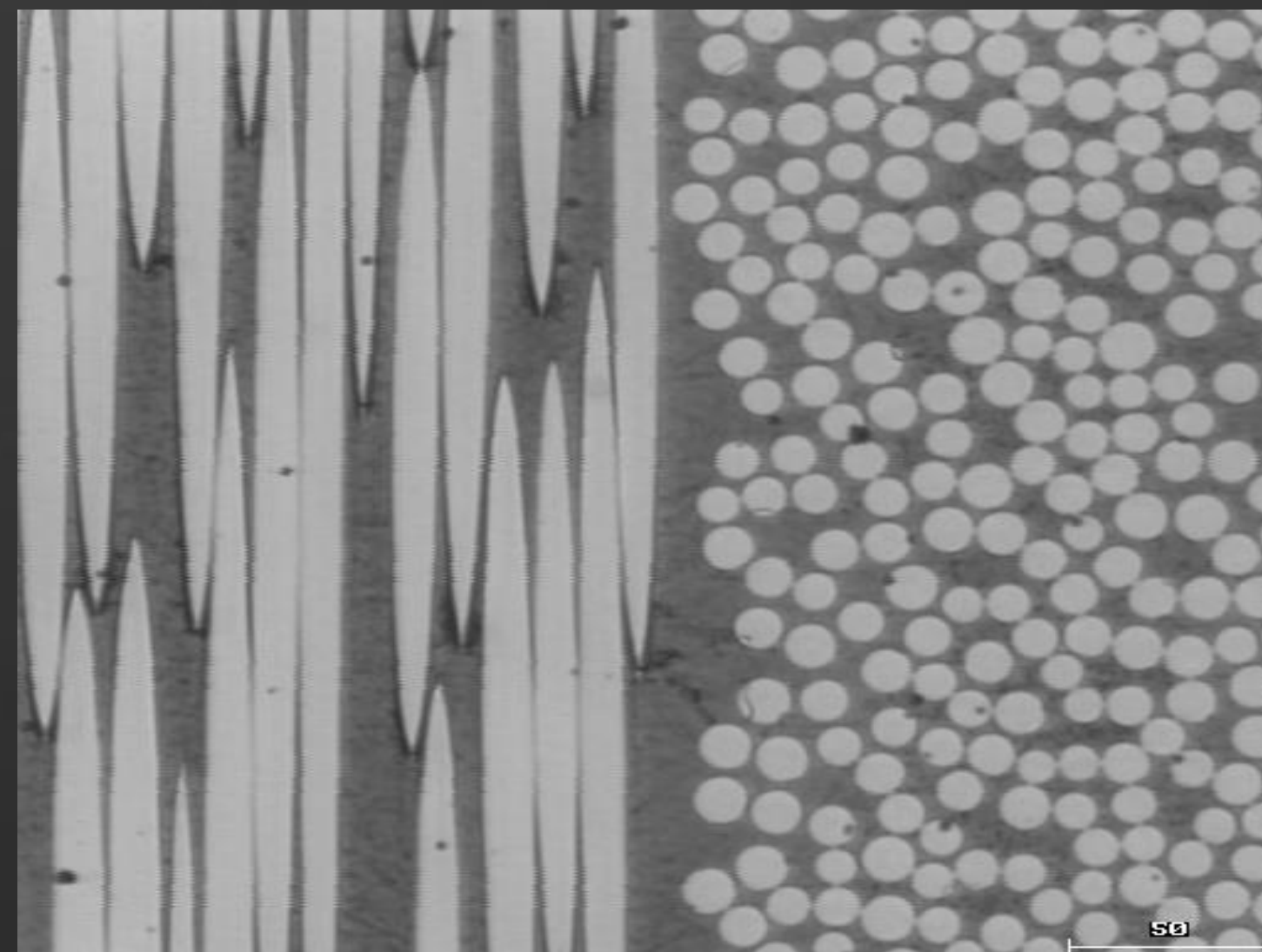
Sample preparation is crucial for obtaining reliable data. The samples to be examined are set into epoxy and polished using various polishing mediums (finest is 0.5 μ m alumina). A plasma etch is finally used (if required) to give contrast between fibres and matrix.



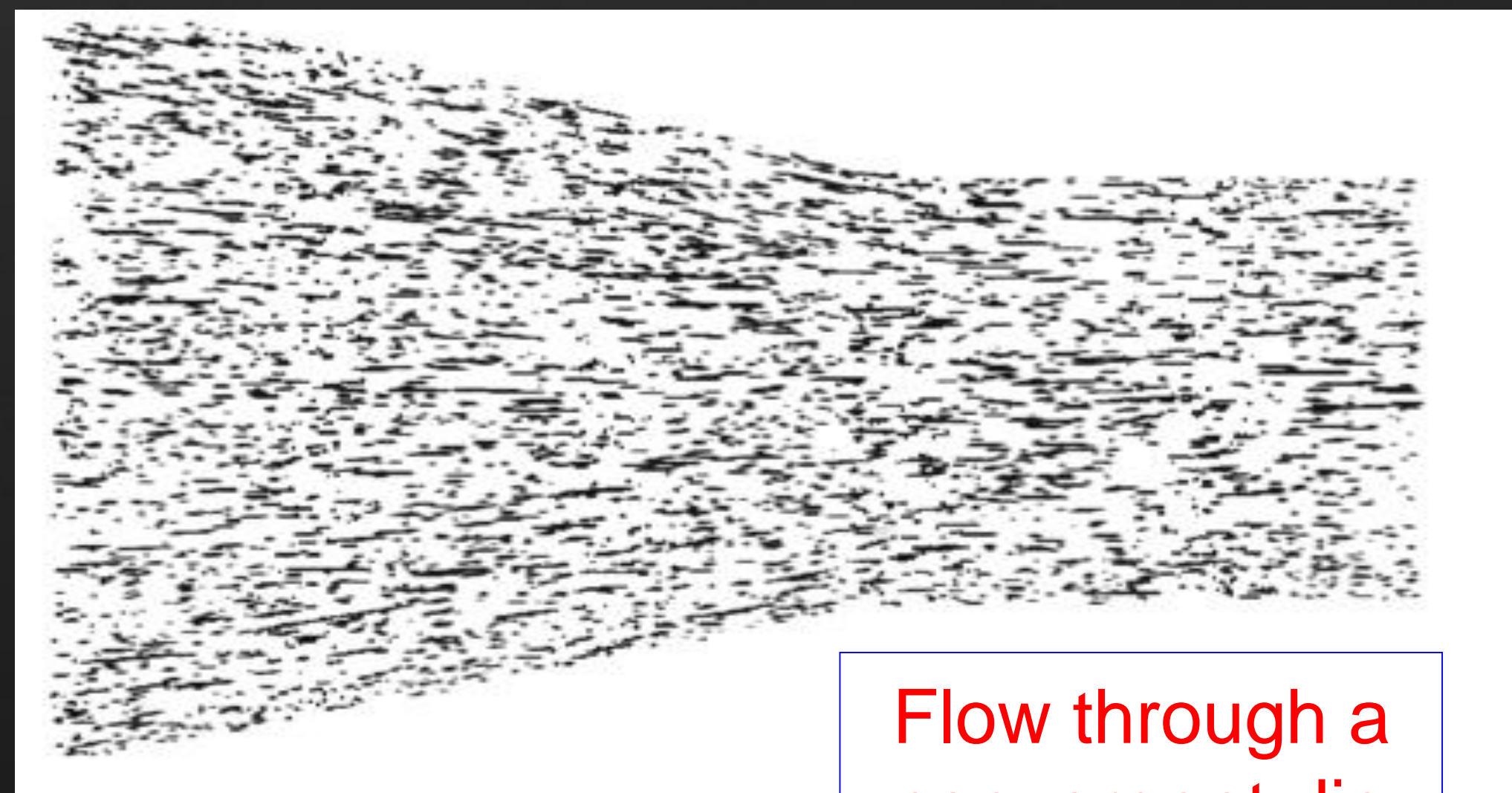
Composite samples are first burnt in a furnace to separate out the fibres. Scanning is carried out using transmitted light and a low magnification (screen size ~ 1mm square).



Section through an injection
moulded gear tooth



Long glass fibre
reinforced epoxy:
junction between
laminates



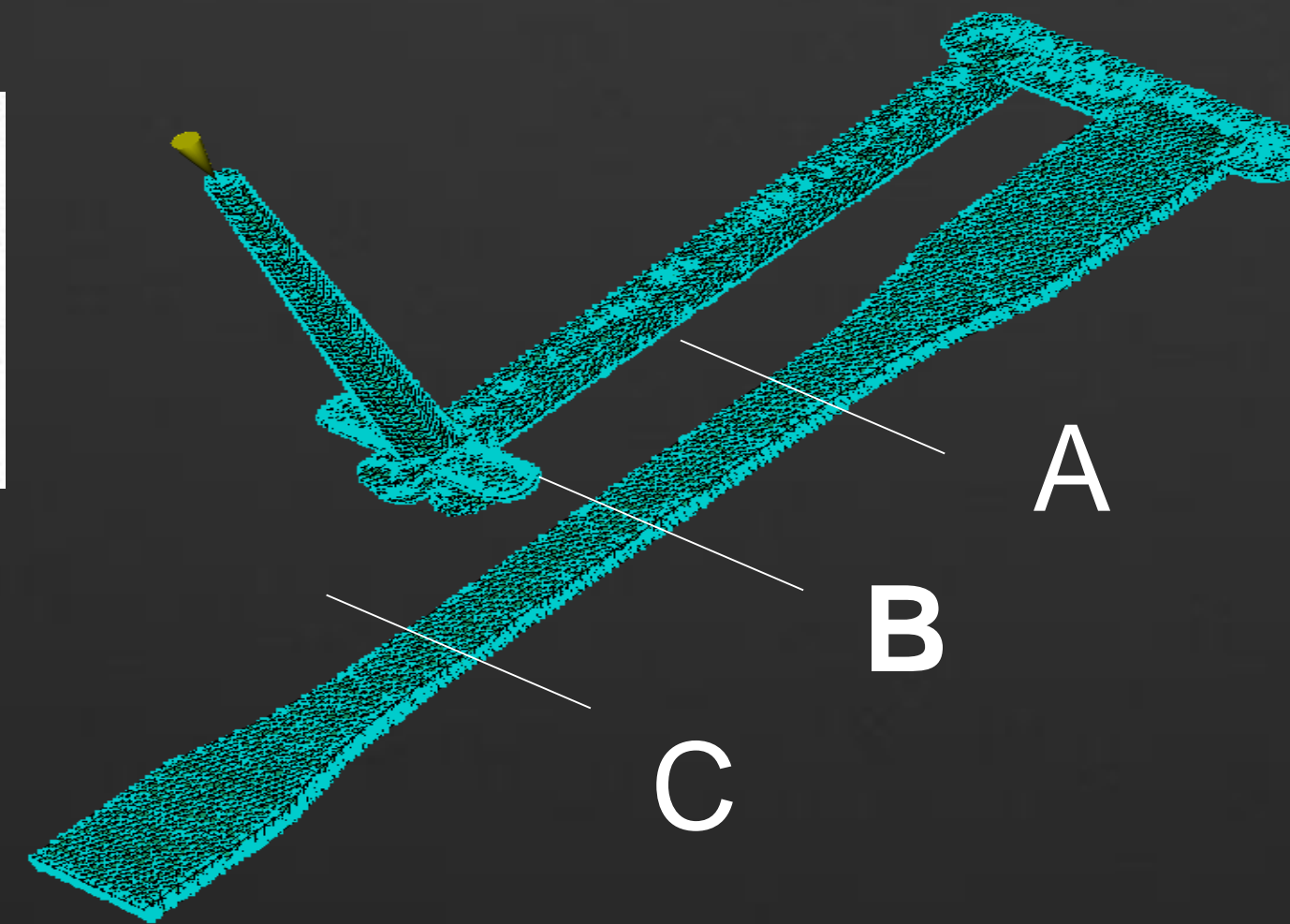
Flow through a
convergent die

Fibre Orientation Predictions

Typical Fibre Orientation Distribution Plots



A



A

B

C



C



B

This data would normally be used to calibrate a midplane or 3D Moldflow model

Fiber orientation prediction

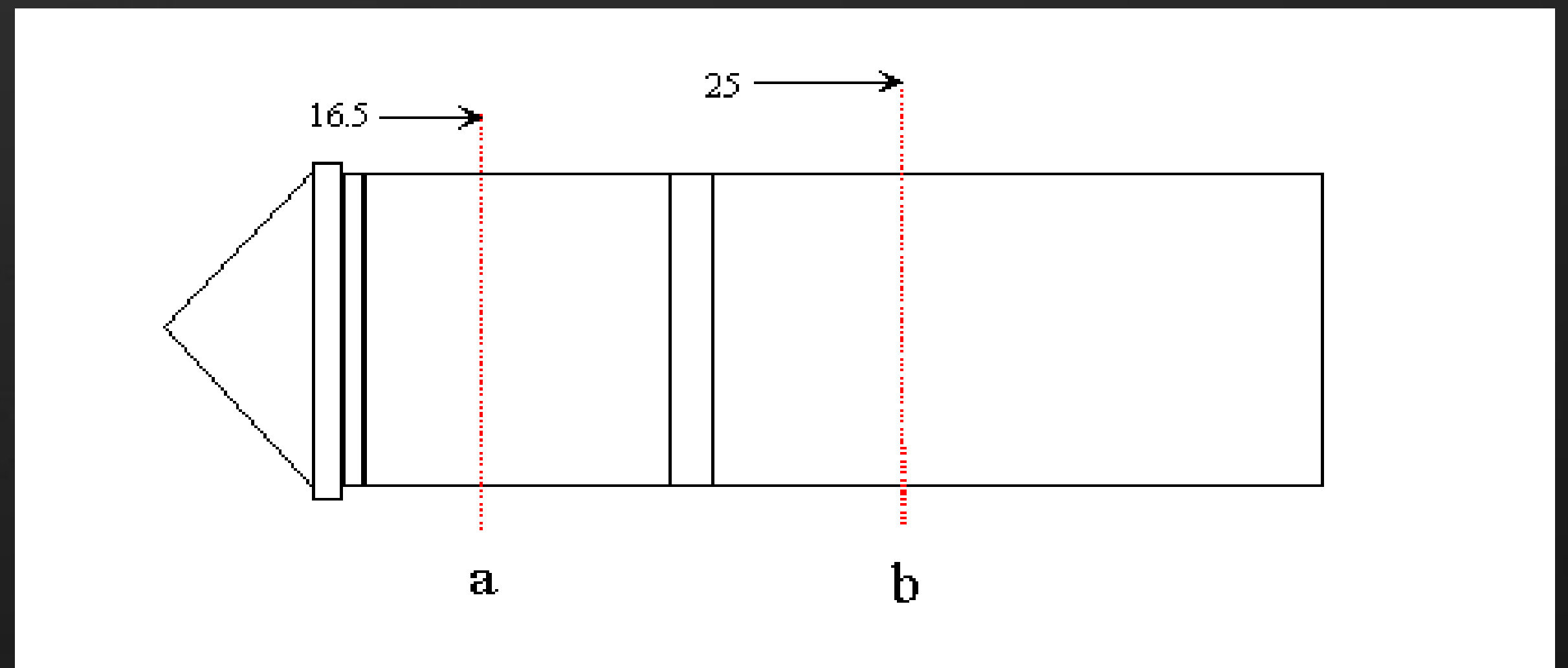
Midplane / Dual-domain	3D
Folgar-Tucker	Folgar-Tucker (Default)
Modified Folgar-Tucker (Dz) : (Default)	-
RSC	RSC

Test Case 1 – Flat Plate

Test geometries

Two geometries have been investigated in both midplane and three-dimensional analyses. All parts were moulded from Rhodia Technyl C216V40 (40% glass filled Nylon)

2 and 4 mm thick flat plate,
40 mm wide 120 mm long
with a 1 and 2 mm thick fan
gate.



- how to set ci, dz, rsc

Midplane Analysis – Folgar-Tucker (2mm plate)

- Various c_i values have been tested and compared to experimental fibre orientation data at both locations. $c_i = 0.03$ was found to be optimum.

table of c_i values
fixed $dz=1$

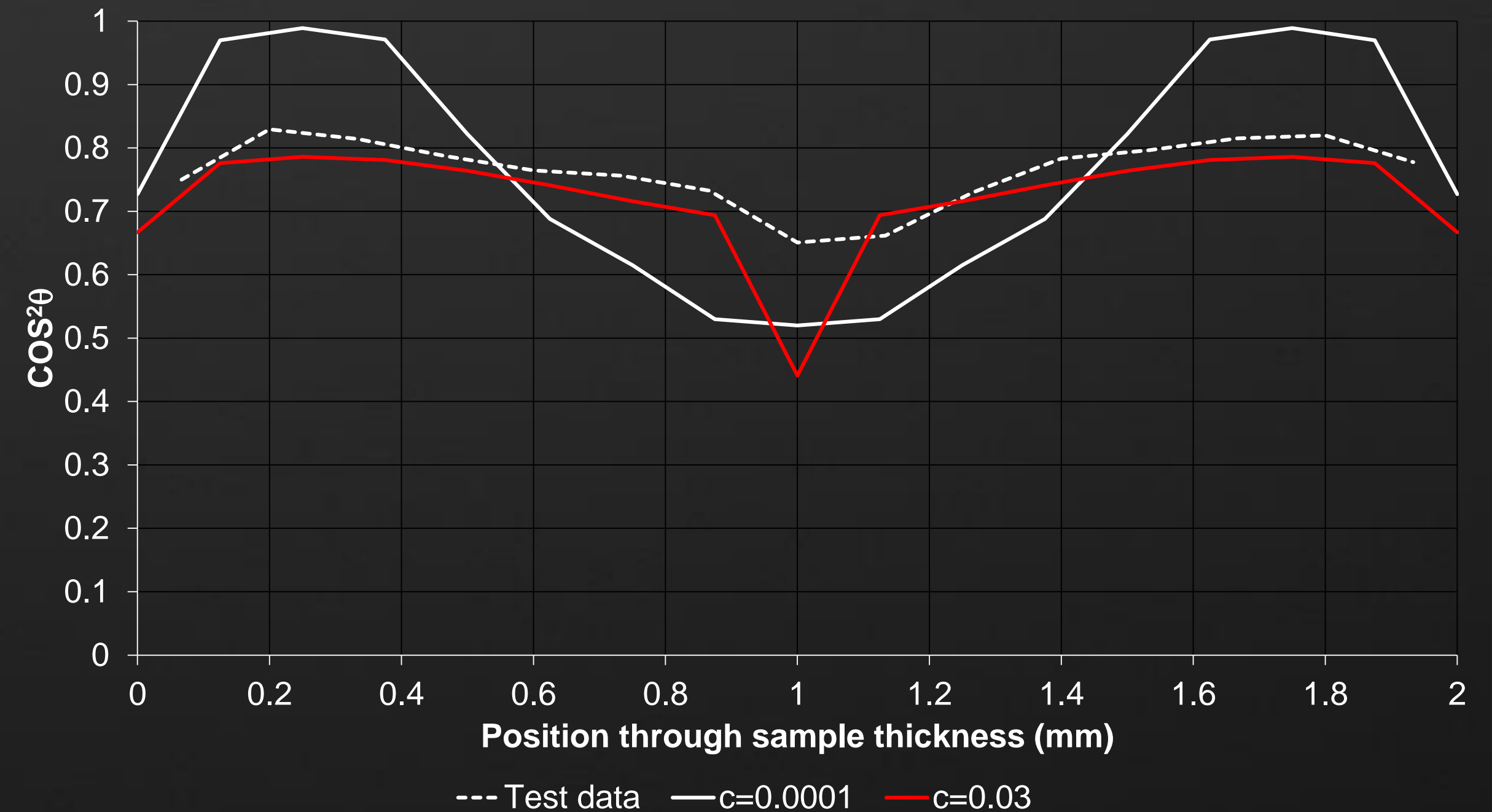
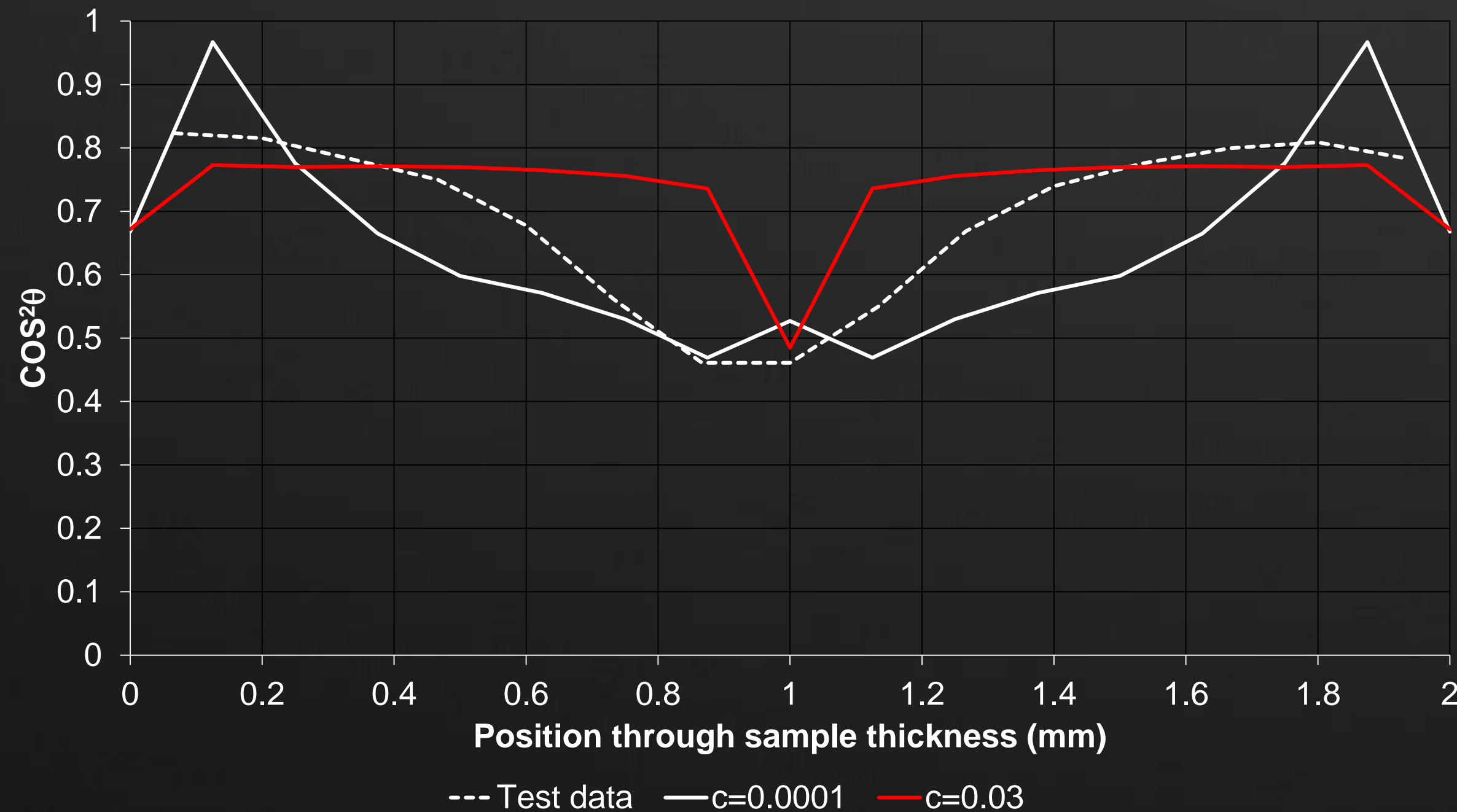
insert video c_i step dance

Location A

Location B

Midplane Analysis – Folgar-Tucker (2mm plate)

- Various c_i values have been tested and compared to experimental fibre orientation data at both locations. $c_i = 0.03$ was found to be optimum.



Location A

Location B

Midplane Analysis – Folgar-Tucker (2mm plate)

- Various c_i values have been tested and compared to experimental fibre orientation data at both locations. $c_i = 0.03$ was found to be optimum.

insert Moldflow default

Location A

Location B

Midplane Analysis – Folgar-Tucker (2mm plate)

- Various c_i values have been tested and compared to experimental fibre orientation data at both locations. $c_i = 0.03$ was found to be optimum.

table of dz values
fixed $c_i = ?$

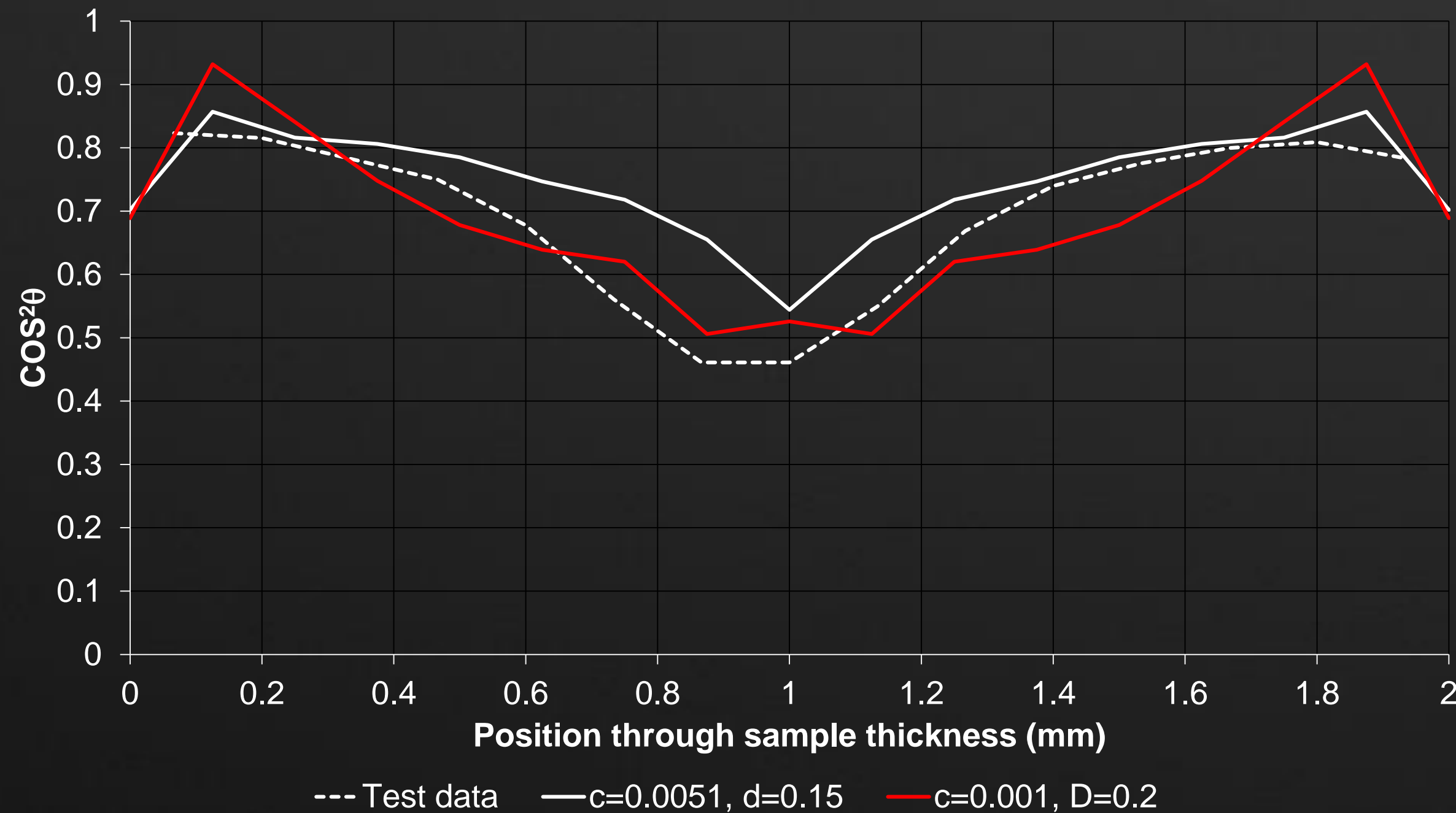
insert video Dz step dance

Location A

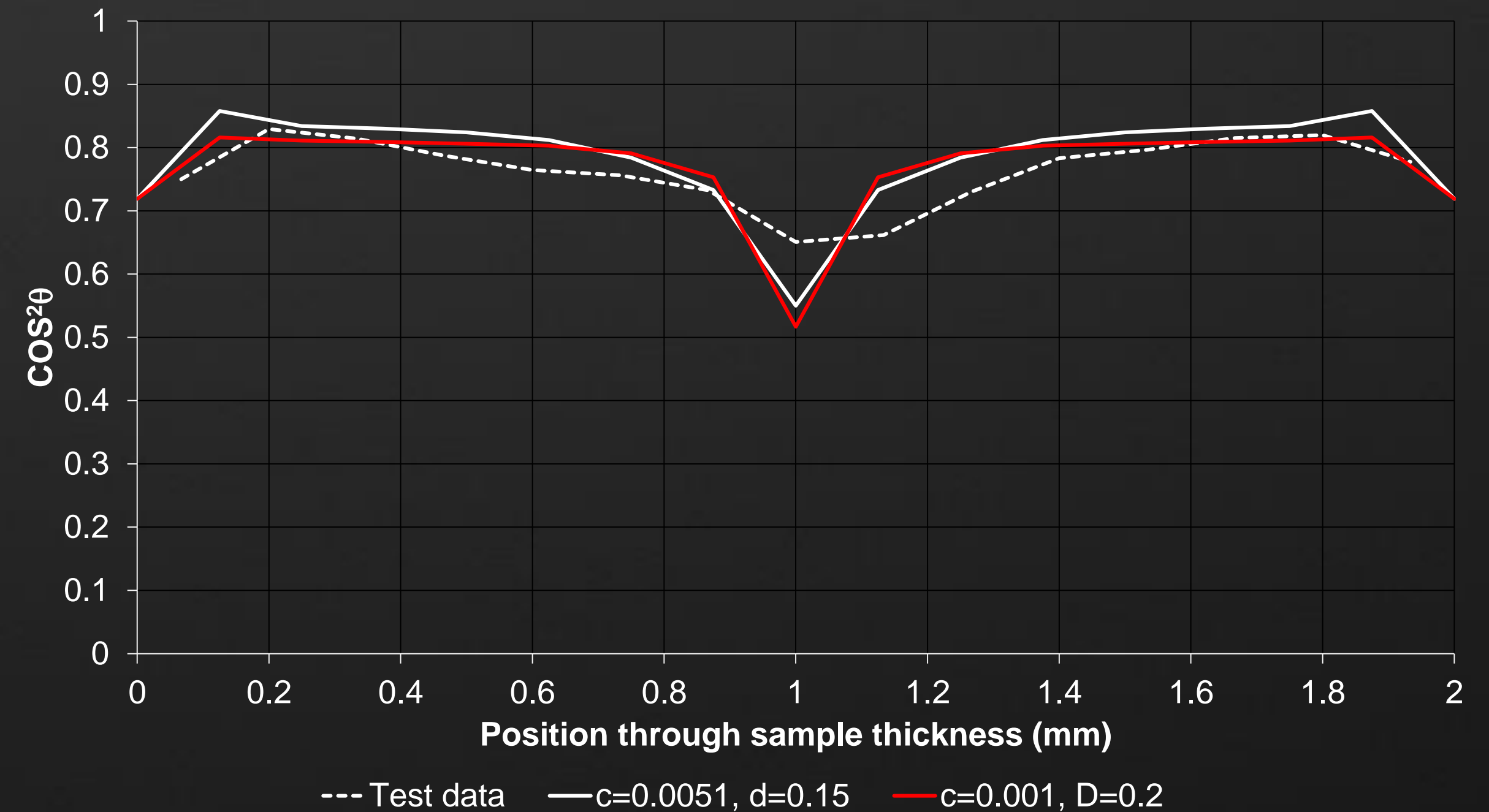
Location B

Midplane Analysis – modified Folgar-Tucker (2mm plate)

- Combinations of D_z and c_i were also trialed and found to significantly improve fibre orientation predictions compared to the unmodified case.



Location A



Location B

Midplane Analysis – Folgar-Tucker (2mm plate)

- Various c_i values have been tested and compared to experimental fibre orientation data at both locations. $c_i = 0.03$ was found to be optimum.

insert Moldflow default

Location A

Location B

Midplane Analysis – Folgar-Tucker (2mm plate)

- Various c_i values have been tested and compared to experimental fibre orientation data at both locations. $c_i = 0.03$ was found to be optimum.

table of RSC values
fixed $c_i = ?$

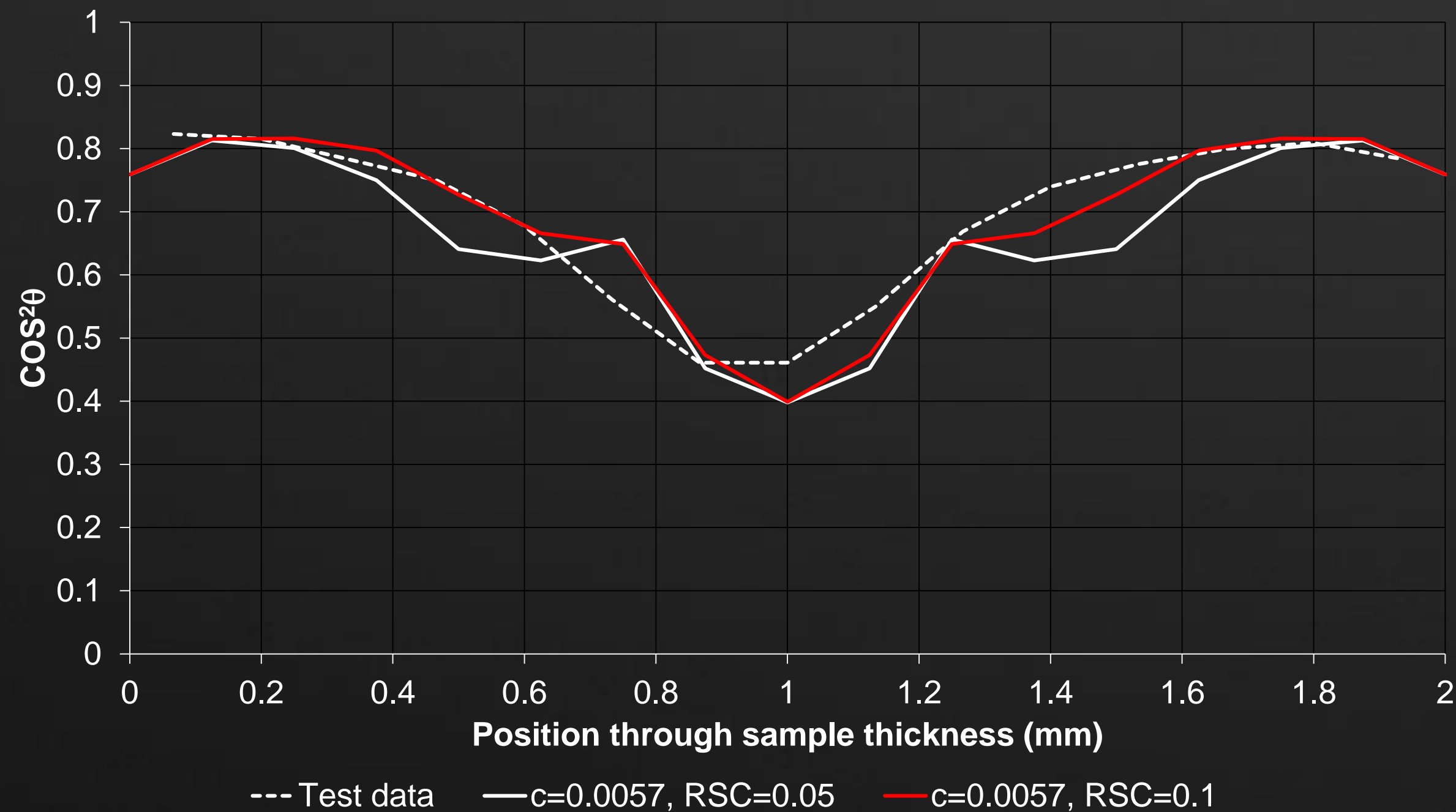
insert video RSC step dance

Location A

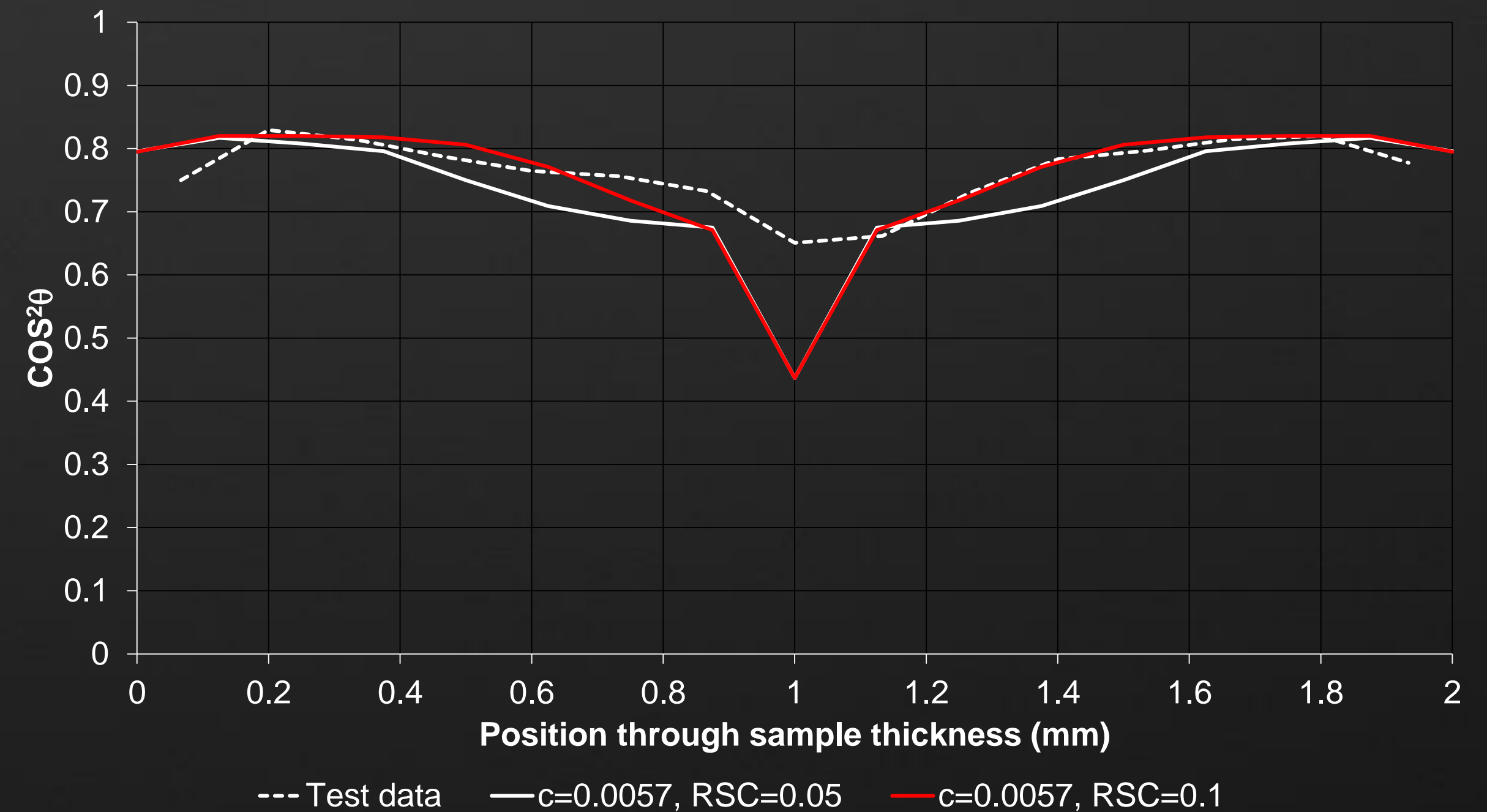
Location B

Midplane Analysis – RSC (2mm plate)

- The RSC analysis was found to closely predict measured fibre orientation with a c_i value of 0.057 and RSC of 0.05.



Location A



Location B

Midplane Analysis – Folgar-Tucker (2mm plate)

- Various c_i values have been tested and compared to experimental fibre orientation data at both locations. $c_i = 0.03$ was found to be optimum.

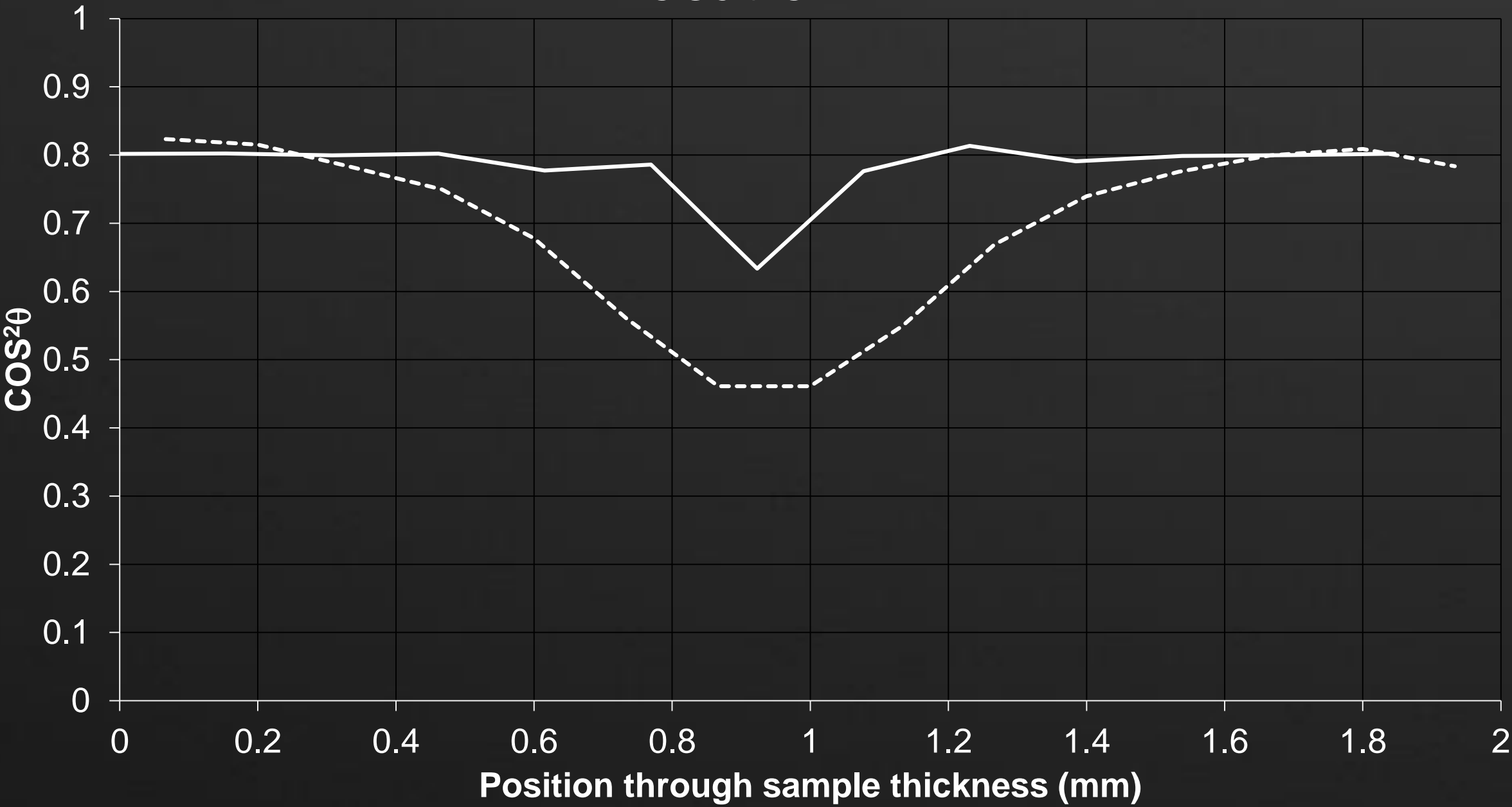
insert Moldflow default

Location A

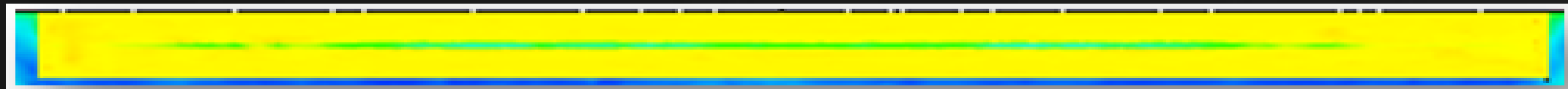
Location B

Three-Dimensional Analysis – Folgar-Tucker (2mm)

Location A

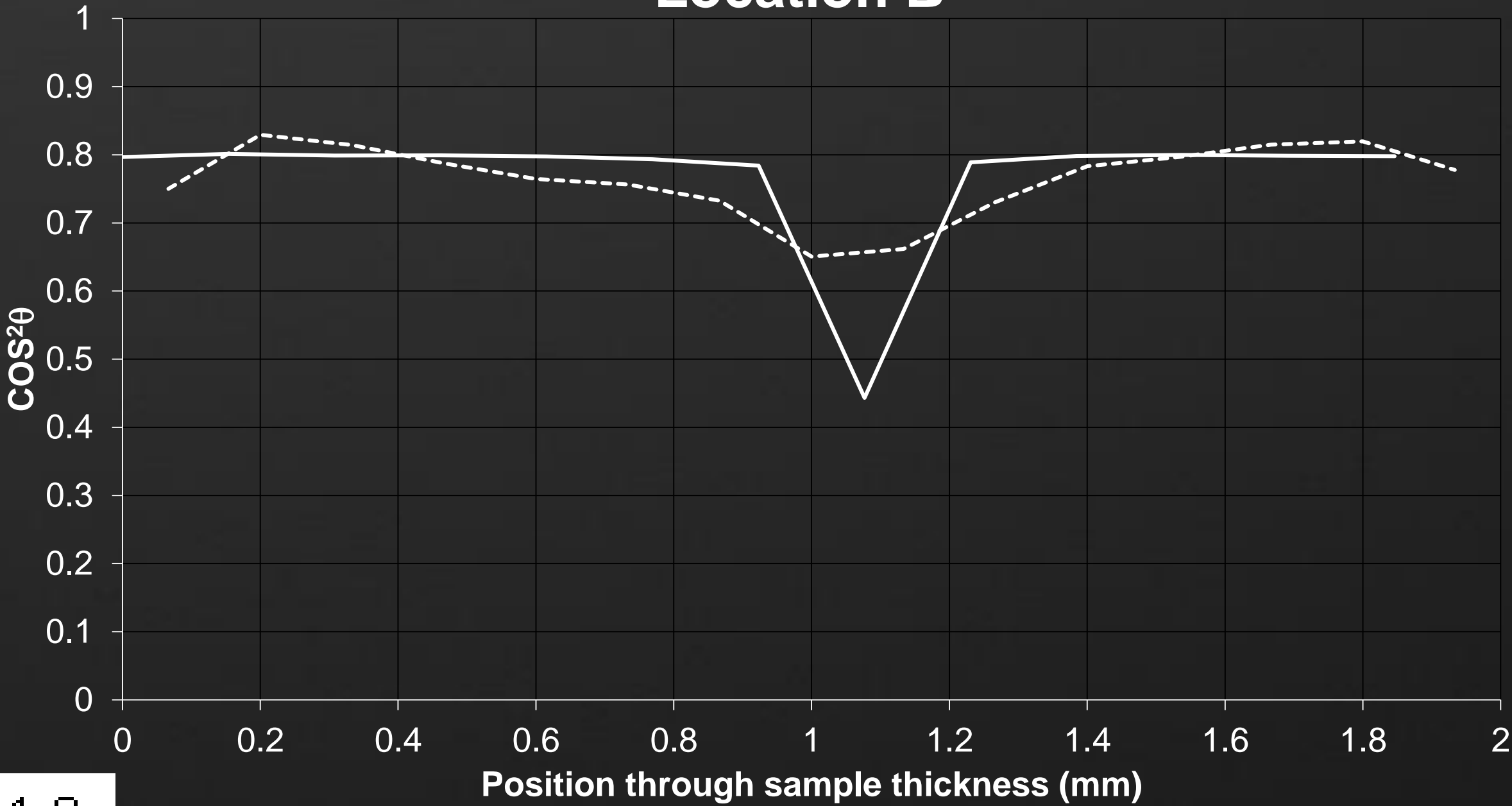


--- Test data

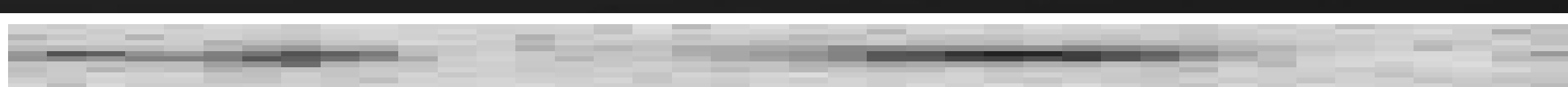


$c_i=0.03$

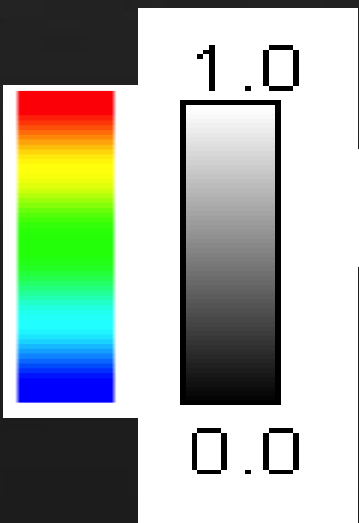
Location B



--- Test data

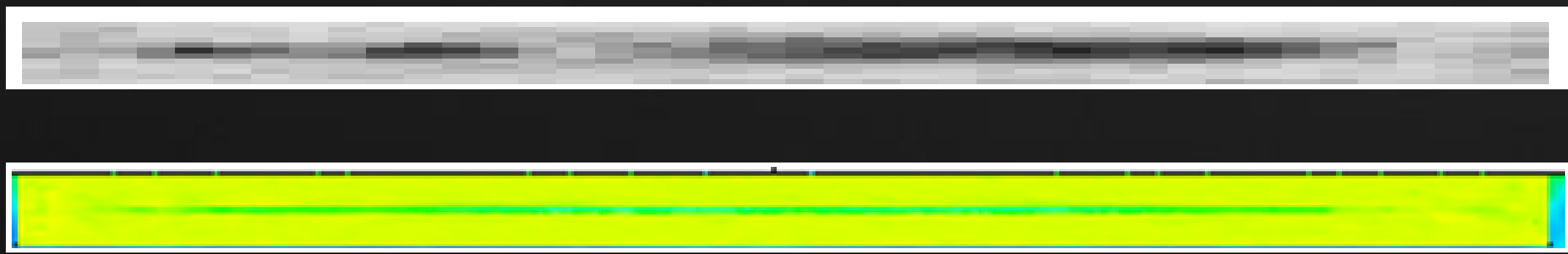
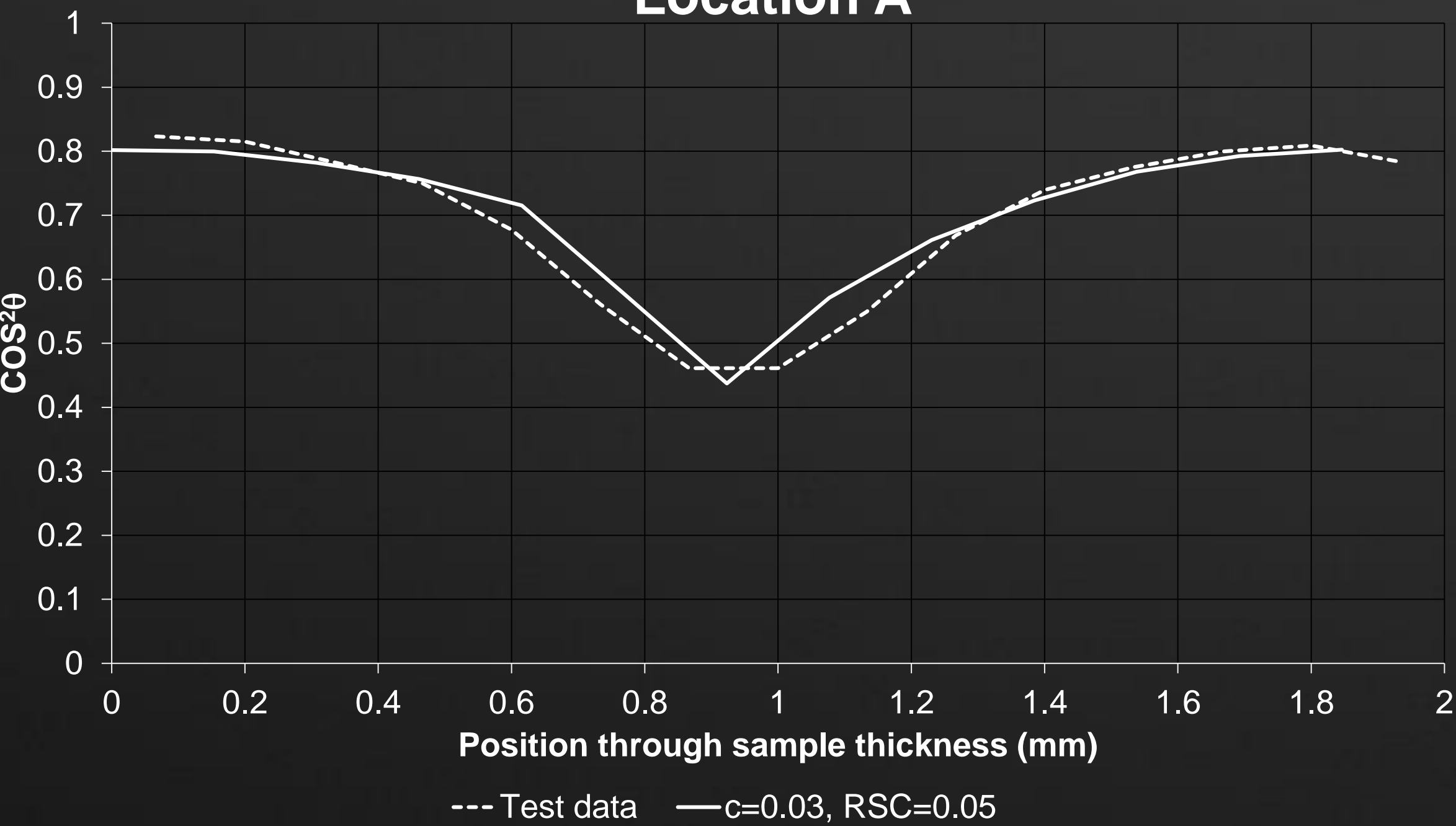


$c_i=0.03$



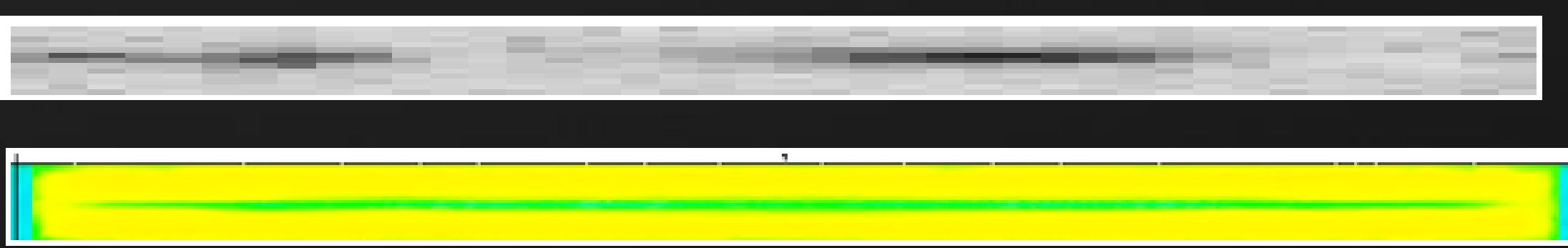
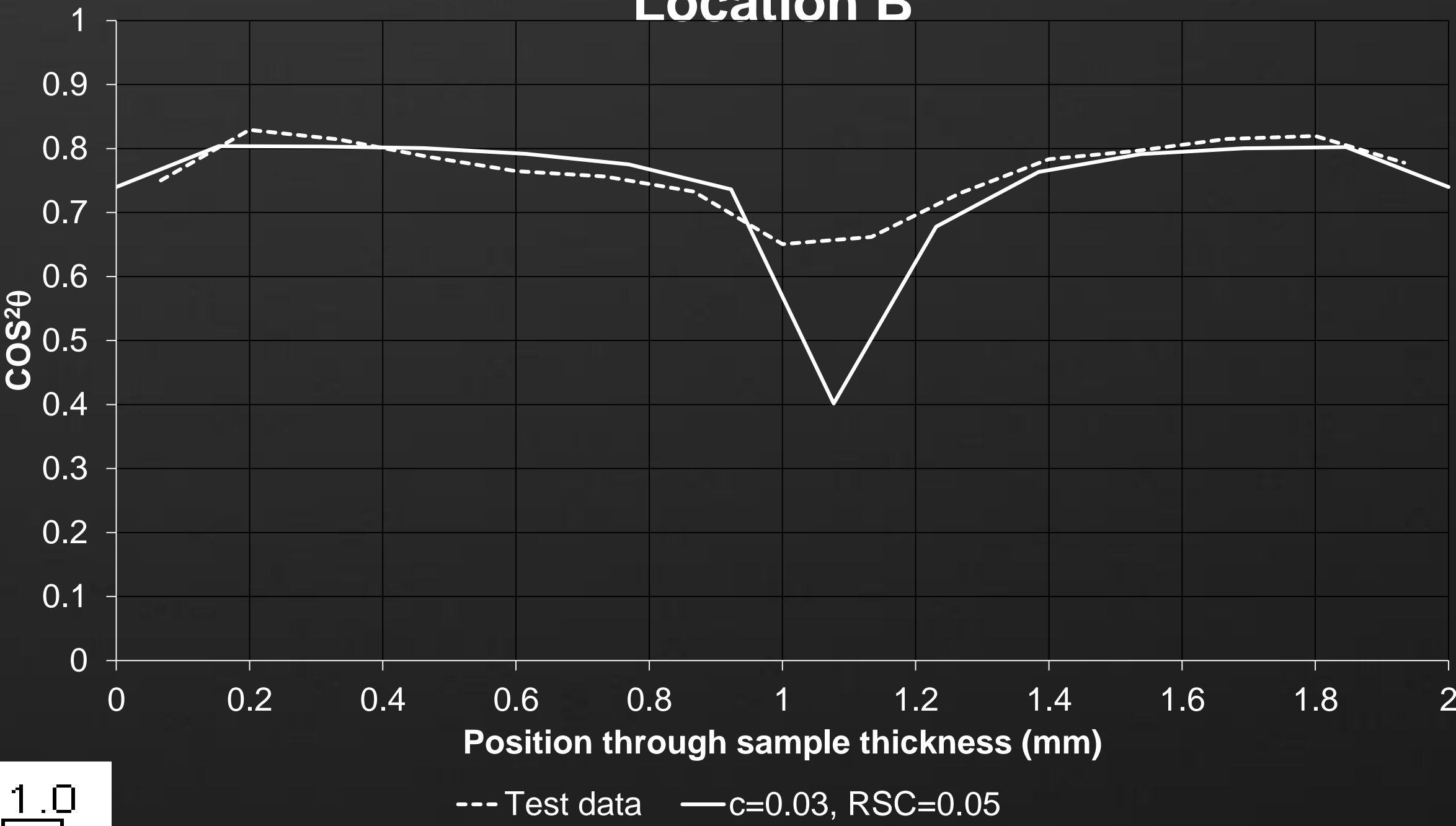
Three-Dimensional Analysis – RSC (2mm)

Location A



$c_i=0.03$, $\text{RSC}=0.05$

Location B

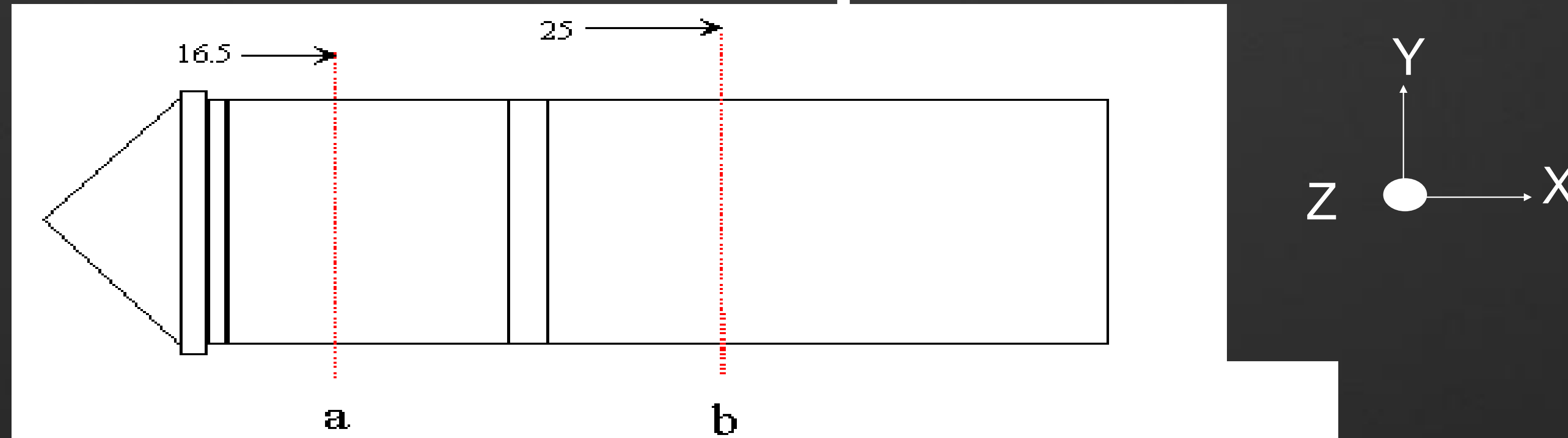


$c_i=0.03$, $\text{RSC}=0.05$

Effect on Final Product Properties

EXPERIMENTAL STUDIES

FOD characterisation: Ribbed plate

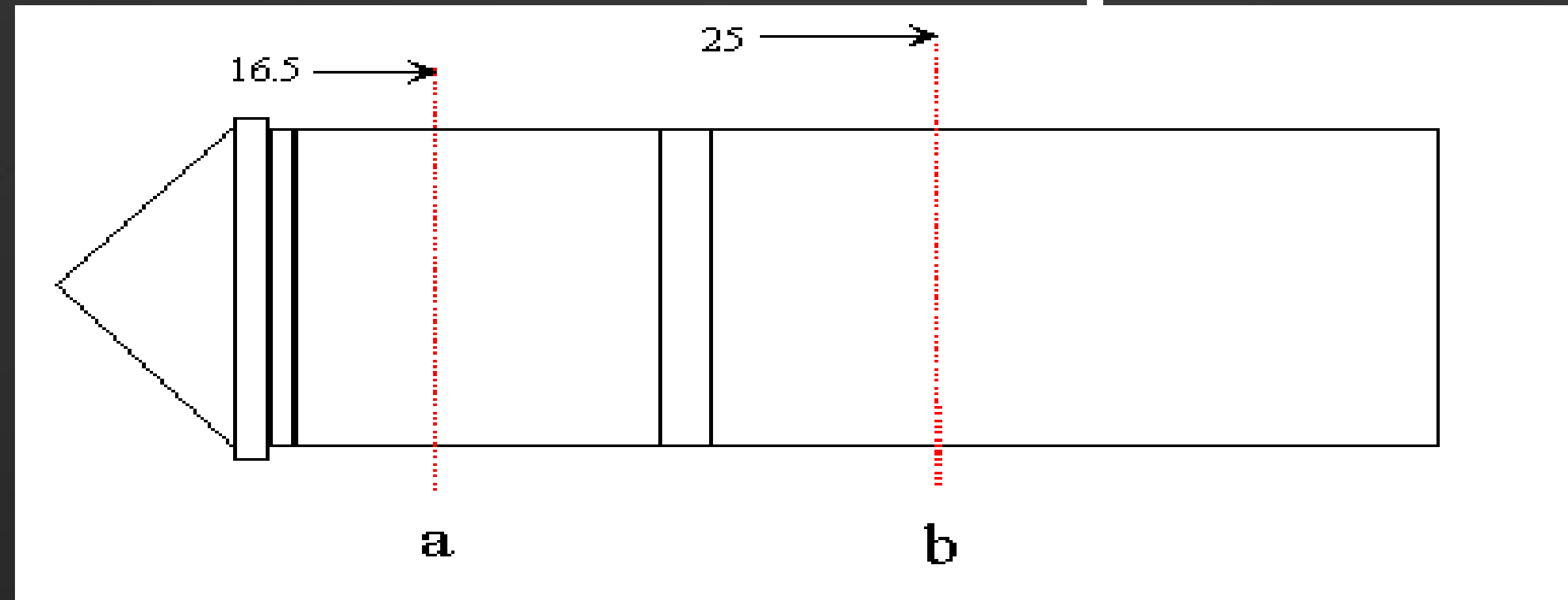


	E_{xx}	E_{yy}
Position a	5.28 ± 0.08	5.00 ± 0.17
Position b	6.46 ± 0.19	3.96 ± 0.17

- Differences in the FOD structures at the two positions lead to a significant difference in elastic properties at the two positions.

EXPERIMENTAL STUDIES

FOD characterisation: Ribbed plate



	Sample 1	Sample 2	Sample 3	Average
E_{XX}	5.35	5.20	5.30	5.28 ± 0.08
E_{YY}	5.20	4.90	4.90	5.00 ± 0.17
E_{ZZ}	2.15	2.15	2.15	2.15

- Maximum random error (<5%) similar to measurement error.
- If parts are made under carefully controlled processing conditions then the FOD (and hence mechanical properties) should be very similar

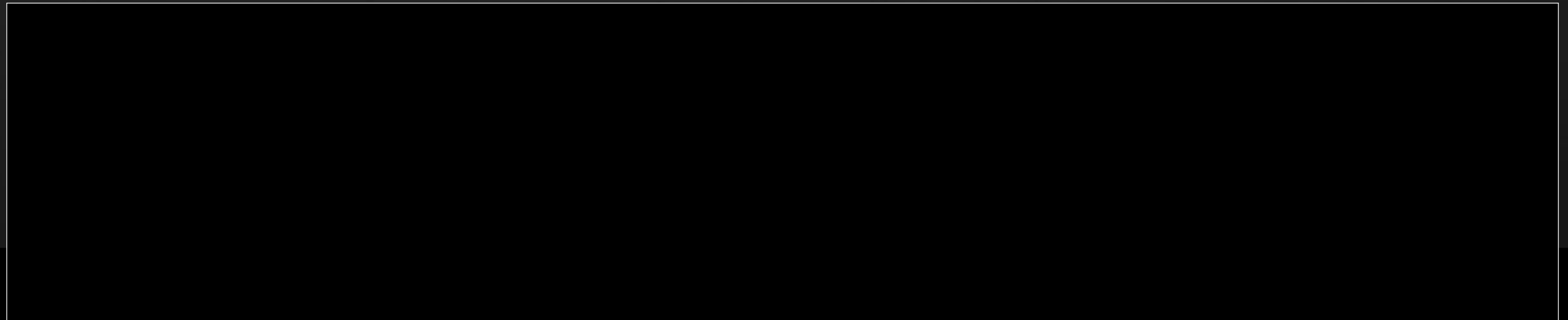
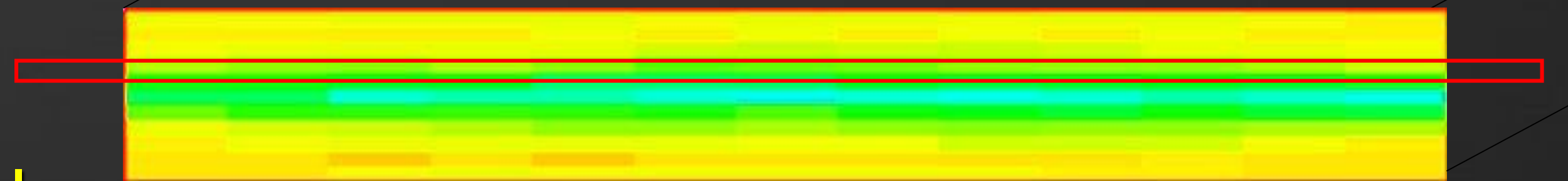
Finite Element Material Model

Experimentally determined FOD translation

FOD measurements were averaged into 11 laminates through the sample thickness, for locations A and B

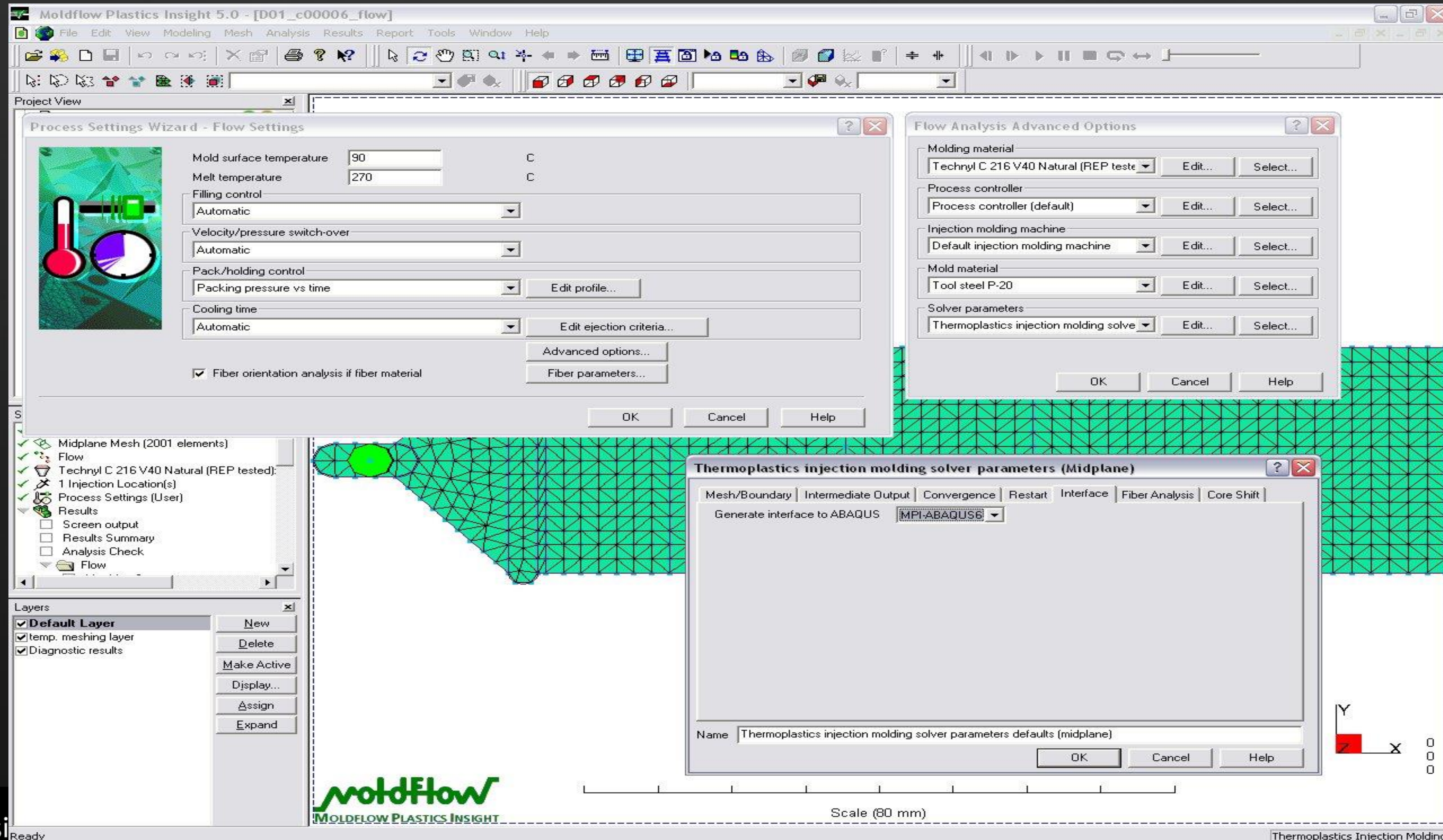
Using the Tandon-Weng model the modulus of the matrix and glass along with 2nd and 4th order orientation tensor allowed the construction of a simplified experimentally determined material model. This has been implemented as a composite lamina shell within ABAQUS

Location B FOD



Finite Element Material Model

Direct translation from numerical predictions



Finite Element Material Model

Direct translation from numerical predictions

Moldflow MPI 5.0 and ABAQUS 6.3 Translator

Two output files are created during the translation

- .pat file defines the finite element mesh

- .osp file describes material properties and residual stresses. Material property data includes elastic and thermal expansion coefficients for each element. For fibre filled materials elastic moduli are given in terms of lamina composite shell material constants oriented in terms of elemental principal directions.

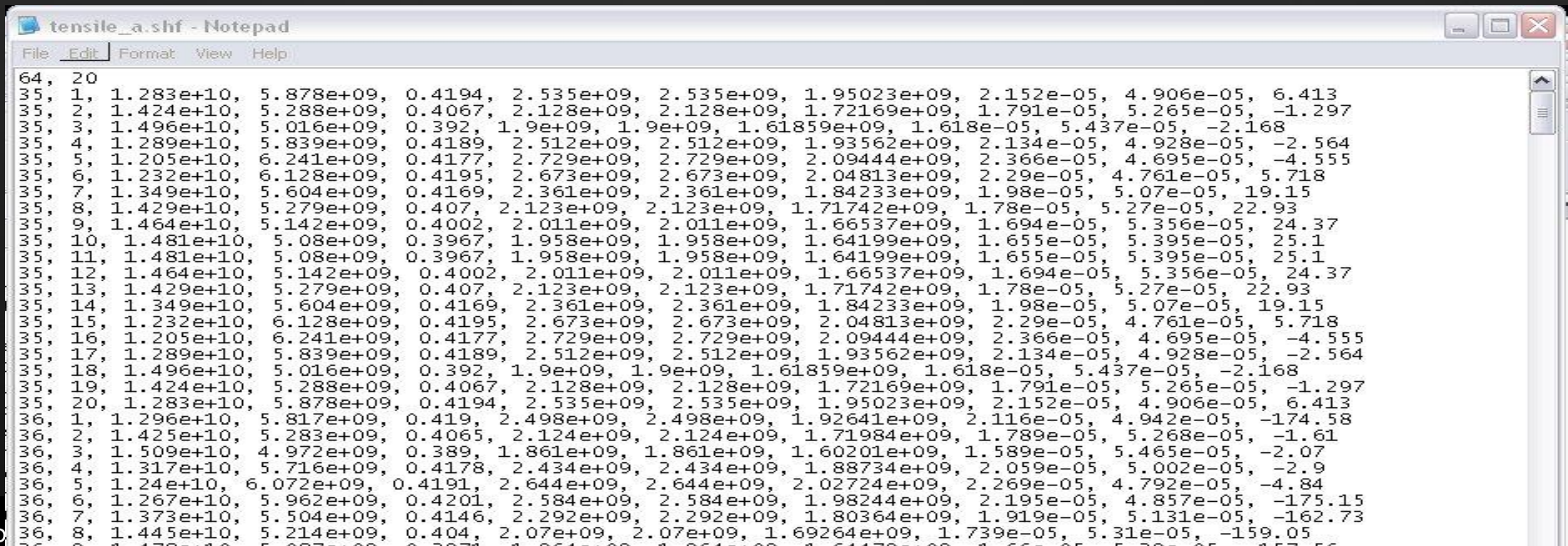
An additional ABAQUS interface (ABAQUS MOLDFLOW) is required to interpret .pat and .osp files

Users are also required to provide composite material property selections ranging from the closure approximation model (Orthotropic 3), thermal expansion coefficient model (Chamberlain) and micro-mechanics model (Tandon-Weng)

Finite Element Material Model

Direct translation from numerical predictions

Translated material properties are described in terms of laminates (20) for each element. Each data set defines the element number, layer identifier, moduli in the two principal elemental directions, poisson's ratio, bulk moduli, principal thermal expansion coefficients and fibre (material) angle



```
tensile_a.shf - Notepad
File Edit Format View Help
64, 20
35, 1, 1.283e+10, 5.878e+09, 0.4194, 2.535e+09, 2.535e+09, 1.95023e+09, 2.152e-05, 4.906e-05, 6.413
35, 2, 1.424e+10, 5.288e+09, 0.4067, 2.128e+09, 2.128e+09, 1.72169e+09, 1.791e-05, 5.265e-05, -1.297
35, 3, 1.496e+10, 5.016e+09, 0.392, 1.9e+09, 1.9e+09, 1.61859e+09, 1.618e-05, 5.437e-05, -2.168
35, 4, 1.289e+10, 5.839e+09, 0.4189, 2.512e+09, 2.512e+09, 1.93562e+09, 2.134e-05, 4.928e-05, -2.564
35, 5, 1.205e+10, 6.241e+09, 0.4177, 2.729e+09, 2.729e+09, 2.09444e+09, 2.366e-05, 4.695e-05, -4.555
35, 6, 1.232e+10, 6.128e+09, 0.4195, 2.673e+09, 2.673e+09, 2.04813e+09, 2.29e-05, 4.761e-05, 5.718
35, 7, 1.349e+10, 5.604e+09, 0.4169, 2.361e+09, 2.361e+09, 1.84233e+09, 1.98e-05, 5.07e-05, 19.15
35, 8, 1.429e+10, 5.279e+09, 0.407, 2.123e+09, 2.123e+09, 1.71742e+09, 1.78e-05, 5.27e-05, 22.93
35, 9, 1.464e+10, 5.142e+09, 0.4002, 2.011e+09, 2.011e+09, 1.66537e+09, 1.694e-05, 5.356e-05, 24.37
35, 10, 1.481e+10, 5.08e+09, 0.3967, 1.958e+09, 1.958e+09, 1.64199e+09, 1.655e-05, 5.395e-05, 25.1
35, 11, 1.481e+10, 5.08e+09, 0.3967, 1.958e+09, 1.958e+09, 1.64199e+09, 1.655e-05, 5.395e-05, 25.1
35, 12, 1.464e+10, 5.142e+09, 0.4002, 2.011e+09, 2.011e+09, 1.66537e+09, 1.694e-05, 5.356e-05, 24.37
35, 13, 1.429e+10, 5.279e+09, 0.407, 2.123e+09, 2.123e+09, 1.71742e+09, 1.78e-05, 5.27e-05, 22.93
35, 14, 1.349e+10, 5.604e+09, 0.4169, 2.361e+09, 2.361e+09, 1.84233e+09, 1.98e-05, 5.07e-05, 19.15
35, 15, 1.232e+10, 6.128e+09, 0.4195, 2.673e+09, 2.673e+09, 2.04813e+09, 2.29e-05, 4.761e-05, 5.718
35, 16, 1.205e+10, 6.241e+09, 0.4177, 2.729e+09, 2.729e+09, 2.09444e+09, 2.366e-05, 4.695e-05, -4.555
35, 17, 1.289e+10, 5.839e+09, 0.4189, 2.512e+09, 2.512e+09, 1.93562e+09, 2.134e-05, 4.928e-05, -2.564
35, 18, 1.496e+10, 5.016e+09, 0.392, 1.9e+09, 1.9e+09, 1.61859e+09, 1.618e-05, 5.437e-05, -2.168
35, 19, 1.424e+10, 5.288e+09, 0.4067, 2.128e+09, 2.128e+09, 1.72169e+09, 1.791e-05, 5.265e-05, -1.297
35, 20, 1.283e+10, 5.878e+09, 0.4194, 2.535e+09, 2.535e+09, 1.95023e+09, 2.152e-05, 4.906e-05, 6.413
36, 1, 1.296e+10, 5.817e+09, 0.419, 2.498e+09, 2.498e+09, 1.92641e+09, 2.116e-05, 4.942e-05, -174.58
36, 2, 1.425e+10, 5.283e+09, 0.4065, 2.124e+09, 2.124e+09, 1.71984e+09, 1.789e-05, 5.268e-05, -1.61
36, 3, 1.509e+10, 4.972e+09, 0.389, 1.861e+09, 1.861e+09, 1.60201e+09, 1.589e-05, 5.465e-05, -2.07
36, 4, 1.317e+10, 5.716e+09, 0.4178, 2.434e+09, 2.434e+09, 1.88734e+09, 2.059e-05, 5.002e-05, -2.9
36, 5, 1.24e+10, 6.072e+09, 0.4191, 2.644e+09, 2.644e+09, 2.02724e+09, 2.269e-05, 4.792e-05, -4.84
36, 6, 1.267e+10, 5.962e+09, 0.4201, 2.584e+09, 2.584e+09, 1.98244e+09, 2.195e-05, 4.857e-05, -175.15
36, 7, 1.373e+10, 5.504e+09, 0.4146, 2.292e+09, 2.292e+09, 1.80364e+09, 1.919e-05, 5.131e-05, -162.73
36, 8, 1.445e+10, 5.214e+09, 0.404, 2.07e+09, 2.07e+09, 1.69264e+09, 1.739e-05, 5.31e-05, -159.05
```


Finite Element Material Model

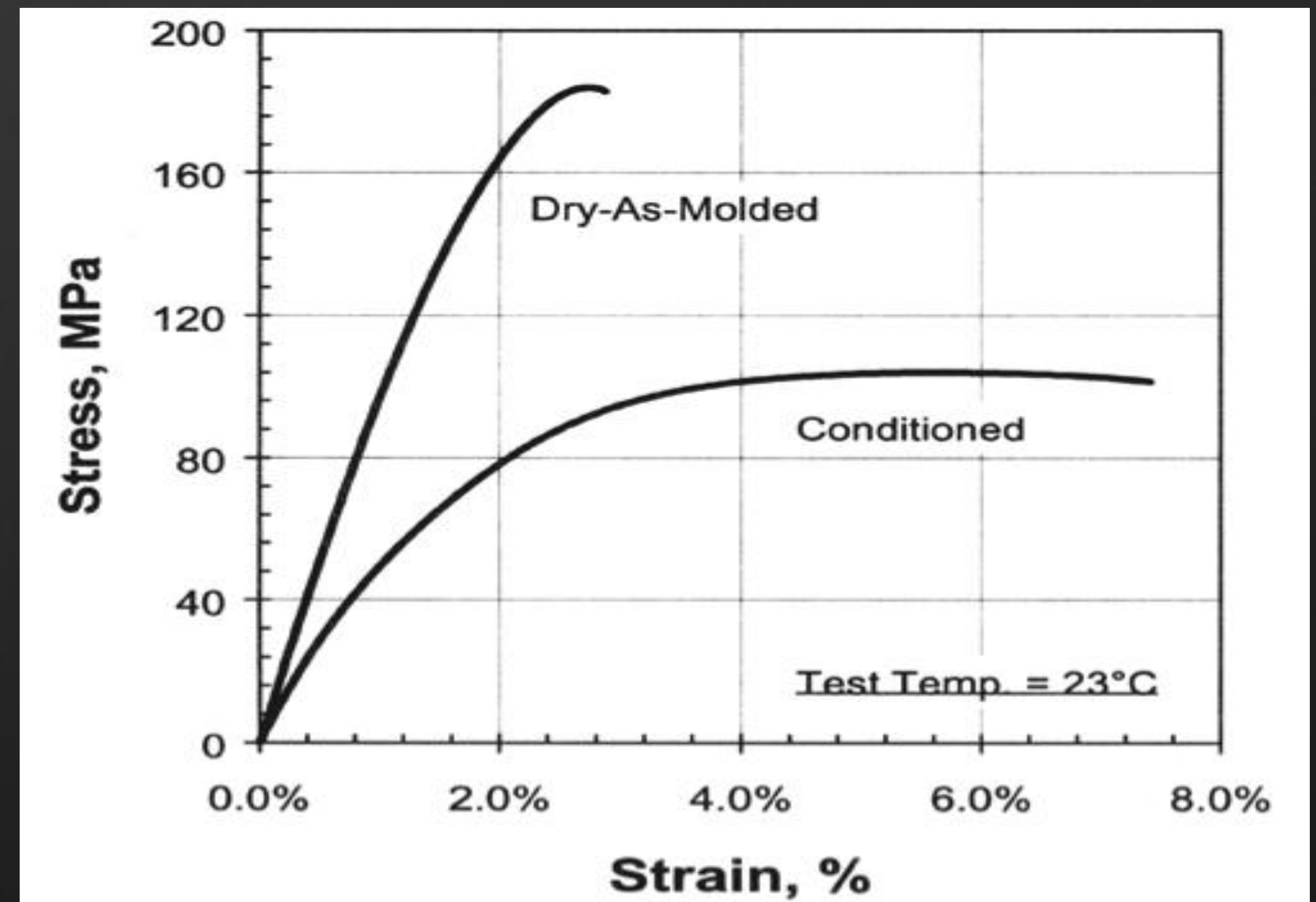
Adjustments due to material behaviour

Matrix material properties employed during Moldflow MPI 5.0 to ABAQUS conversion were based upon 'dry as moulded' modulus, room temperature and zero humidity

Material manufacturer supplies two values for modulus based on environmental conditions which can have a significant effect on final product performance

Room temp, 0% humidity
E - 2800 MPa

Room temp, 50% humidity



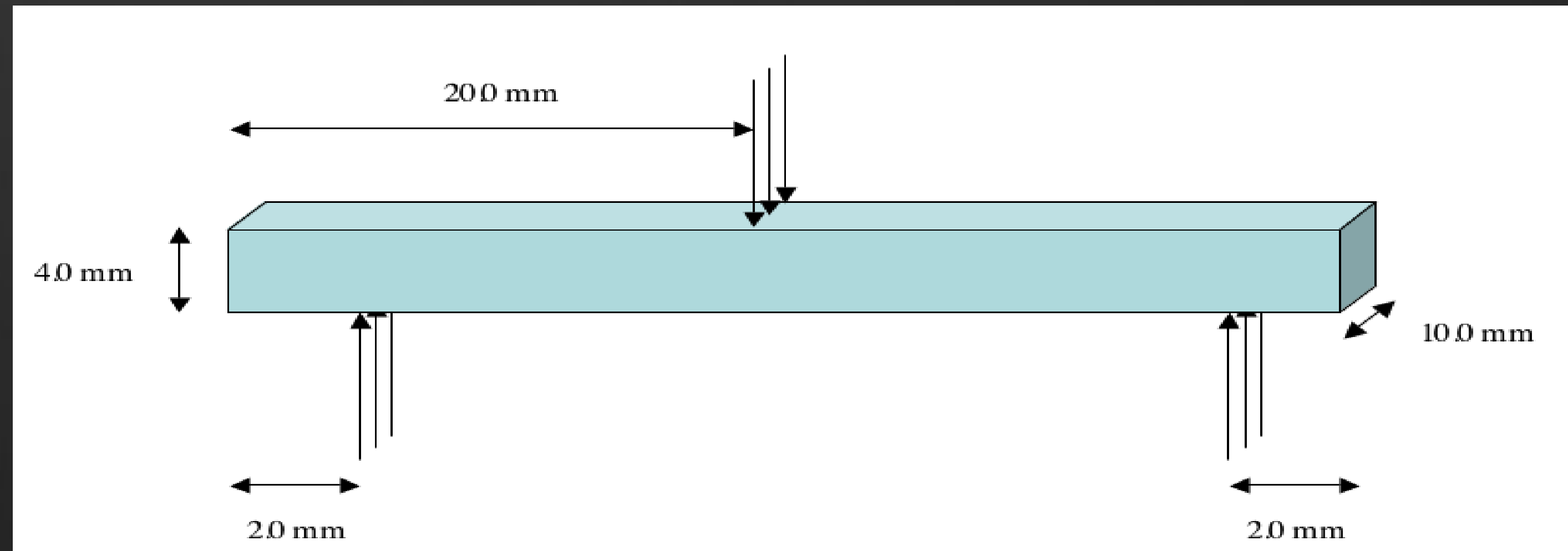
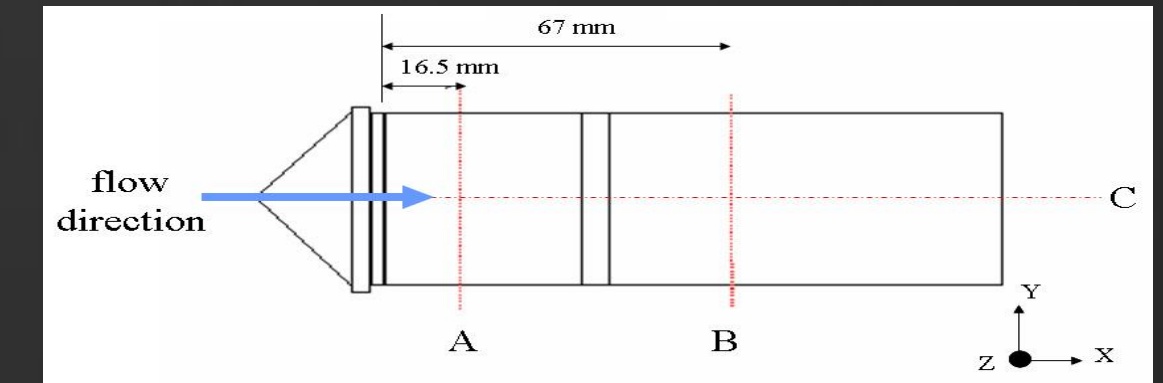
Load Case 1

Three point bending

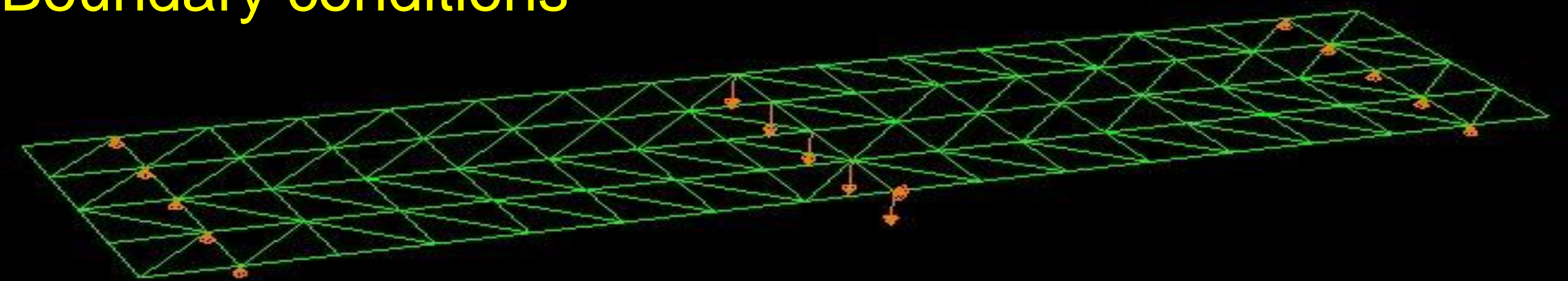
Three point bend tests were initially used to determine the validity of composite material models

10 mm wide sections taken from locations A and B were subjected to 1 mm imposed central displacement

Reaction forces experienced during experimental and finite element analysis were compared for the three material cases.

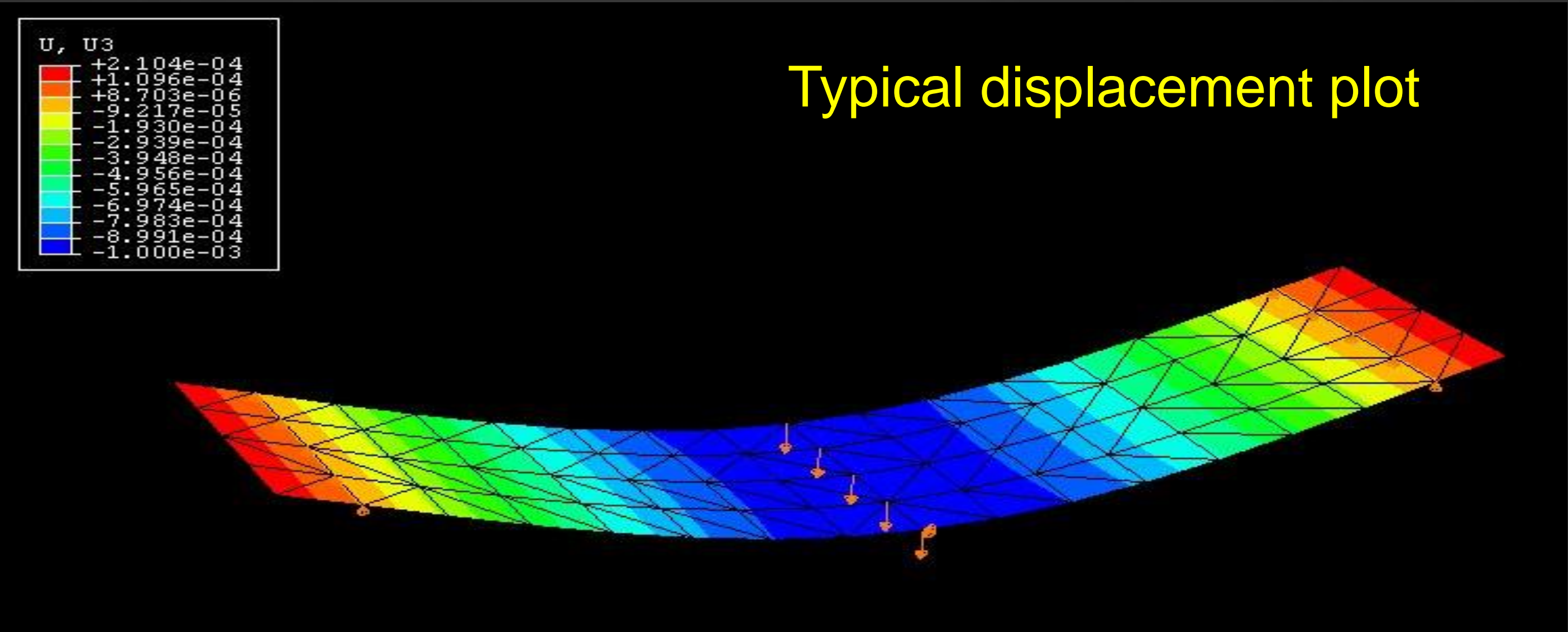


Boundary conditions



Load Case 1

Three point bending



	Experimental	FE model using Moldflow FOD	FE model using adjusted material data	FE model using measured FOD
Location A	162 N	437 N	330 N	193
Location B	127 N	361 N	266 N	155 N

Load Case 2

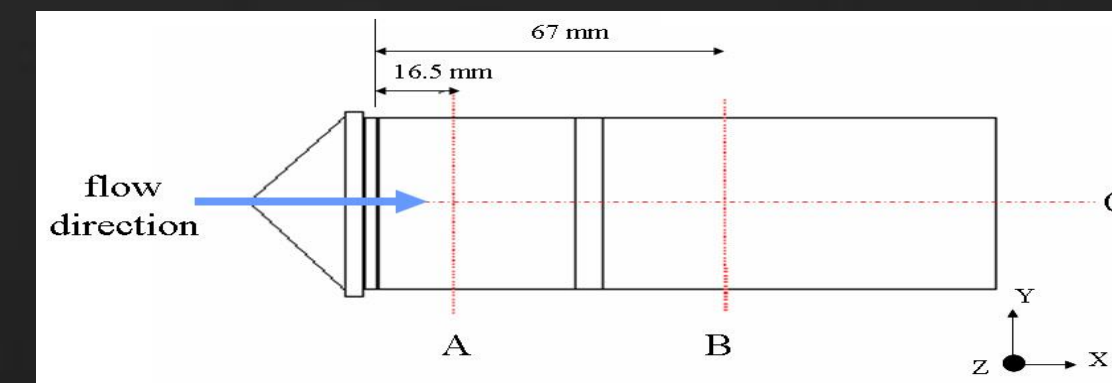
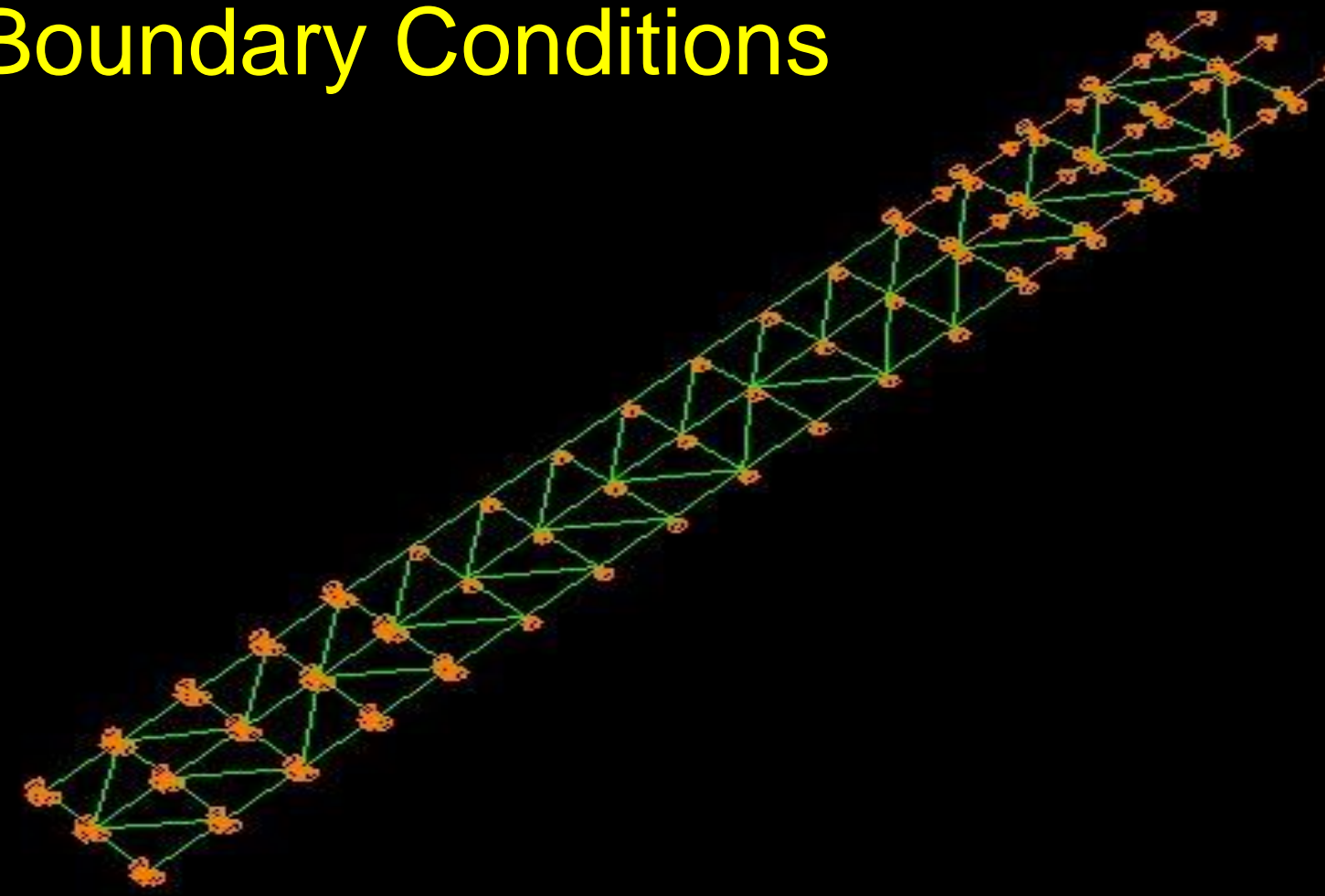
Tensile

Tensile tests were used to determine the validity of composite material models

5.0 mm wide sections taken from locations A and B were subjected to 5 mm imposed tensile displacement 10 mm from the outside edge. The base of the sample was constrained in the vertical direction.

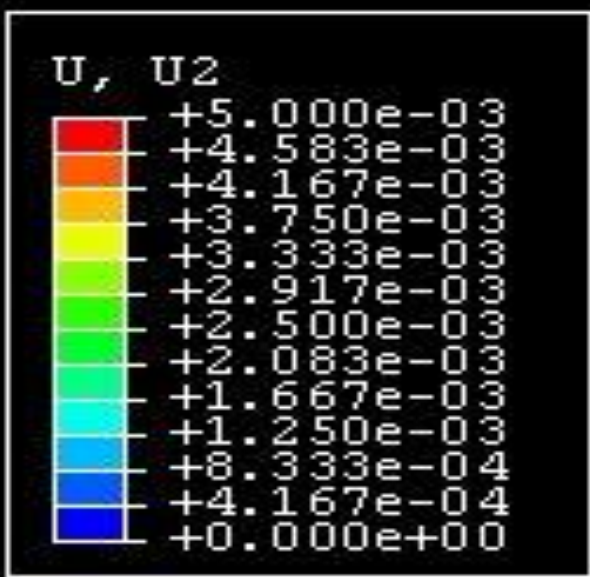
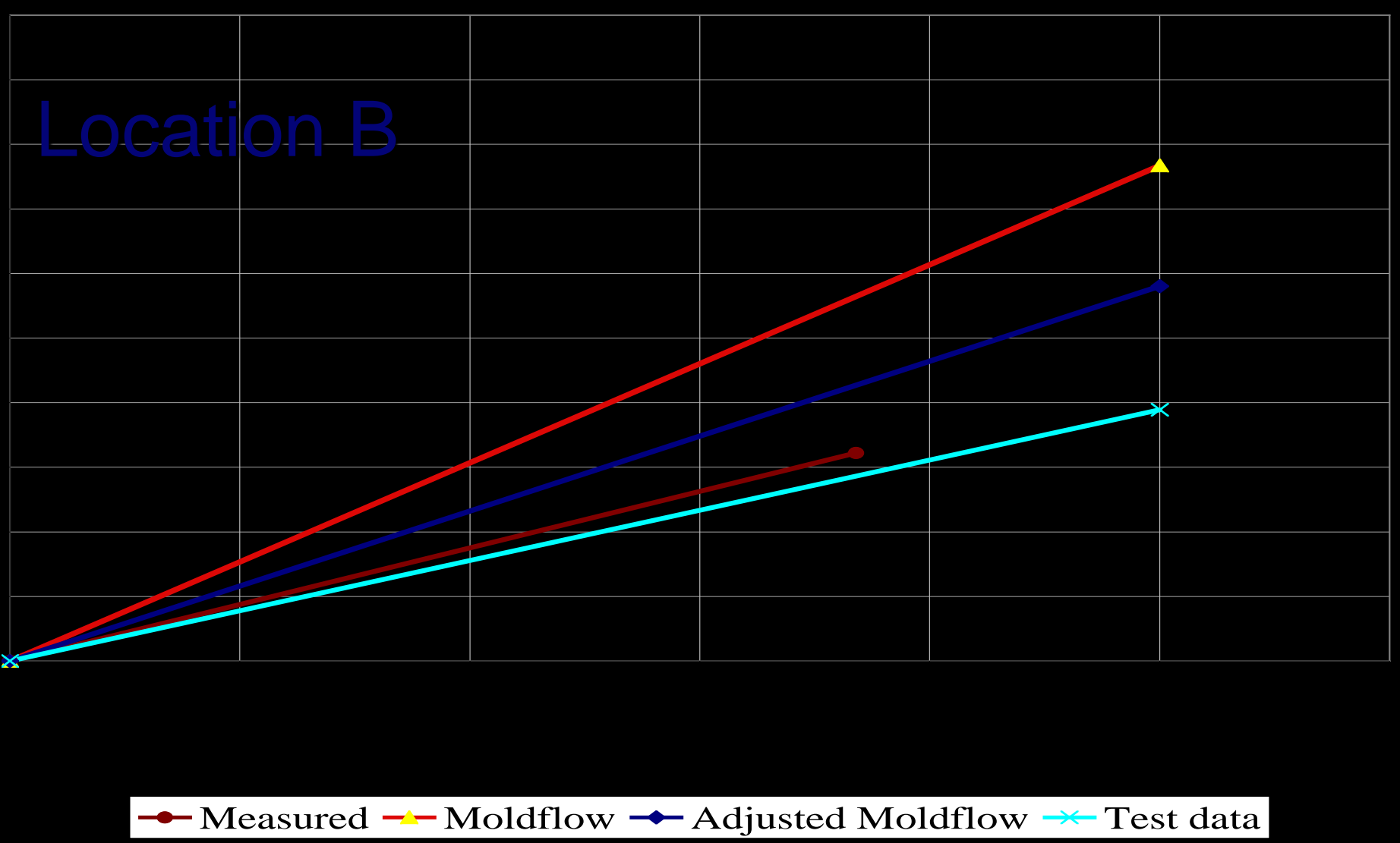
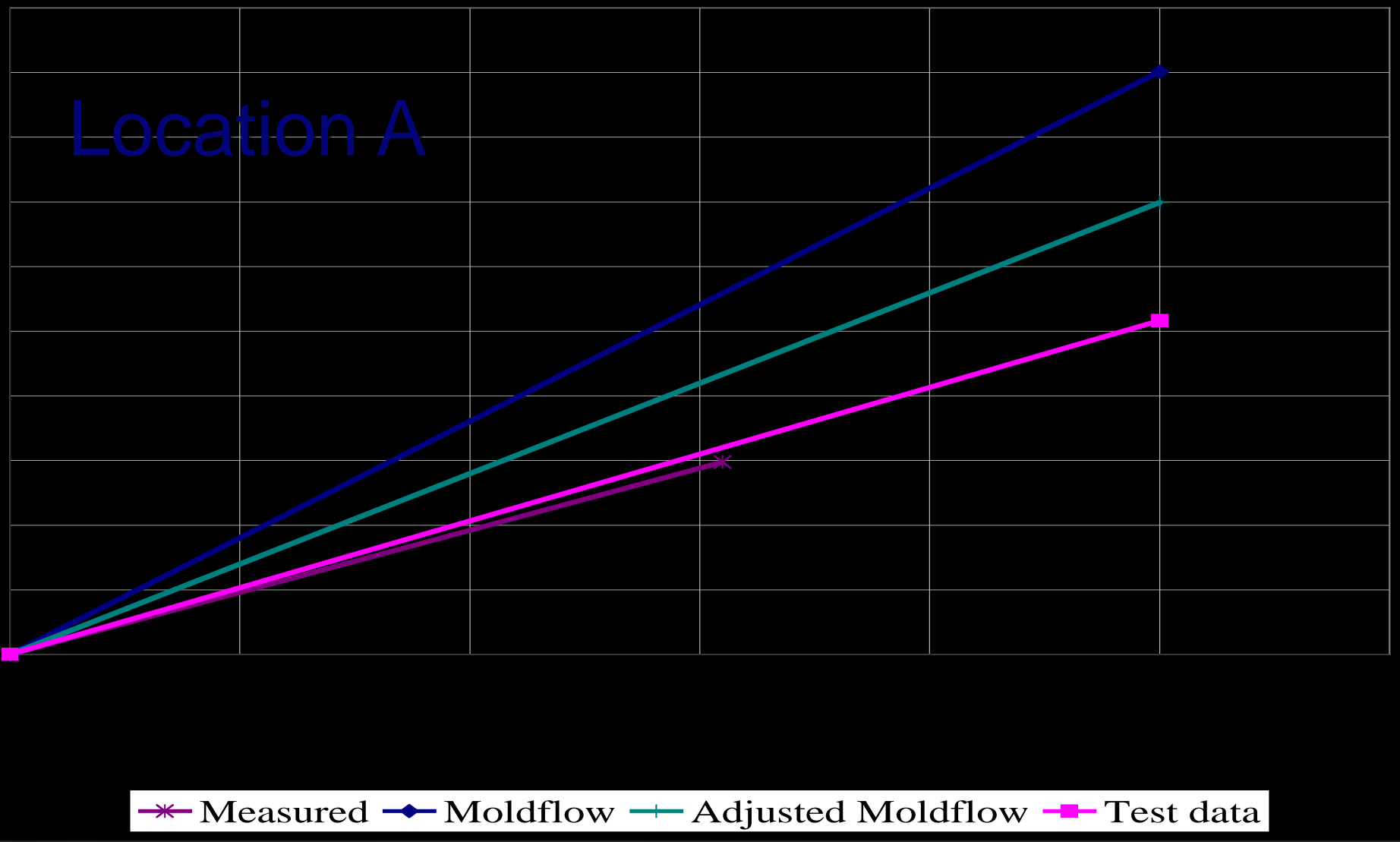
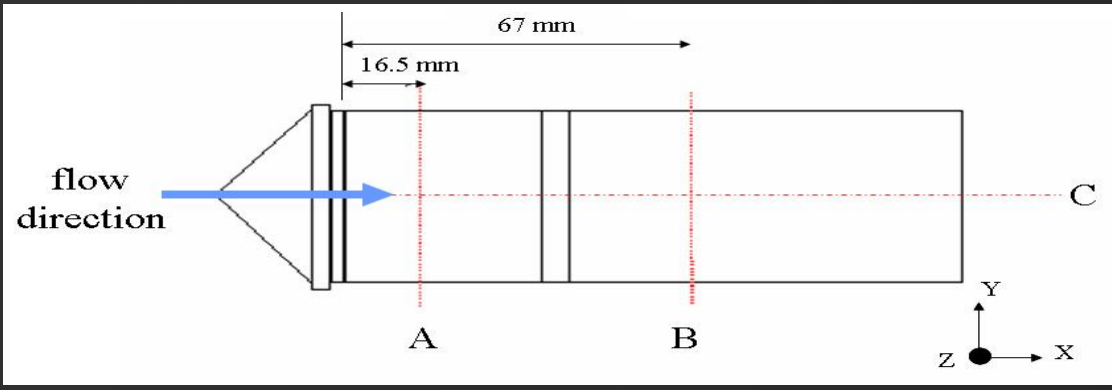
Reaction forces experienced during experimental and finite element analysis were compared for the three material cases.

Boundary Conditions

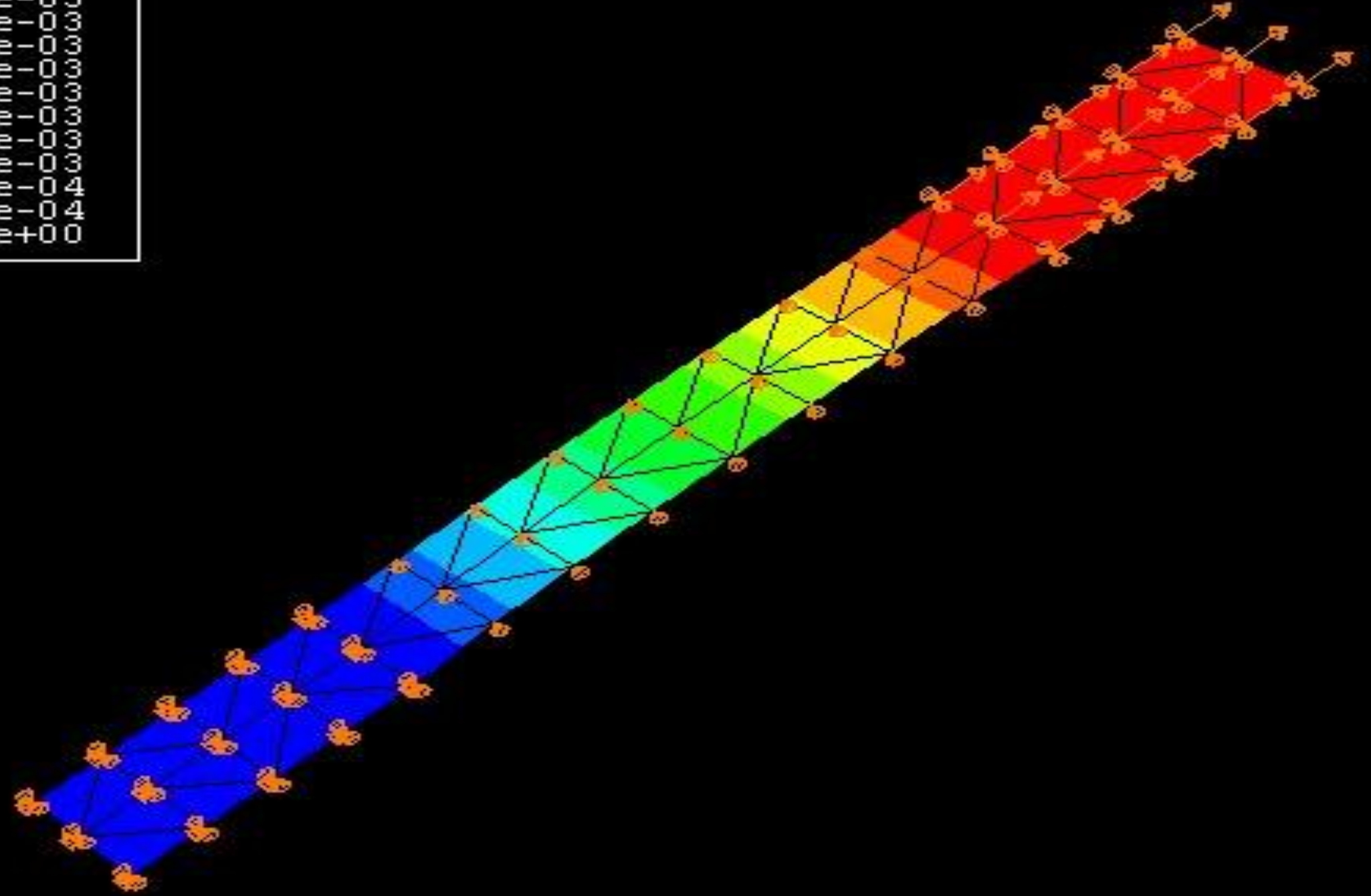


Load Case 2

Tensile



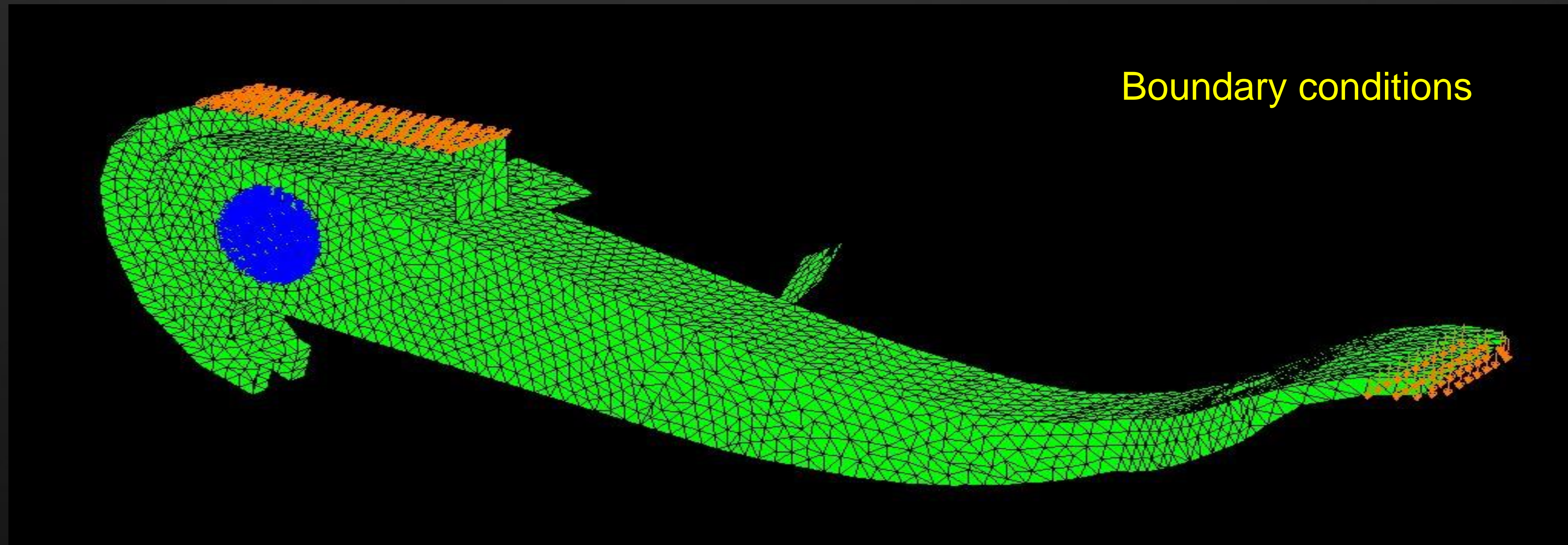
Typical displacement plot



Commercial Application

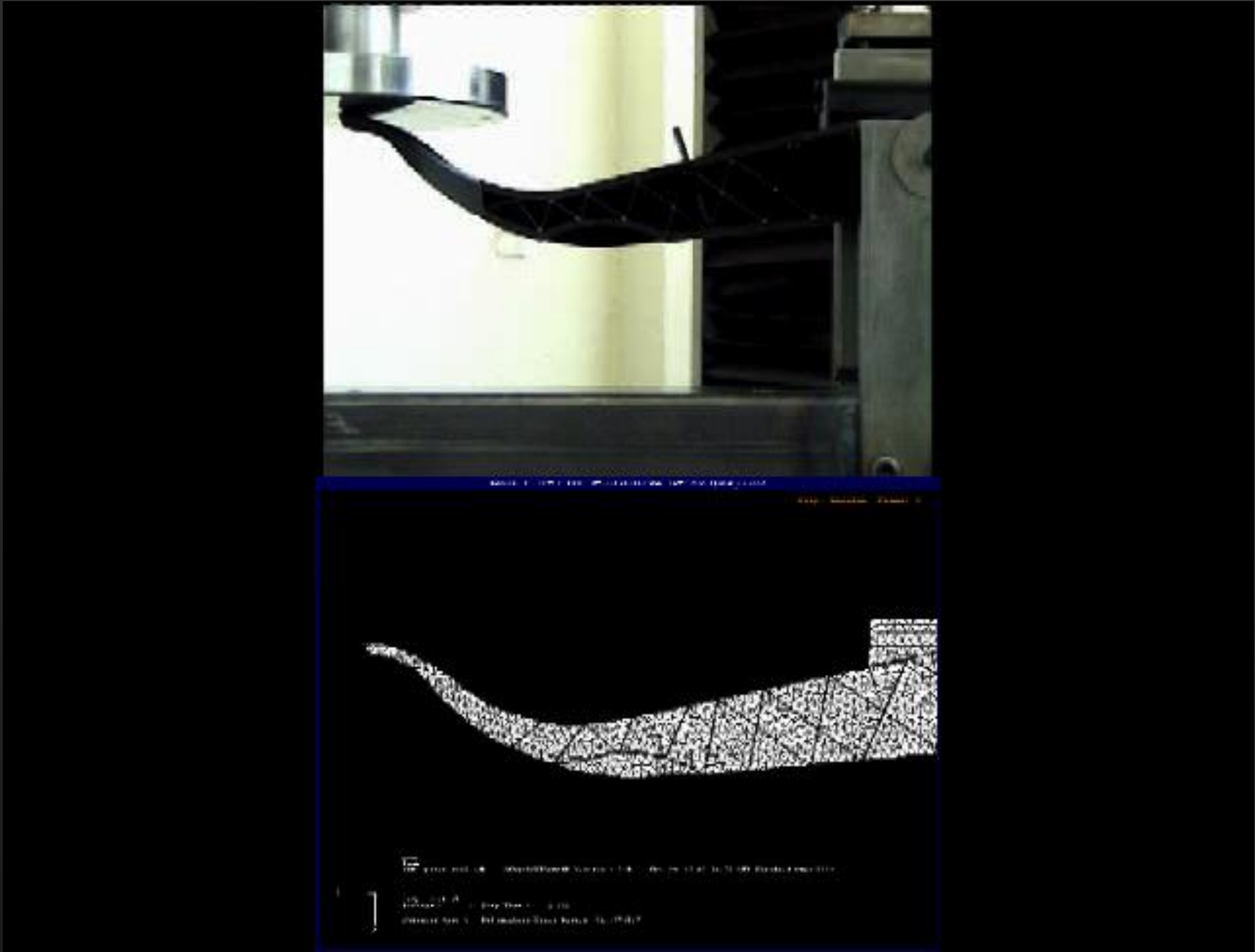
Automotive pedal

An automotive pedal was moulded from 40 % Rhodia Technyl C216 V40, (40% w/w glass filled nylon). As with the three-point bend test and tensile investigations the pedal was analysed using Moldflow MPI 5.0 and ABAQUS.



Commercial Application

Automotive pedal



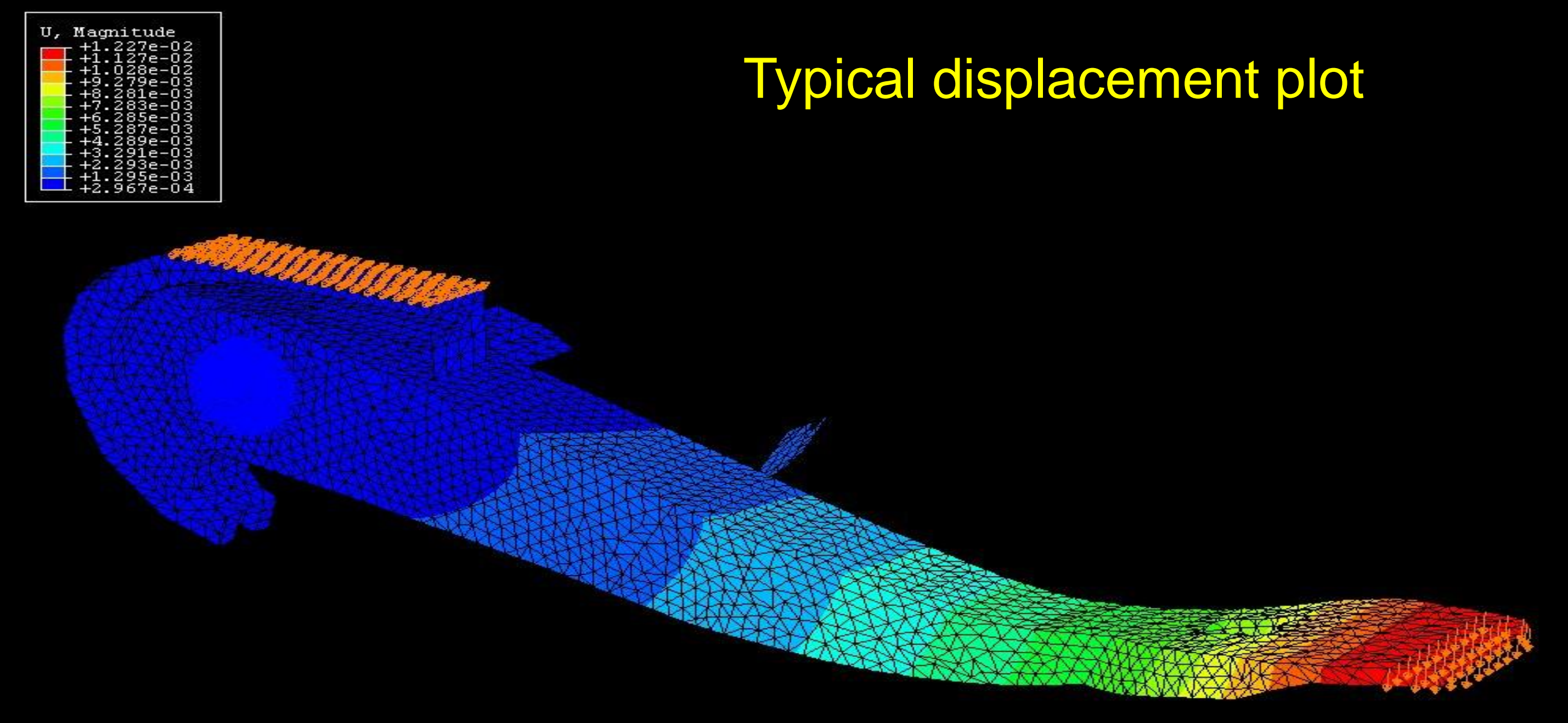
Commercial Application

Automotive pedal



Commercial Application

Automotive pedal



	Experimental	FE model using Moldflow FOD	FE model using adjusted material data
Reaction force	350 N	1200 N	700 N

Test Case 2 – Automotive Component

Warpage

Automotive component supplied by Jaguar, moulding from Birkby's plastics.

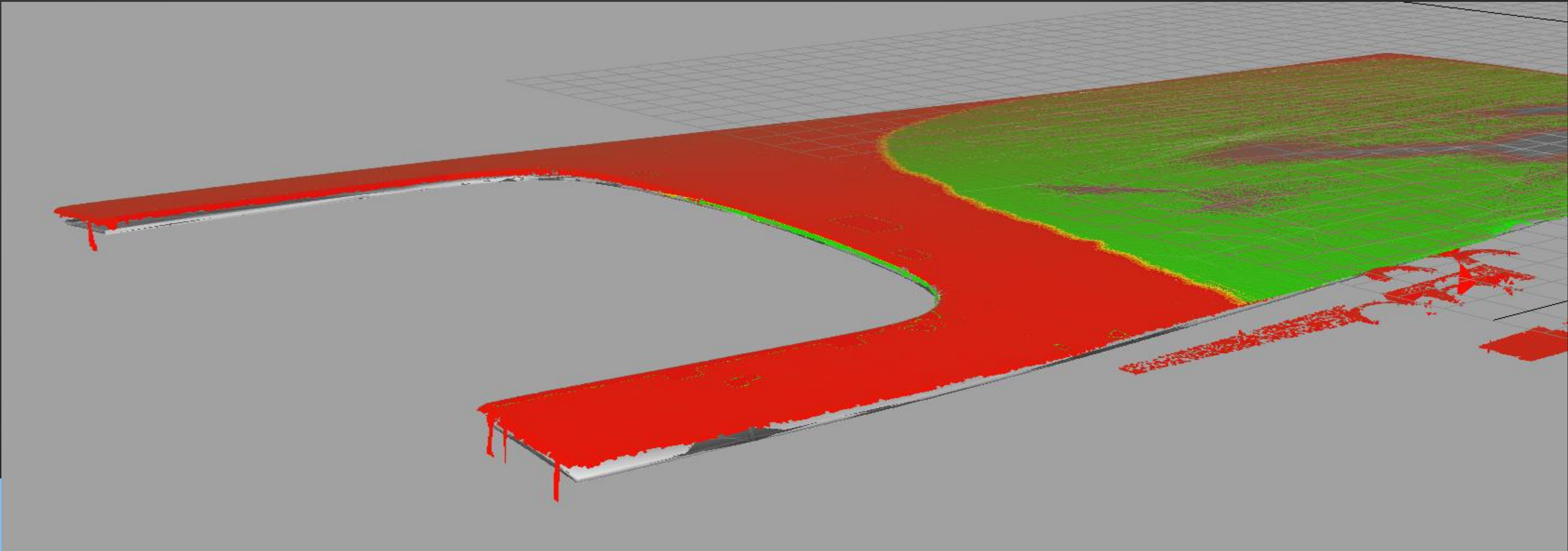
PA66 – 50% short glass fibre

Sample surface digitised using a 3D laser scanner with height resolution of 0.1 mm. 10 samples scanned

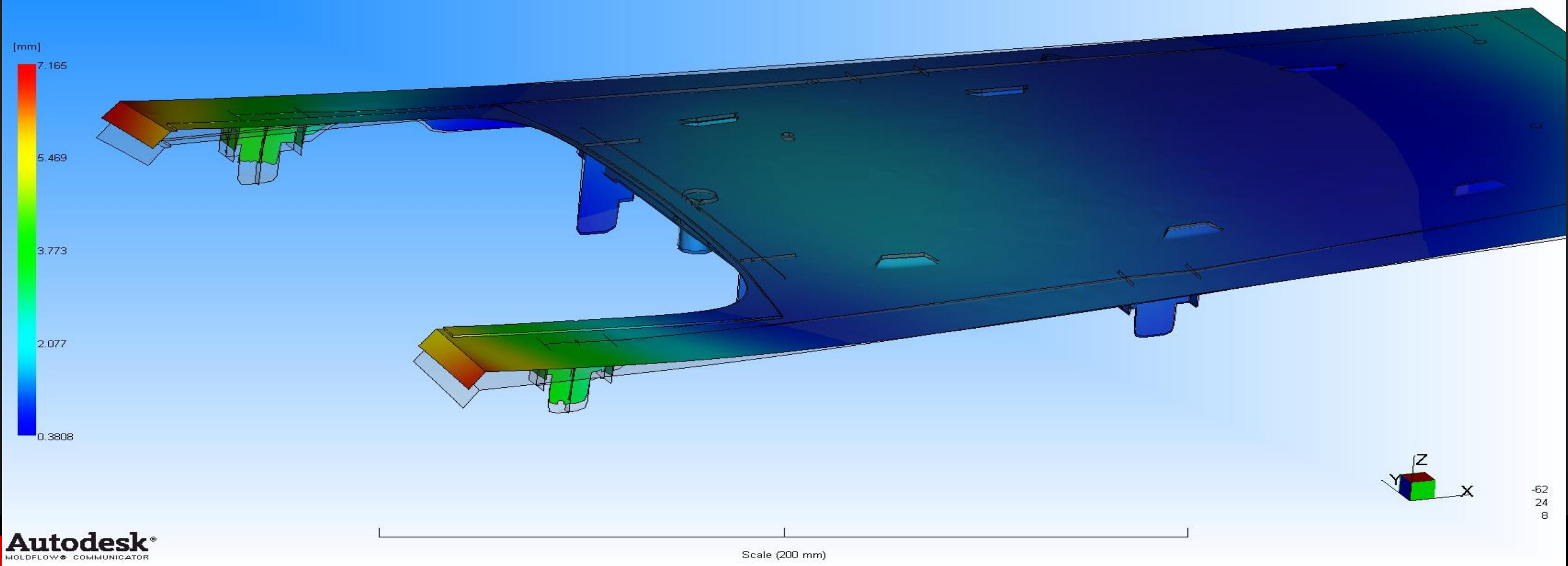


- Insert Moldflow to Alias translational information, cloud point data acquisition and meshing information

Warpage



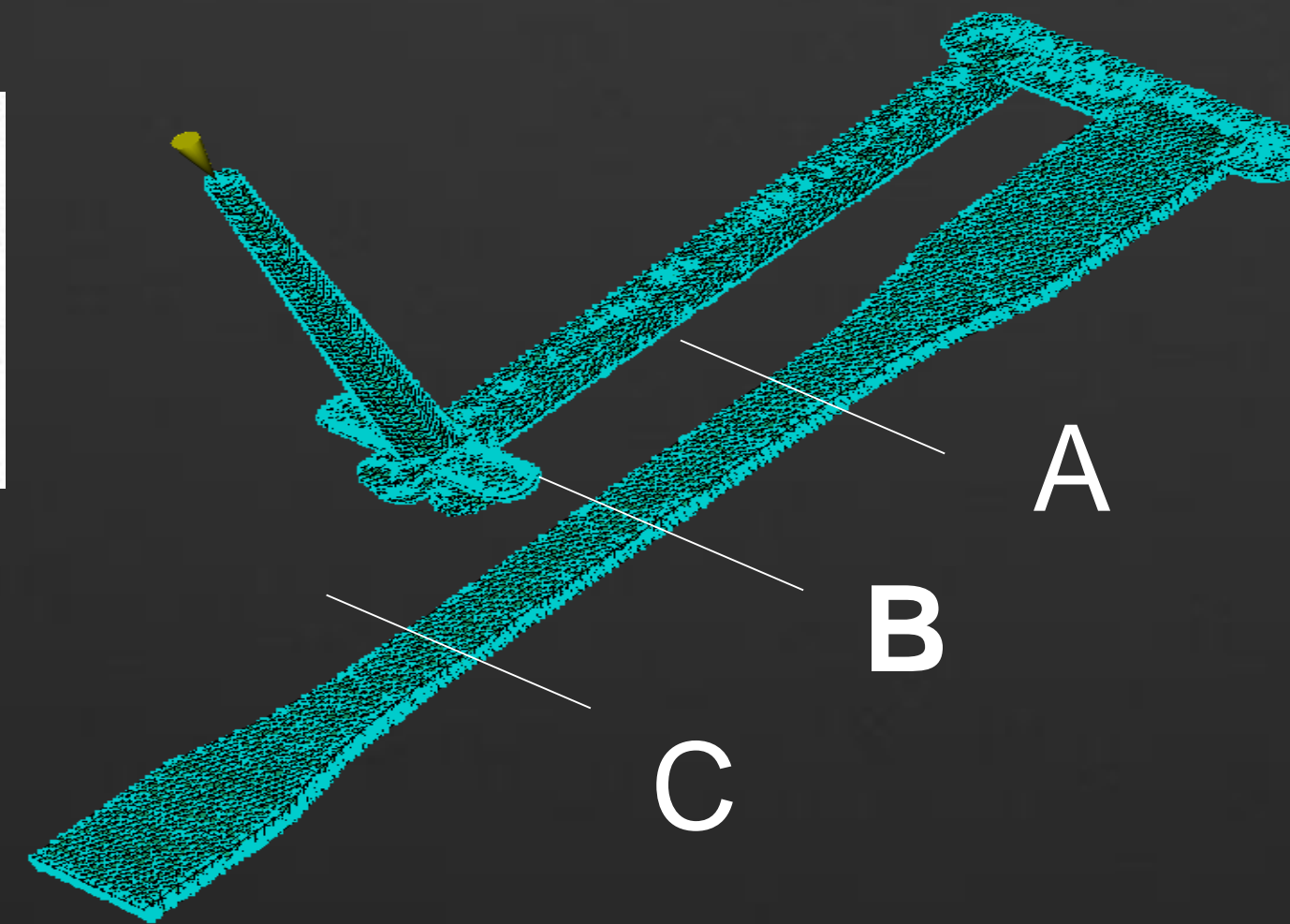
Deflection, all effects.Deflection
Scale Factor = 1.000



Look to the Future



A

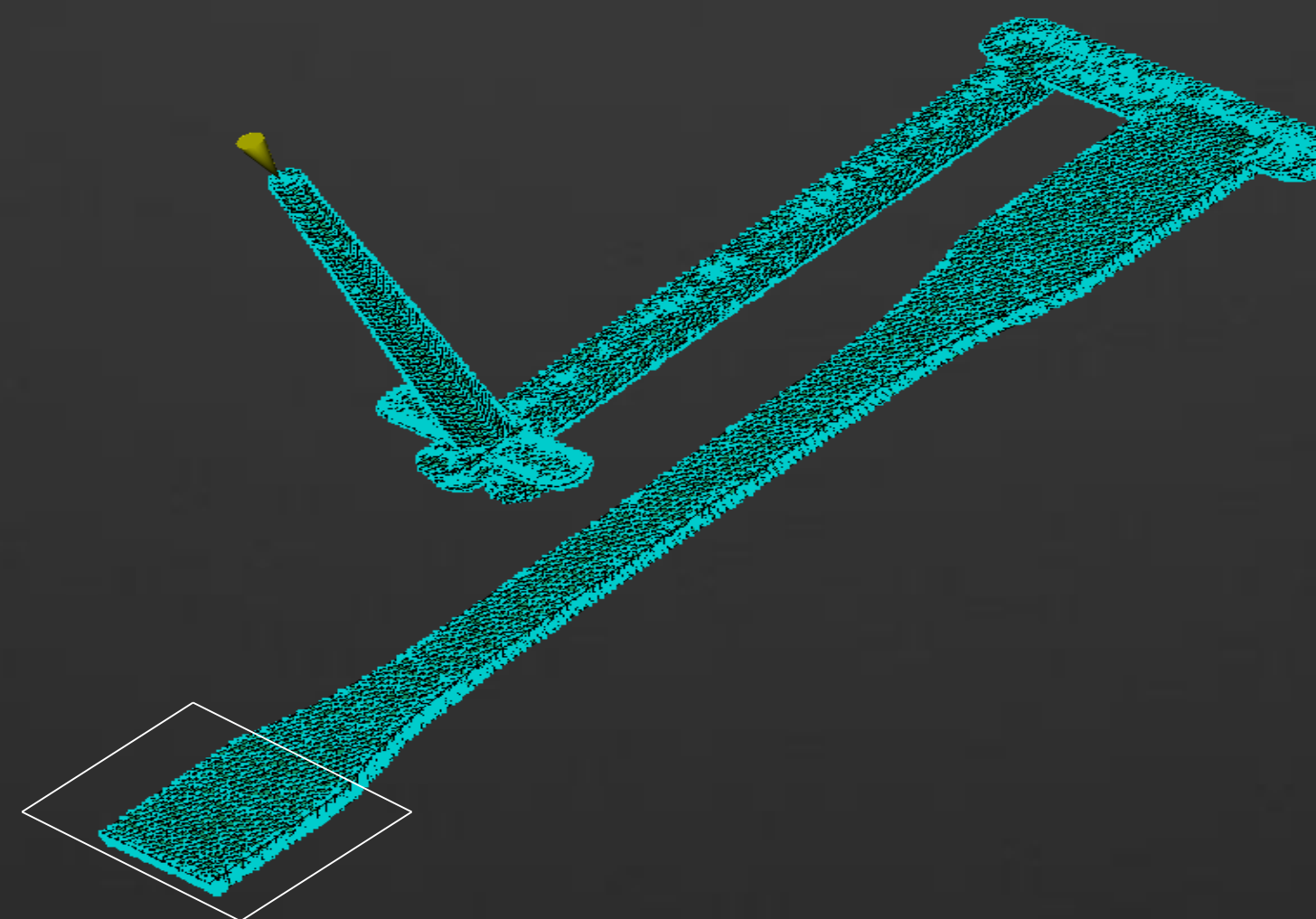


B

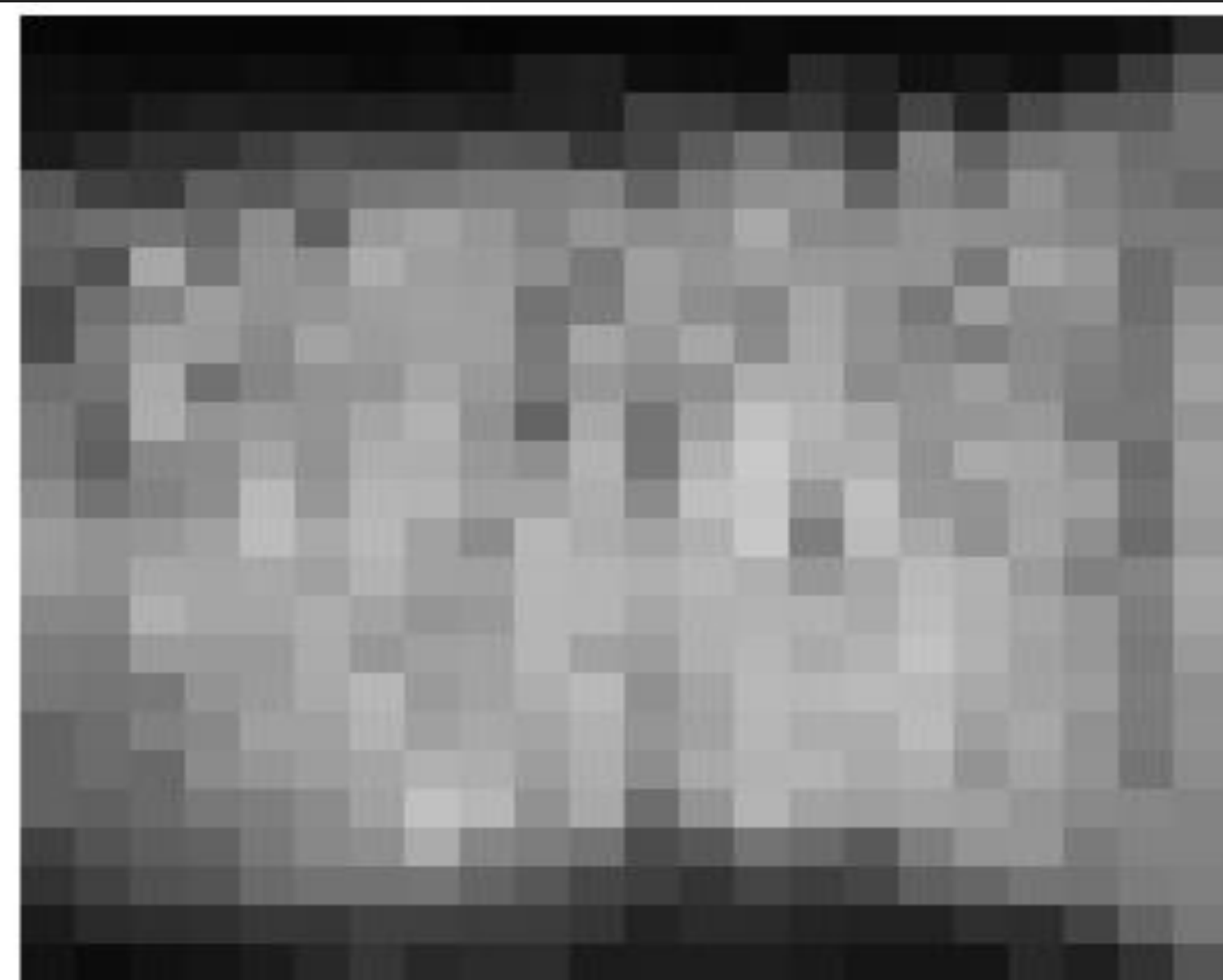


C

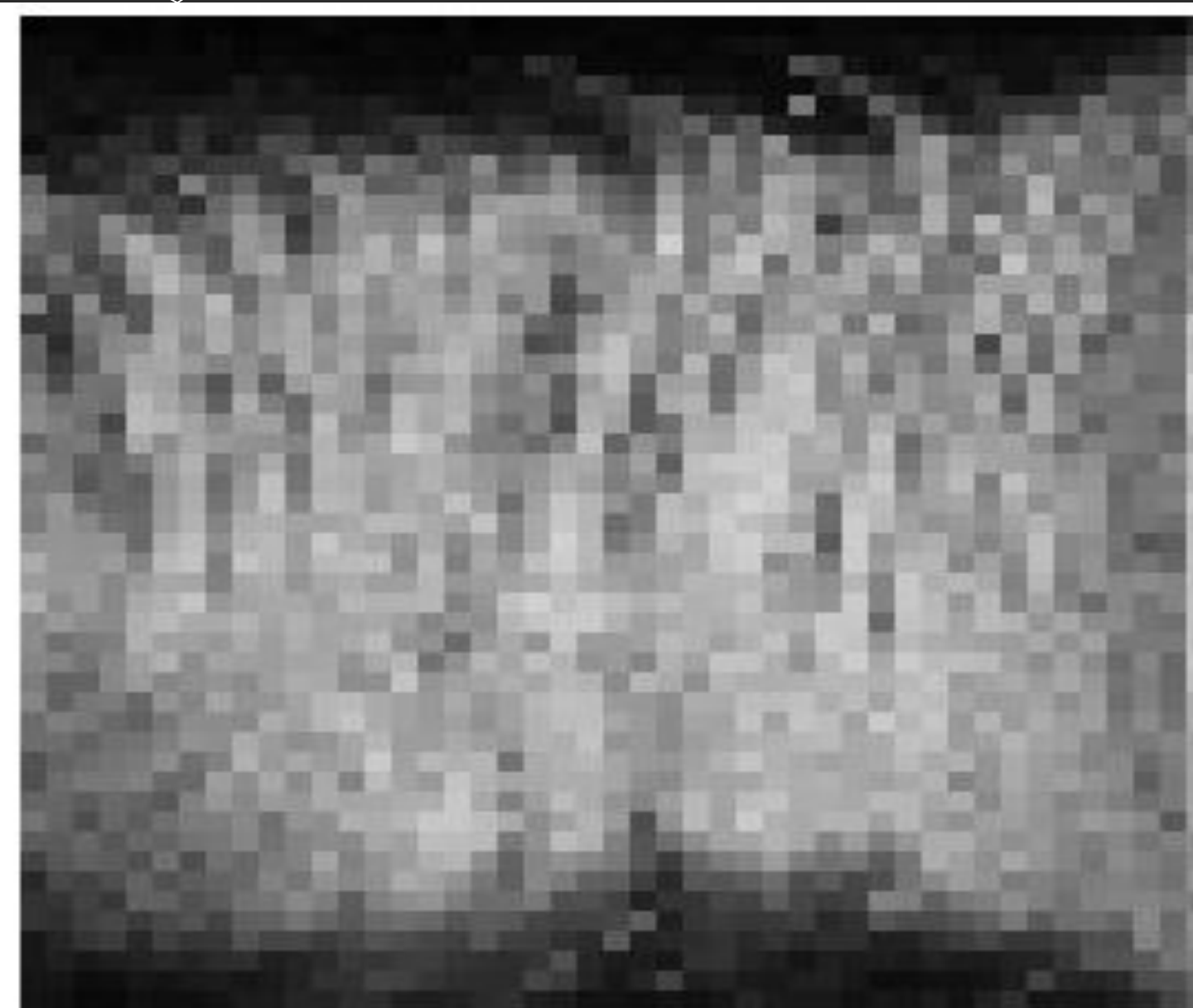
This data would normally be used to calibrate a midplane or 3D Moldflow model



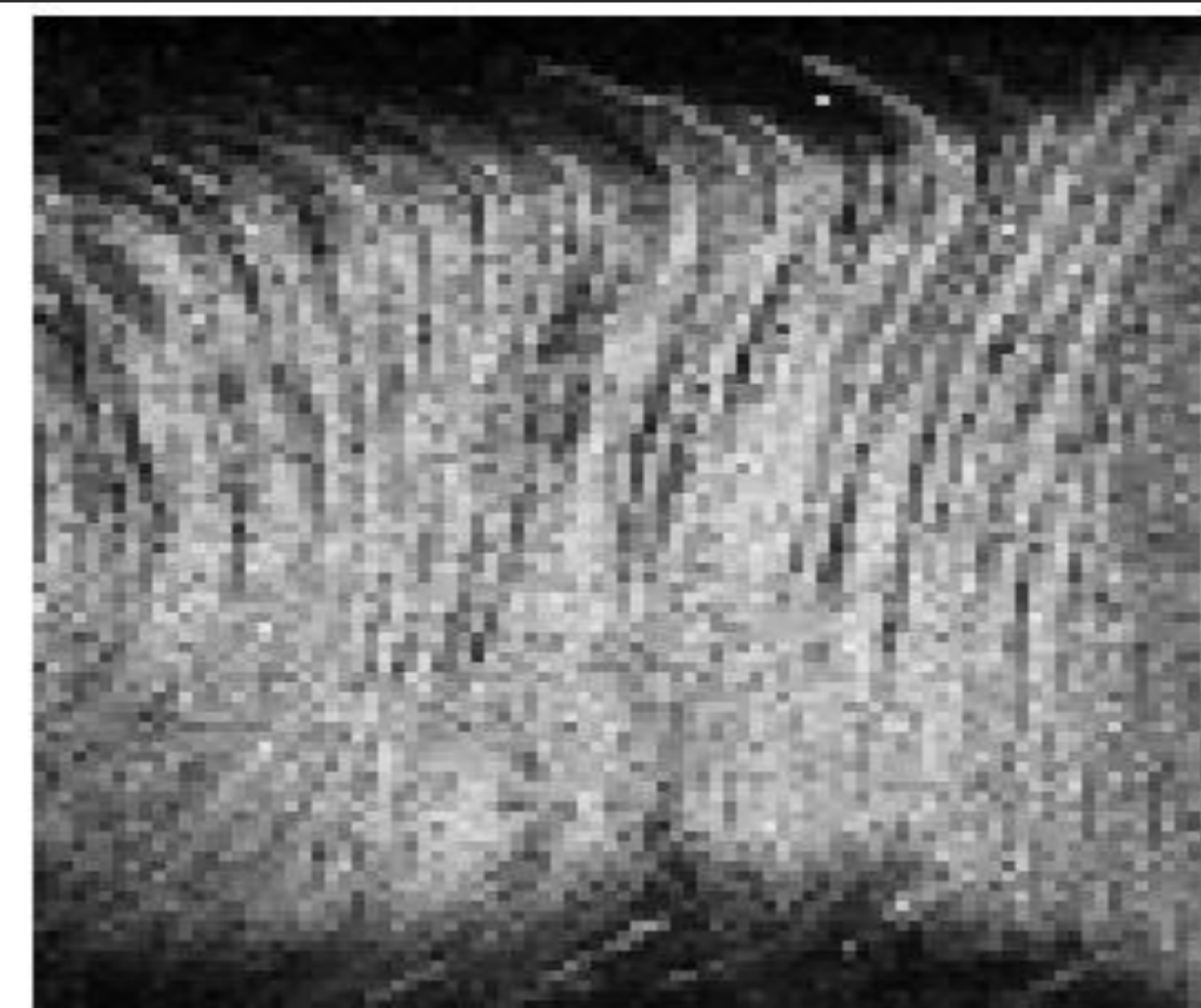
Slices through the core of the sample show complex orientation effects at higher magnification



22 x 25

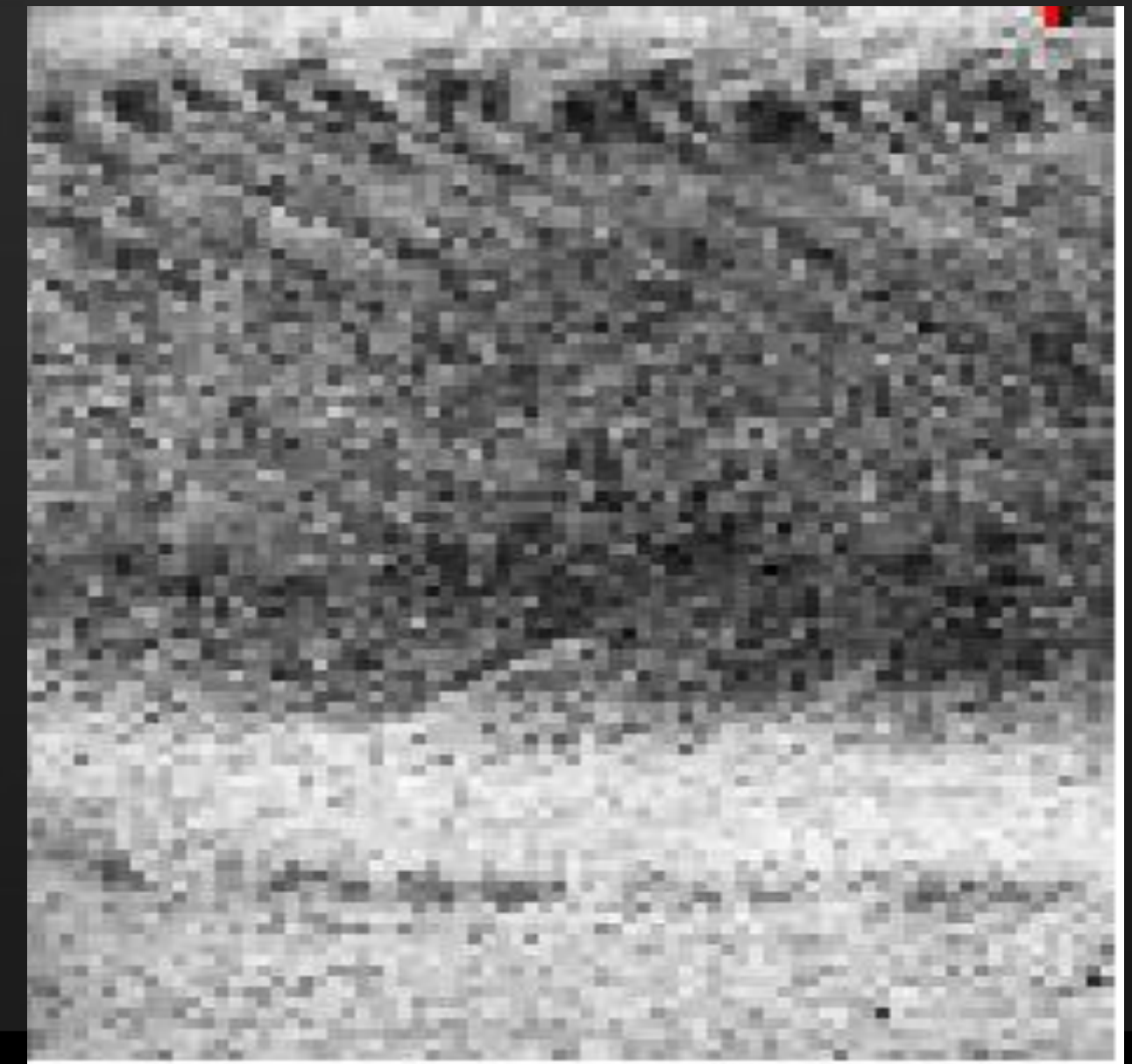
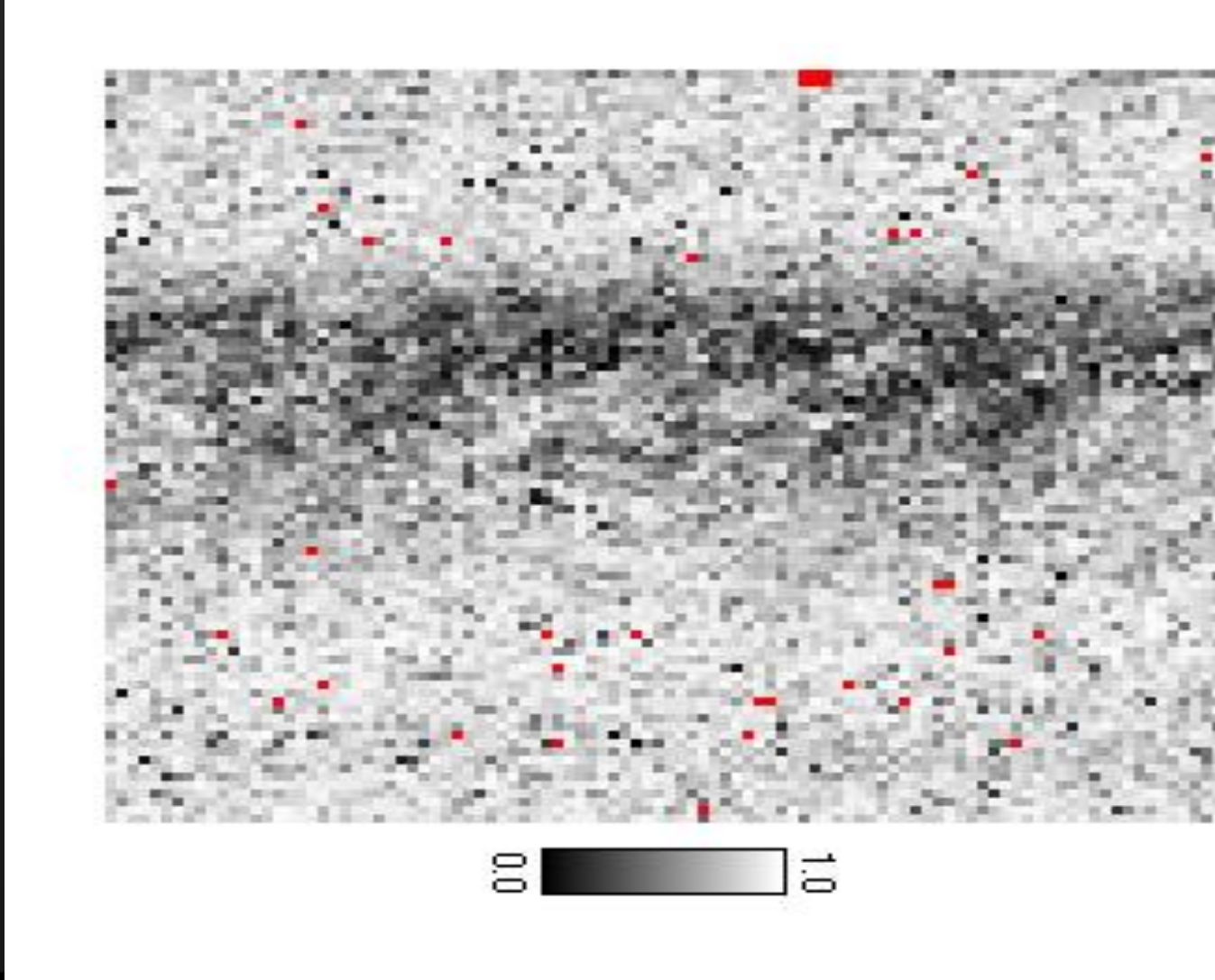
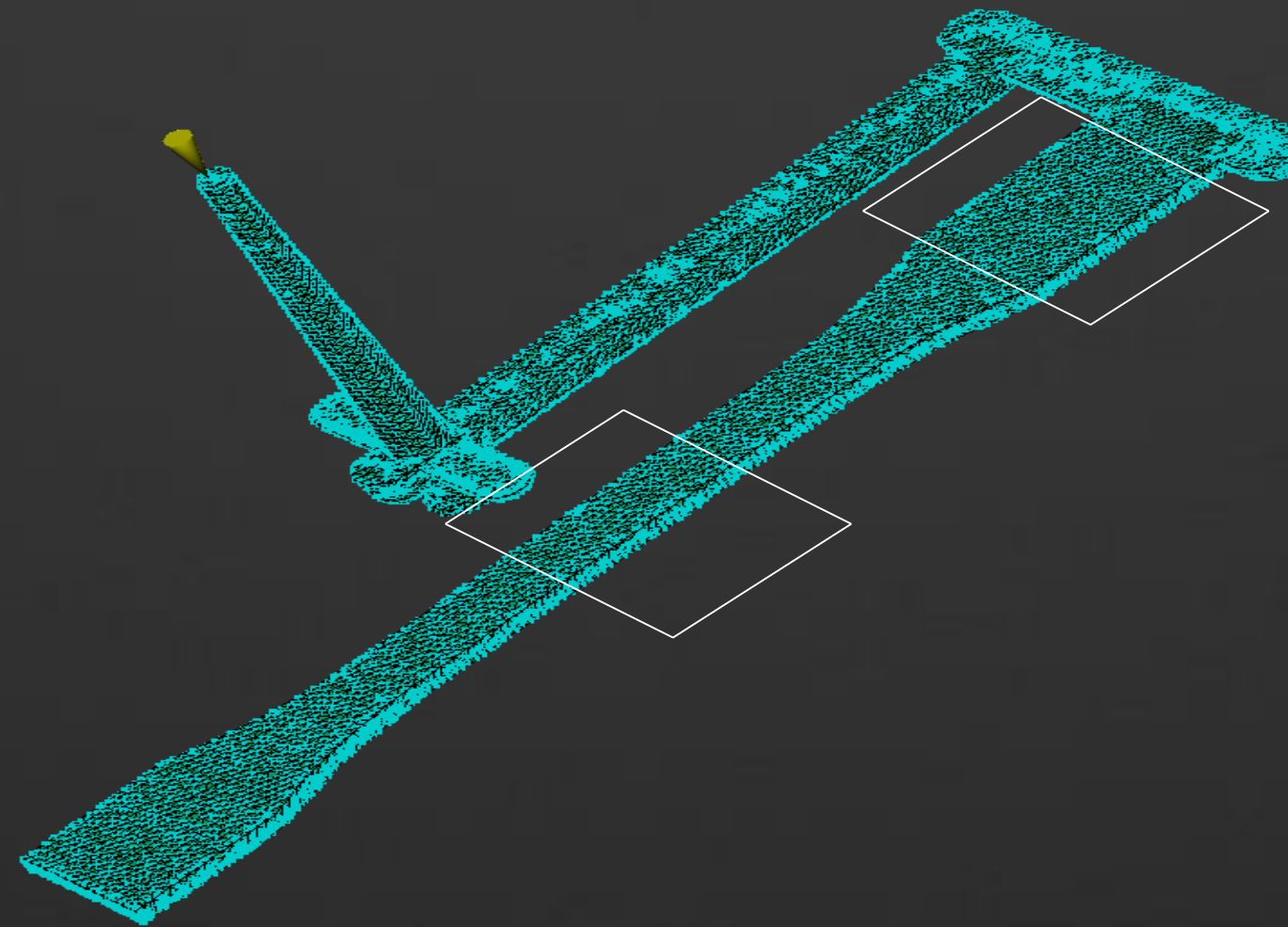


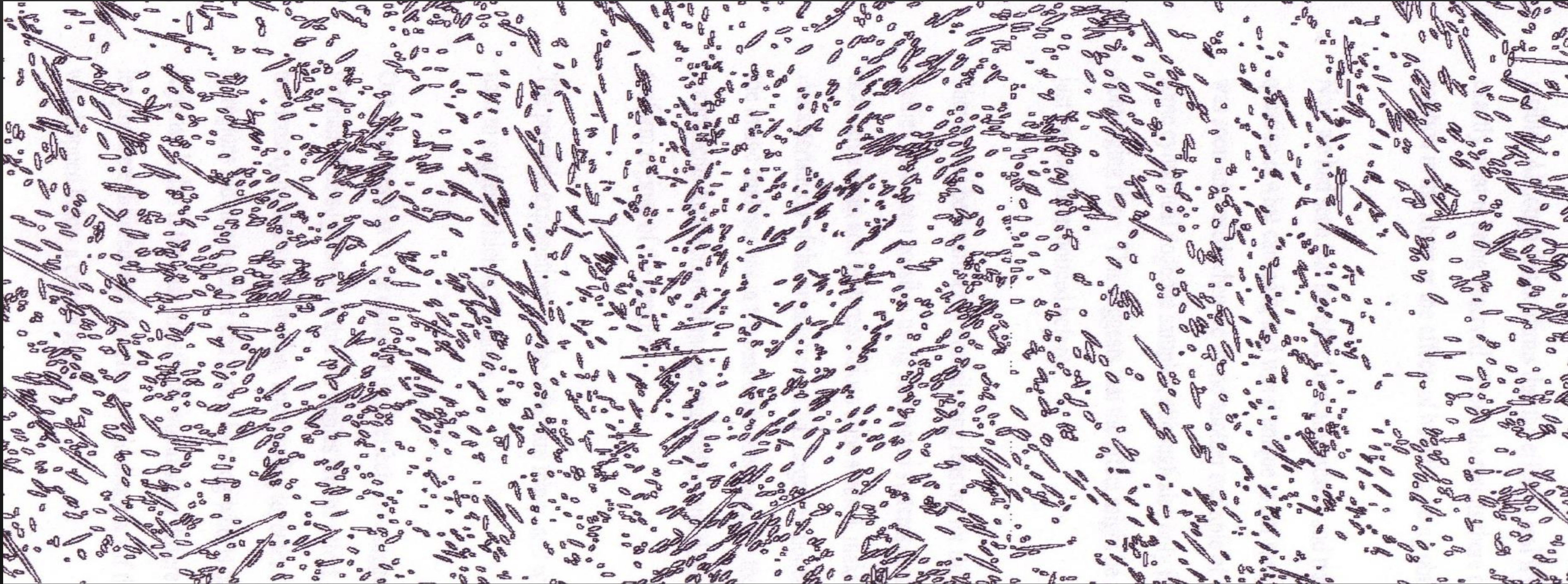
45 x 50



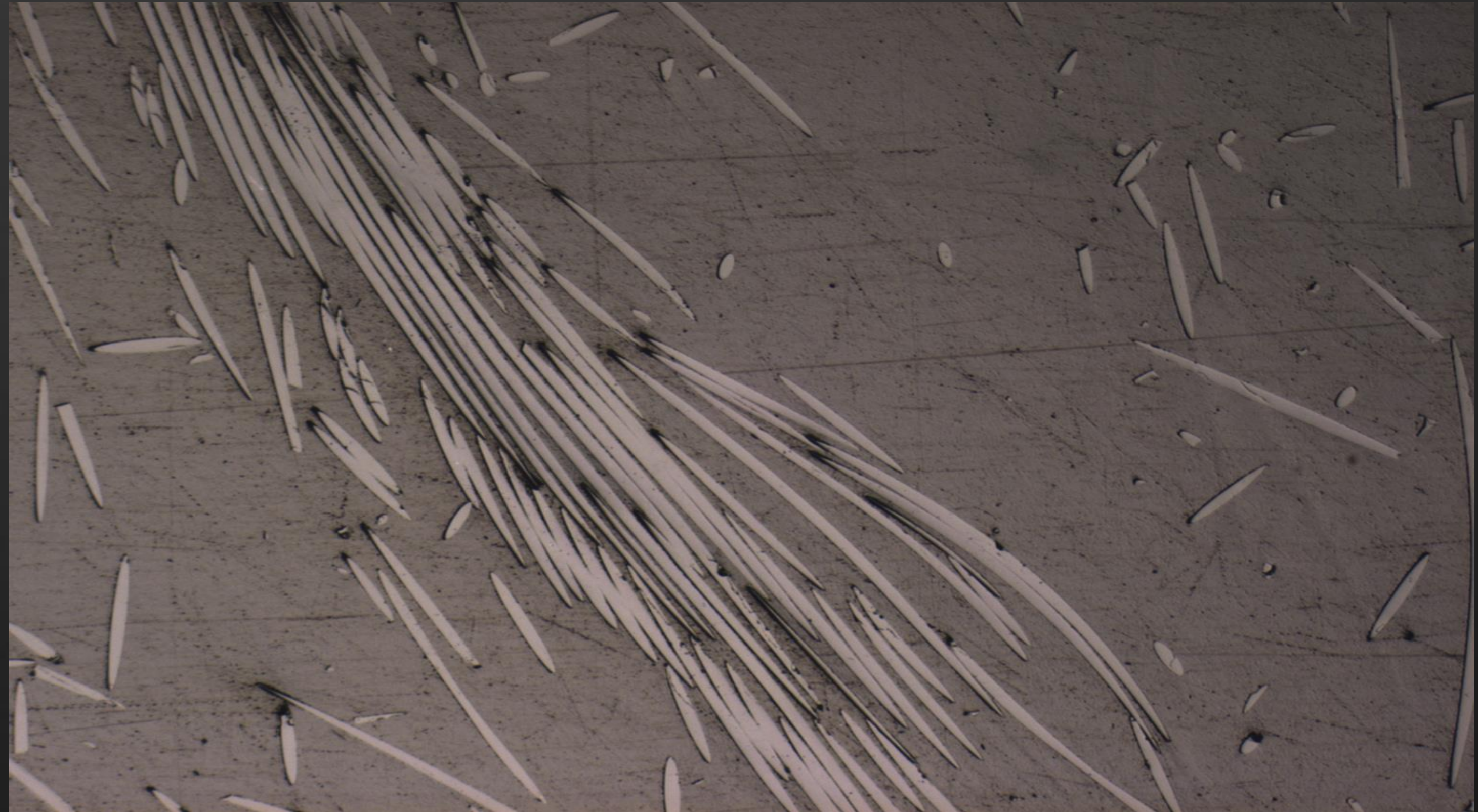
90 x 100



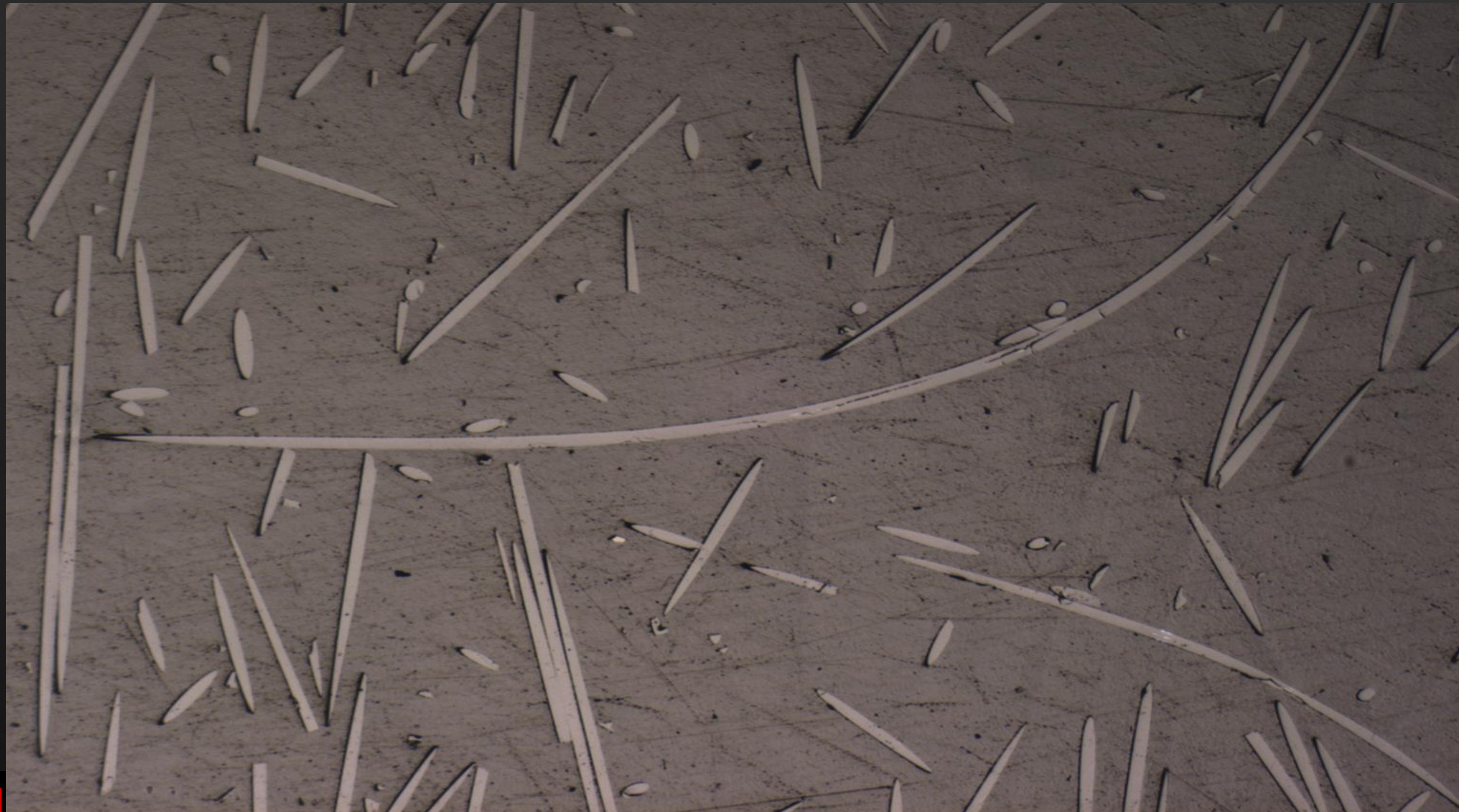




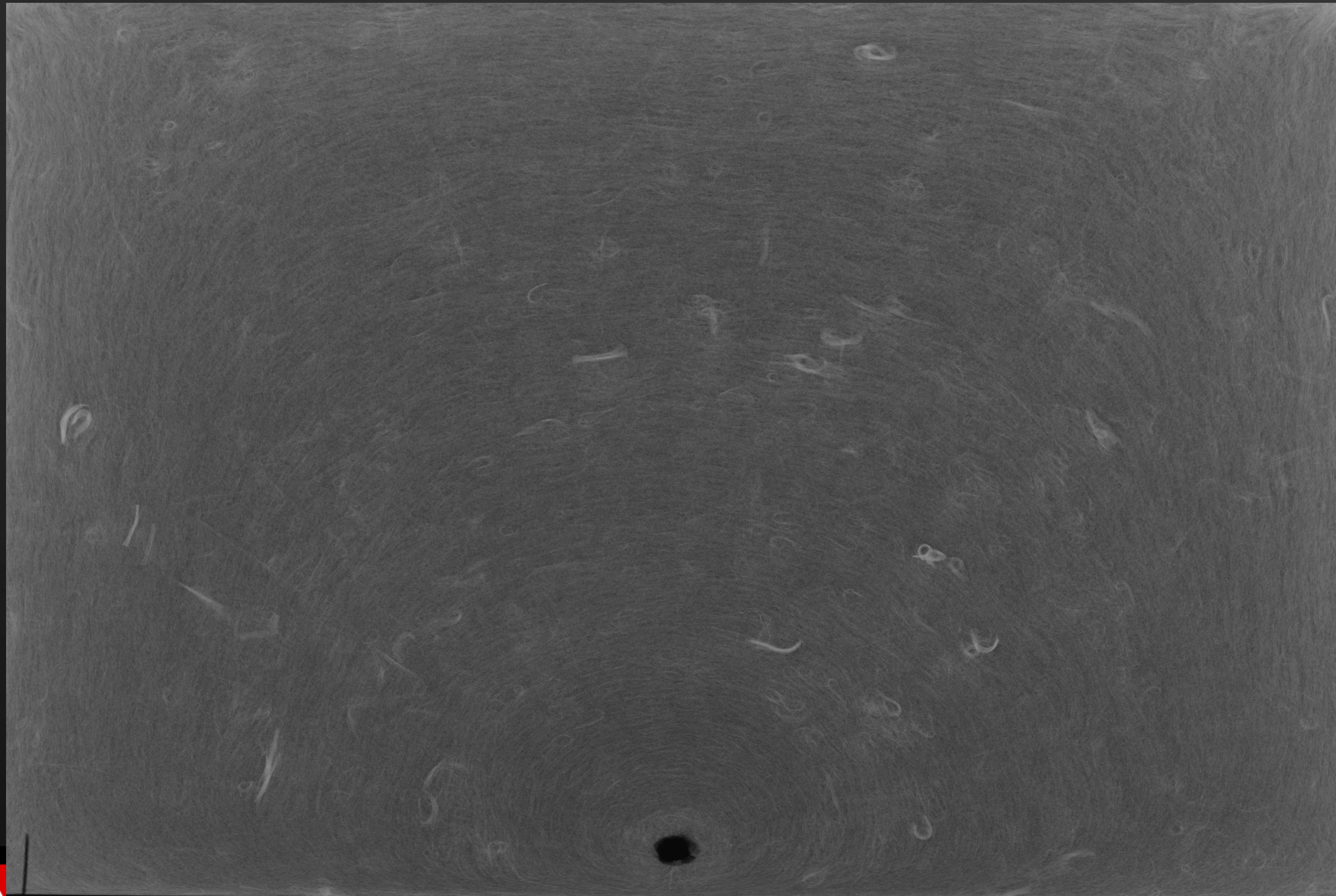
Long fibre orientation



Long fibre orientation



Alternative fibre orientation measurement



Fibre diameter has increased from $\sim 10\ \mu\text{m}$ (short) to $\sim 20\ \mu\text{m}$ (medium to long).

This increase in length makes microCT a viable option for fibre orientation measurement

Fibre Orientation - Future

1. Experimentally determined fibre orientation

- Existing system has shown more complex fibre orientation than previously thought. The significance of fibre bundling on final product properties requires further work.
- Existing Leeds system is currently being evaluated for long fibre orientation. MicroCT has shown promising results although further investigation is needed.

2. Fibre prediction models

- Apply RSC model to commercially relevant geometries
- Post injection component performance, with specific interest in warpage and non-linear mechanical properties

3. Long fibre reinforcement

- Need to consider fibre curvature, break and bundling and the subsequent mechanical properties

Any questions?

